

Investigation of Neuropeptide Y as a metabolic marker and its effects on adipose vasculature and brainstem astrocytes

Carlo Casale

**Adipokines and Metabolism Research Group
Division of Medicine**



**A thesis submitted for the degree of Doctor of Philosophy in the
Division of Medicine at University College London**

Declaration

No part of this thesis has been submitted in support of an application for any other degree or qualification at the University College London or any other university or institute. All the work presented is my own and all collaborations have been acknowledged.

Signature:**Date:**

Abstract

Subsets of morbidly obese patients do not appear to exhibit the expected comorbidities, as well as the fact that heightened sympathetic nervous system (SNS) activity has been known to affect metabolism. In this study, Neuropeptide Y (NPY), an SNS co-transmitter is explored as a possible biomarker for unhealthy obesity. The aims of the study were to identify a normoinsulinemic/insulin sensitive morbidly obese Caucasian patient cohort, compare differences in NPY levels in the circulation and adipose tissue between the normoinsulinemic and hyperinsulinemic subjects. I explored the hypothesis that elevated circulating peripheral NPY causes metabolic abnormalities by mediating changes in the normal function of brain stem regulatory mechanisms via inflammation of astrocytes as shown in an *in vitro* model of primary cell line of human fetal brain stem astrocyte cell line.

Blood and abdominal adipose tissue samples were obtained from consenting, morbidly obese patients awaiting bariatric surgery for recruitment in the study. Adipokines and NPY were measured as well as gene and protein expression by real-time PCR and histology. Effect of NPY was determined on a human brainstem astrocytic primary cell-line using immunohistochemistry, real time PCR, cytokine ELISA, intracellular secondary messengers via ELISA and fluorescence microscopy. Secreted lactate levels were measured by calorimetric assays. Differences were found between metabolically healthy obese (MHO) and pathologically obese (PO)/diabetic groups in certain adipokines and insulin sensitivity, which were maintained after surgical weight loss. Differences in adipocyte cell size were visible between the two groups both in subcutaneous and omental adipose tissue depots but inflammatory cell infiltration was not different. Brain stem astrocytes expressed NPY receptors and IL-6 secretion from the astrocytes increased when exposed to a combination of NPY and noradrenaline, reflected by changes in intracellular cAMP. Cytokine array showed increases in various inflammatory cytokines under the same treatment. IL-6 treatment increased astrocyte lactate levels.

In astrocytes there was greater level of adrenergic signalling and secretion of IL-6 and lactate by the cells, which could mean different metabolic balance of astrocytes and long-term effects on astrocyte chemosensing function. These findings suggest differences in susceptibility to obesity associated pathologies linked to a synergistic modulation between the intracellular signalling pathways of astrocytes, being regulated at least partially by components of the CNS and having a direct effect on the cells. Perhaps these would pave the way for targeted treatment modalities. In vivo studies in an analogous animal model would further clarify the connection between elevated peripheral NPY and its central effects on the brainstem astrocytes in mediating metabolic disease.

Acknowledgments

First and foremost I would like to thank Giulia. Without your help, loving support and the strength you were able to give me (and remind me of having within), this thesis would have never been possible. Then my family: my parents Francesco and Isabella, for giving me the constant support and opportunities to reach the point where I am today, as well as Adriano and Alice in making my family a place to regain strength and resolve.

My supervisors Vidya Mohamed-Ali and Nephtali Maria-Gonzalez for the help and patience shown and my colleagues Shen and Noora, with whom I've shared a lab for three years, and with all the ups and downs of the time spent there and all the fun moments that I will never forget. I'd like to also thank Binara for our lengthy talks and help (which I hope I've been able to reciprocate) and all the people at the Division of Medicine that have made this project and my three years at UCL possible and so special.

Special thanks also to my dear friend An-Rui, with whom the years in London could have never been better.

Thank you all.

Table of Contents

Abstract	2
Acknowledgments	4
Table of Contents	5
List of figures	10
List of tables	12
Publications arising from this project.....	13
Conference Proceedings	13
Manuscripts under review	13
Abbreviations (in alphabetical order)	14
1.2.1 Cardiovascular disease and obesity	19
1.2.2 Obstructive Sleep Apnoea (OSA) and obesity	21
1.2.3 Non-Alcoholic Fatty Liver Disease (NAFLD) and obesity	21
1.3.1 Insulin resistance and skeletal muscle	24
1.3.2 Insulin resistance and the liver.....	25
1.4.1 Adipose tissue: an endocrine organ	26
1.4.2 Adipose tissue remodelling and insulin resistance in obesity: Hypertrophy vs. hyperplasia.....	27
1.4.3 FFA and insulin resistance in adipose tissue	32
1.4.4 Obesity or metabolism? The need to explore the heterogeneity of obesity.....	34
1.5.1 Metabolically Healthy Obese (MHO) individuals	34
1.5.2 Implications of MHO individuals in the clinical setting	36
1.6.1 Adipokine profile differences	38
1.6.2 Inhibition of Adipogenesis.....	39
1.6.3 Dysfunction in the regulation of SREBP Proteins and the lipogenic/lipid homeostasis pathway	40
1.6.4 The need for a biomarker.....	41
1.7.1 The sympathetic nervous system in breathing and blood pressure control.....	42

1.7.3 Direct effectors of the SNS: catecholamines and adrenoceptors	45
1.7.4 The role of astrocytes in the sympathetic nervous system	47
1.7.5 Neuropeptide Y and the sympathetic nervous system	50
1.7.6 NPY and the periphery: adipose tissue	51
1.8.1 Hypothesis: NPY as a possible link between periphery and CNS	53
1.8.2 Overall aims	54
1.8.3 Patient recruitment and characterisation	54
1.8.4 Assessment of adipokine differences and search for possible biomarkers....	55
1.8.5 Differences in Morphological and local secretory function between subcutaneous (SC) and omental (OM) adipose tissue	55
1.8.6 Adipogenic/metabolic gene expression differences	55
1.8.7 Circulating NPY levels	55
1.8.7 Effects of NPY/NA levels simulating heightened SNS activity on human astrocytes	55
2.1.1 Patient Recruitment	57
2.1.2 Statistical analysis.....	71
2.1.3 Blood samples	58
2.1.4 MHO/PO characterisation criteria.....	58
2.2.1 Histology sample preparation	59
2.2.2 Hematoxylin and Eosin staining	59
2.2.3 NPY/CD68 Immunohistochemistry.....	59
2.2.4 Adipocyte size calculation	59
2.2.5 Quantification of CD68/NPY receptor DAB stain	60
2.3.1 Organ explant cultures	62
2.3.2 Protein extraction.....	62
2.3.3 Circulating and local adipokine/NEFA levels	63
2.3.4 Induction of IL-6 secretion by IL-1 β	63
2.4.1 RNA extraction	63
2.4.2 cDNA synthesis	64

2.4.3 Real-time PCR	64
2.4.5 siRNA knockdown in adipose tissue	65
2.5.1 Astrocyte cell culture.....	66
2.5.2 Astrocyte incubations.....	66
2.5.3 Quantification of astrocyte pSTAT3, cAMP, IL-6 and lactate levels	67
2.5.4 Astrocyte Immunohistochemistry.....	68
2.5.5 Cytokine array	68
2.5.6 Astrocyte gene silencing.....	69
2.5.7 Astrocyte intracellular calcium imaging	71
3.1.1 General patient characteristics	73
3.1.2 Circulating adipokines	74
3.1.3 Locally secreted adipokines from adipose tissue explants	74
3.1.4 IL-1 β induction of IL-6 secretion.....	75
3.2.1 Adipocyte area	79
3.2.2 Adipose tissue CD68+ cells.....	81
3.2.3 NPY receptor staining in tissue.....	83
Table 8: NPY receptor expression.	83
Immunohistochemistry quantification in arbitrary units (AU).....	83
3.2.4 Blood vessel-associated NPY receptor quantification.....	86
3.3 Adipose tissue transcriptional studies	89
3.3.1 Adipogenesis: adipocyte PPAR γ expression	89
3.3.2 Metabolism: adipocyte SCD1 expression	90
3.3.3 Adipocyte NPY receptor expression	92
3.3.4 Adipose tissue siRNA knockdown	93
3.4 Brain stem astrocyte in vitro studies.....	95
3.4.1 Astrocyte NPY receptor immunohistochemistry.....	95
3.4.2 Astrocyte NPY receptor transcription modulation in response to NPY	97
3.4.3 Astrocyte NPY/adrenergic receptor transcription in simulated SNS activity	99
3.4.4 Astrocyte inflammatory mediator secretion.....	102

3.4.5 Intracellular signalling molecules and IL-6 secretion	104
3.4.6 Intracellular secondary messengers and IL-6 secretion	108
3.4.7 IL-6 incubation and astrocyte lactate release	109
3.4.8 Astrocyte cytokine array quantification	110
3.4.9 Astrocyte gene silencing.....	112
3.4.10 Astrocyte intracellular calcium signalling in response to NA and NPY.....	113
4.1 Clinical data	118
4.1.1 Patient population results	118
4.1.2 Adipose tissue explants secretion	119
4.1.3 IL-6 secretion in response to IL-1 β stimulation.....	120
4.1.4 Summary of clinical data	120
4.2 Histology.....	121
4.2.1 Adipocyte area	121
4.2.2 CD68+ cell infiltration in adipose tissue	121
4.2.4 NPY receptor staining in adipose tissue vessels.....	122
4.2.5 Summary of histological investigation data	123
4.3 Tissue RNA transcriptional studies.....	125
4.3.1 PPAR γ expression in adipose tissue	125
4.3.2 SCD1 expression	126
4.3.3 NPY receptor expression	126
4.3.4 Adipose tissue siRNA electroporation and knockdown of miR-146b	128
4.3.5 Summary of transcription data	128
4.4 Astrocyte data	130
4.4.1 NPY receptor immunohistochemistry data.....	130
4.4.2 Responsiveness of the receptors to NPY at the mRNA level.....	130
4.4.3 Astrocyte receptor mRNA transcription in response to SNS activity (Noradrenaline/NPY) data	131
4.4.4 Astrocyte inflammatory cytokine secretion data.....	132
4.4.5 Intracellular secondary messengers and IL-6.....	133

4.4.6 cAMP levels and IL-6 release in brain stem astrocytes	135
4.4.7 IL-6 and lactate release data	135
4.4.8 Astrocyte cytokine array	136
4.4.9 Astrocyte leptin receptor gene silencing	138
4.4.10 Intracellular Ca ²⁺ levels in astrocytes	138
4.4.11 Summary of astrocyte data	140
4.5 Conclusions, limitations and future work	142
4.5.1 Intracellular boost of noradrenergic signalling by NPY via Ca ²⁺ levels.....	142
4.5.2 Limitations of the astrocyte model and future work	145
4.5.3 Development of an animal model.....	146
4.5.4 DPP-IV and its effects on NPY signalling.....	147
4.5.5 Precise NPY detection	148
4.5.6 The need for a common MHO definition	148
Bibliography.....	150

List of figures

<i>Figure 1: Number of hospital episodes for bariatric surgery in England by sex 2003/4-2009/10</i>	18
<i>Figure 2: Mechanisms linking the obese state and hypertension</i>	20
<i>Figure 3: Hyperinsulinemia in obesity</i>	22
<i>Figure 4: Crosstalk of insulin-sensitive tissues in the bod</i>	24
<i>Figure 5: Insulin resistance in the liver</i>	25
<i>Figure 6: Adipose tissue adipokines</i>	27
<i>Figure 7: Adipose tissue hypertrophy and its local effects in obesity</i>	28
<i>Figure 8: Adipose tissue remodelling in obesity</i>	30
<i>Figure 9: Role of lipotoxicity via adipose tissue FFAs in obesity</i>	33
<i>Figure 10: Profiles of MHO vs. MAO (PO) patients</i>	35
<i>Figure 11: Genes regulated by SREBP activity in cholesterol and fatty acid synthesis pathways</i>	41
<i>Figure 12: Sympathetic control of BP in humans</i>	43
<i>Figure 13: The HPA axis</i>	44
<i>Figure 14: lipolysis pathway</i>	46
<i>Figure 15: Models of metabolic coupling in the neuron/astrocyte interaction</i>	47
<i>Figure 16: Possible pathways of astrocyte chemo-detection in the ventral surface of the medulla oblongata (VMS)</i>	49
<i>Figure 17: Possible hypothesis for SNS interference with energy homeostasis and BP regulation</i>	53
<i>Figure 18: clinical study structure</i>	57
<i>Figure 19: adipocyte size calculation method</i>	60
<i>Figure 20: Secretion of IL-6 following stimulation with IL-1beta after 65hours in human subcutaneous adipose tissue</i>	76
<i>Figure 21: Adipocyte area calculation</i>	80
<i>Figure 22: CD68+ DAB staining in SC and OM adipose tissue</i>	82
<i>Figure 23: NPY receptors Y1 and Y5 in MHO and PO adipose tissue</i>	84
<i>Figure 24: NPY receptors Y1 and Y5 associated with vessels in adipose tissue</i>	87
<i>Figure 25: PPARγ2 expression in adipose tissue</i>	89
<i>Figure 26: SCD1 RNA expression in adipose tissue</i>	91

Figure 27: NPY receptor 1 and 5 RNA expression in adipose tissue _____	92
Figure 28: miR-146b expression knockdown in adipose tissue after electroporation and 65h incubation	93
Figure 29: Subcutaneous adipose tissue IL-6 secretion following tissue electroporation and IL-18 stimulation after 65 hours _____	94
Figure 30: Astrocyte receptor Y1 and Y5 immunohistochemistry _____	96
Figure 31: Astrocyte RNA expression of Y1, Y5 and Beta2 adrenergic receptors in response to NPY treatment and Leptin receptor expression in response to Leptin treatment _____	98
Figure 32: Relative RNA expression changes in NPY receptor Y1 and adrenergic receptors β_2 and α_2 with respect to control value of 0 in the presence of NPY and/or noradrenaline _____	101
Figure 33: Astrocyte IL-6 (A) and MCP-1(B) secretion after overnight exposure to NA and/or NPY _____	103
Figure 34: cAMP responses for NA and/or NPY _____	104
Figure 35: pSTAT3 responses for NA and/or NPY _____	107
Figure 36: IL-6 secretion following overnight incubations with intracellular cAMP-boosting drugs _____	108
Figure 37: lactate release in astrocytes exposed to IL-6 _____	109
Figure 38: Astrocyte array densitometry and sample array blot _____	111
Figure 39: LEPR gene silencing in cultured human brain stem astrocytes _____	112
Figure 40: Intracellular Ca ²⁺ oscillations in astrocytes _____	115
Figure 41: possible mechanisms for potentiation of IL-6 release from astrocytes caused by noradrenaline and NPY in combination _____	142

List of tables

<i>Table 1: Patient characteristics</i>	73
<i>Table 2: Serum adipokines</i>	74
<i>Table 3: adipose tissue explants (0.045g-0.055g) adipokine secretion after 24h incubation</i>	75
<i>Table 4: Average IL-6 secretion after stimulation with IL-1beta after 65 hours</i>	76
<i>Table 5: Patient follow-up parameters</i>	78
<i>Table 6: Adipocyte size calculations in SC and OM adipose tissue samples</i>	79
<i>Table 7: CD68+ DAB staining in SC and OM adipose tissue of MHO and PO patients</i>	81
<i>Table 8: NPY receptor immunohistochemistry quantification in arbitrary units (AU)</i>	83
<i>Table 9: NPY blood vessel staining quantification</i>	86

Publications arising from this project

Conference Proceedings

Lei Shen, Nelson Orie, **Carlo Casale**, Nephtali Marina, Mick Dashwood, Pratik Sufi, Dugal Heath, Rosaire Gray and Vidya Mohamed-Ali, *Depot- and disease-specific differences in adipose noradrenaline mediated vascular tone and arteriolar structure*. Endocr Rev, 2013, Vol. 34 (03_MeetingAbstracts): OR51-2 (oral presentation)

Carlo Casale, Lei Shen, Sana Malik, Rosaire Gray, Pratik Sufi, Dugal Heath, Nephtali Marina and Vidya Mohamed-Ali, *Systemic Neuropeptide Y Levels Are Suppressed in the Metabolically Healthy Obese*. Endocr Rev, 2013, Vol. 33 (03_MeetingAbstracts): SUN-134

Sana Malik, Lei Shen, **Carlo Casale**, Rosaire Gray, Pratik Sufi, Dugal Heath and Vidya Mohamed-Ali, *Effect of Surgical Weight Loss on Insulin Sensitivity and Lipid Profile of Metabolically Healthy Morbidly Obese Subjects*. Obes Surg. 2012 pp. 981 - 981

Vidya Mohamed-Ali; **Carlo Casale**; Sana Malik; Lei Shen; Pratik Sufi, Dugal Heath, Nephtali Marina, Rosaire Gray, *Prevalence and Treatment of Depression Are Differentially Associated With Pathological Obesity and Metabolically Healthy Obesity*. Obesity, 2011. pp. S92 - S92

Manuscripts under review

Lei Shen, Nelson Orie, **Carlo Casale**, Nephtali Marina, Mohammed Alsayrafi, Pratik Sufi, Rosaire Gray and Vidya Mohamed-Ali, *Norepinephrine-induced contractile insensitivity and collagen deposition in subcutaneous adipose tissue arterioles of diabetic patients*, Submitted to Circulation, 2014.

Lei Shen, **Carlo Casale**, Rosaire Gray, Pratik Sufi, Dugal Heath and Vidya Mohamed-Ali, *Depot- and diabetes-specific differences of angiogenesis and angiogenesis-related gene on human abdominal adipose tissue*, Submitted to Diabetes, 2014.

Abbreviations (in alphabetical order)

AMPA - α -amino-3-hydroxy-5-methyl-4-isoxazolepropionic acid

ADRA2- - Adrenergic receptor alpha 2

ADRB2 – Adrenergic receptor beta 2

BMI – Body mass index

cAMP – Cyclic-adenosine monophosphate

CXCL1 - chemokine (C-X-C motif) ligand 1

dbcAMP – Dibutyryl cyclic adenosine monophosphate

FFA – Free fatty acids

FPG – Fasting plasma glucose

HDL – High-density lipoprotein

HOMA-IR - Homeostatic model assessment – insulin resistance

IBMX - 3-isobutyl-1-methylxanthine

IL-1beta – Interleukin 1 beta

IL-1ra – Interleukin 1 receptor antagonist

IL-6 – Interleukin 6

IL-8 – Interleukin 8

IFNgamma – Interferon gamma

LEPR – Leptin receptor

LDL – Low-density lipoprotein

MCP-1 – Monocyte chemotactic protein 1

MHO – Metabolically healthy obese

MUFA – Monounsaturated fatty acids

NA - Noradrenaline

NAFLD – Non-alcoholic fatty liver disease

NPY – Neuropeptide Y

OGTT – Oral glucose tolerance test

OM – Omental

PO – Pathologically obese

PPAR- γ – Peroxisome proliferator-activated receptor gamma

pSTAT3 – phosphorylated STAT3

PUFA – Polyunsaturated fatty acids

RVLM – Rostro-ventrolateral medulla

SAT – Subcutaneous adipose tissue

SC - Subcutaneous

SCD-1 - Stearoyl-Coenzyme A desaturase 1

SREBP – Sterol regulatory element binding protein

STAT3 - Signal transducer and activator of transcription 3

TC – Total cholesterol

TLR-4 – Toll-like receptor 4

TNF- α – Tumor necrosis factor alpha

Y1 – Neuropeptide Y receptor 1

Y5 – Neuropeptide Y receptor 5

Chapter 1

Introduction

1.1 The obesity epidemic and its impact on society

Obesity is defined as abnormal or excessive fat accumulation that may impair health (1). This excessive fat accumulation is accommodated by the expansion of existing adipose tissue depots of the organism and is mostly caused by an excessive caloric intake coupled with a sedentary lifestyle (2). Obesity is associated with a variety of comorbidities and is currently a growing economic burden on the National Health Service in the United Kingdom, with a growing number of clinical resources being allocated to the treatment of the phenomenon every year. Direct costs of treating obesity and obesity related comorbidities incurred by the NHS have risen from £479.3 million in 1998 to £4.2 billion in 2007, and indirect costs have been estimated to range from £600 million to £1.4 billion in 2007 (3). Modelled projections regarding the current trend of indirect costs estimate them to rise to £27 billion in 2015 (3).

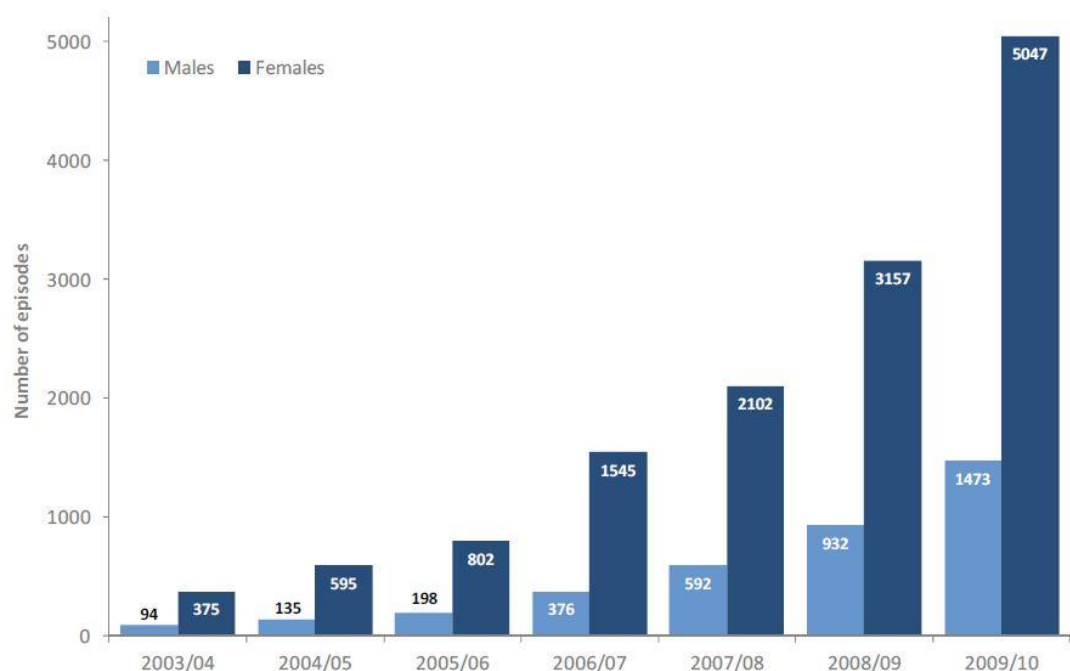


Figure 1: Number of hospital episodes for bariatric surgery in England by sex 2003/4-2009/10 (Source: (4))

As shown in Figure 1, hospital episodes for surgical interventions to facilitate weight loss, such as gastric bypass and gastric banding, have been steadily increasing every year. In the UK currently there are approximately 12.3 of such procedures per 100,000 population (4), reflecting the rising need for treatment for obesity and morbid obesity,. Added to this economic and social burden are the greater numbers of overweight individuals, which, in 2009 were estimated to account for 63% of males and 52% of females(5). In the face of the increasing prevalence of all forms of obesity, the need to tackle the disease and its co-morbidities, along with the costs associated with its treatment, are paramount.

In addition to the monetary considerations of preventing the spread of the obesity epidemic, there is the important disabling effect that the condition can have on the population, calculated in 2002 as 7% of European total Disability Adjusted Life Years (DALY, a figure used to express the quantity of time spent with obesity-related comorbidities and the years of life lost due to the disability compared to the average European lifespan(6). These data make obesity a tripartite issue, comprising of human, economic and demographic components, worthy of greater investigation and a social understanding of the disease, rather than victimisation and stigmatisation of the sufferers(5)

1.2 Obesity and comorbidities

Obesity is associated with the increased risk of numerous metabolic complications, such as insulin resistance, dyslipidaemia, hypertension, and various cancers (7–10). While insulin resistance and endothelial dysfunction are risk factors for all of these metabolic diseases the precise molecular mechanisms that may explain the associations between obesity and its co-morbidities is, as yet, poorly understood. Effective prevention and novel therapies require elucidation of the mechanisms underlying these interactions, which will be described in the following sections.

1.2.1 Cardiovascular disease and obesity

One of the most common comorbidities associated with obesity is the emergence of cardiovascular disease, more commonly arising in the forms of endothelial dysfunction in the

intima media of the blood vessel wall, which can then lead to the formation of atherosclerotic plaques (11,12), or a hypertensive circulatory state. This is observed across various ethnicities as BMI increases in the population (13), with endothelial dysfunction being correlated with visceral adiposity in various obese populations (14). The mechanisms linking obesity to endothelial dysfunction on the other hand are relatively poorly understood, despite evidence from various studies suggesting that an obese state, which leads to increased reactive oxygen species, due to hyperglycaemia and the resulting sequestration of intracellular nitric oxide (15), reduces the vessel's ability to dilate, which could then allow the dysfunction to develop into a full-fledged hypertensive state if left unchecked and allowed to progress as obesity is maintained.

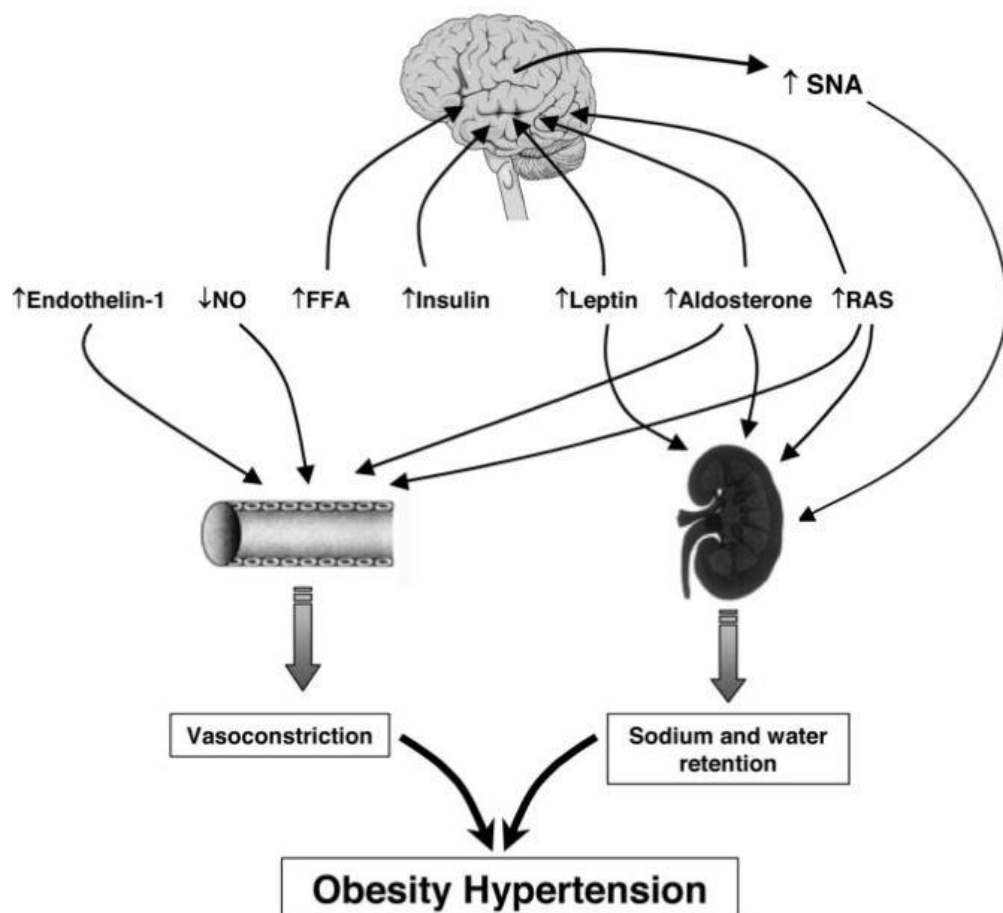


Figure 2: Mechanisms linking the obese state and hypertension (FFA = Free Fatty Acids, SNA = Sympathetic Nervous System Activity, RAS = Renin-Angiotensin System)

Another contributing change which occurs in the obese state and known to contribute to the development of obesity associated hypertension (Figure 2) is the activity of the sympathetic nervous system (SNS). SNS activity is markedly increased in both human and animal models of dietary obesity (16). It is known to affect kidney sodium and water retention capability (17), mediated through the hypothalamic action of circulating leptin levels (15). Also, higher levels of systemic insulin, which often accompany obesity, affect SNS activity (15).

1.2.2 Obstructive Sleep Apnoea (OSA) and obesity

Another common comorbidity associated with a greater body mass is obstructive sleep apnoea (OSA), an episodic and repetitive interruption of the upper airways characterised by oxygen desaturations and sleep fragmentation (18). Despite the symptoms of OSA being detected as daytime tiredness and snoring, the disease has been associated with a number of cardiovascular complications (19), heightened SNS activity (20) and even abnormalities in glucose homeostasis regulation (18,20). The mechanisms for these types of abnormalities still has to be elucidated, but SNS activity which is known to be heightened may account for the changes in blood pressure and breathing control observed in OSA patients (21).

1.2.3 Non-Alcoholic Fatty Liver Disease (NAFLD) and obesity

A high-energy dietary intake is also associated with the presence of greater amounts of saturated fatty acids (SFAs) which is metabolised by the liver. In a normal and fed state, the monosaccharides and amino acids that enter the circulation are taken up by hepatocytes and converted into fatty acid-CoA through an acetyl-CoA intermediate step. The first fatty acid products are in the saturated form and polyunsaturated fatty acids are created with modifications by desaturase enzymes (e.g. SCD1). Newly synthesized fatty acids are inserted into complex lipids, which in turn are packed into very low density lipoprotein (VLDL) particles and thus secreted (22). Impairment in any of the steps of this pathway, may it be due to oversaturation of lipid supply (23), either through the increase of intracellular reactive oxygen species generated by mitochondrial dysfunction (24), which in turn cause heightened intracellular inflammation signalling, or hyperinsulinemia triggered by greater levels of glucose

in overfeeding (25), causes a build-up of fatty acids, with histologically visible cytosolic lipid vacuoles in hepatocytes. The way these lipid droplets are accumulated can vary with genetic variance in the expression and function of droplet trafficking-associated genes, some of which are currently under study as a factor for predisposition to NAFLD (such as Liver Triglyceride Hydrolase, TGH) and that could impair liver function in the face of heightened lipogenesis (26).

This build-up of intracellular lipids then causes fibrotic injuries which are similar to the resulting damage caused in alcoholic liver disease (25), with impaired liver function and cirrhosis at later stages if left untreated. The mechanisms underlying a predisposition to the disease in an obese population are yet not fully understood, and need further study in order to elucidate the molecular mechanisms involved in NAFLD and the possible metabolic differences that could underlie the incidence of the disease in obese populations worldwide.

1.3 Obesity and insulin resistance

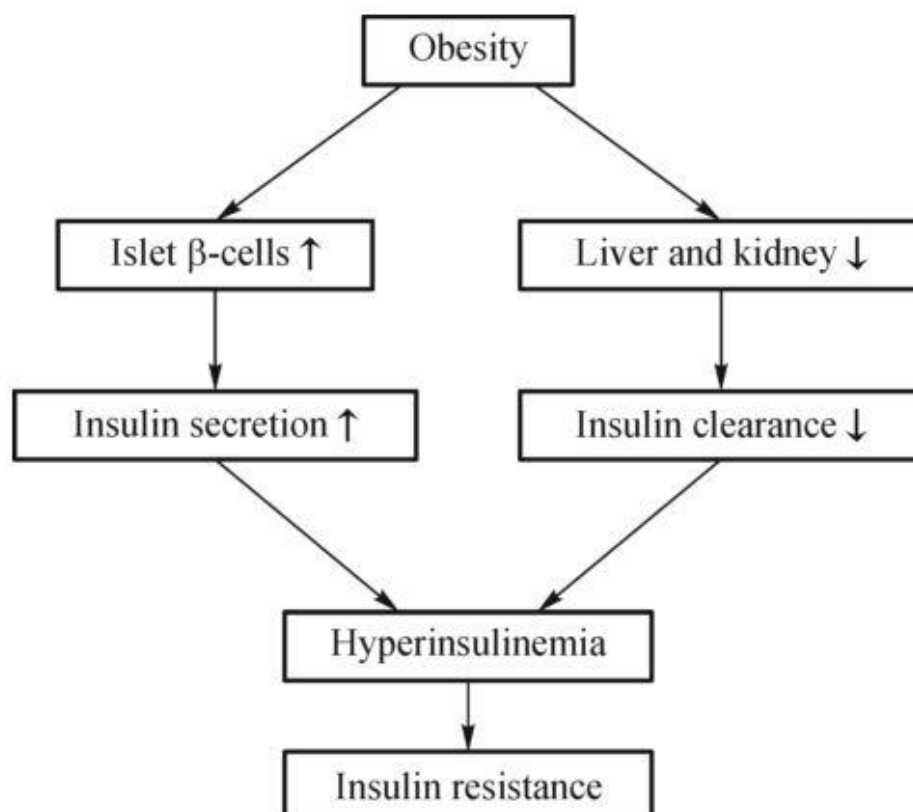


Figure 3: Hyperinsulinemia in obesity (Source: (27))

The most important and significant comorbidity associated with obesity, mainly due to its effects on the onset of other disease characteristics is insulin resistance (IR). Insulin resistance may be defined as a progressive resistance of various insulin-responsive organs in the body to the effects of circulating insulin. The current understanding of the overall mechanisms that explain insulin resistance in obesity (Figure 3), suggests that the onset of IR is preceded by increased insulin secretion by the β -cells along with lower clearance of insulin by the liver and kidneys leading to systemic hyperinsulinemia. The development of the IR may be to compensate for this hyperinsulinemia to maintain glucose homeostasis before deteriorating into frank diabetes. The cross-talk between insulin-responsive tissues is illustrated in Figure 4, where in response to glucose levels rising in the bloodstream insulin secretion is stimulated and causes uptake of glucose by the skeletal muscle and adipose tissue. High insulin levels also decrease free fatty acid (FFA) levels through inhibition of lipolysis by the adipose tissue, and decrease gluconeogenesis in the liver, as well as increasing leptin secretion by the adipose tissue. The resulting pathologies arising from the development of insulin resistance could alter the balance of this crosstalk, with a shift to rising FFA levels due to the lack of the lipolysis-inhibiting effect of insulin signalling on adipose tissue, as well as impaired control of gluconeogenesis and glucose uptake, which could ultimately lead to Type 2 diabetes mellitus as the disease progresses and this balance is altered chronically (8,28,29).

The correlation between obesity and insulin resistance has been investigated using various techniques (8,28), including oral glucose tolerance tests (OGTT) and the (8,28), the euglycaemic hyperinsulinaemic clamp, often described as the gold standard for measuring insulin sensitivity in vivo. Insulin sensitivity in humans effectively decreases by 30-40% when body weight increases past ideal levels by >35-40% (28) and the development of insulin resistance has been directly shown to occur in response to experimental overfeeding in normal weight individuals (2). Progressive exacerbation of insulin resistance to type 2 diabetes following a prolonged state of hyperinsulinemia has also been reported (8,28,30). The symptomatic manifestation of insulin resistance involves the concerted action of all of the insulin-responsive tissues (as shown in

Figure 4) in the body: skeletal muscle, the liver and adipose tissue, with varying effects at the systemic level: all of which will be briefly reviewed in the next section.

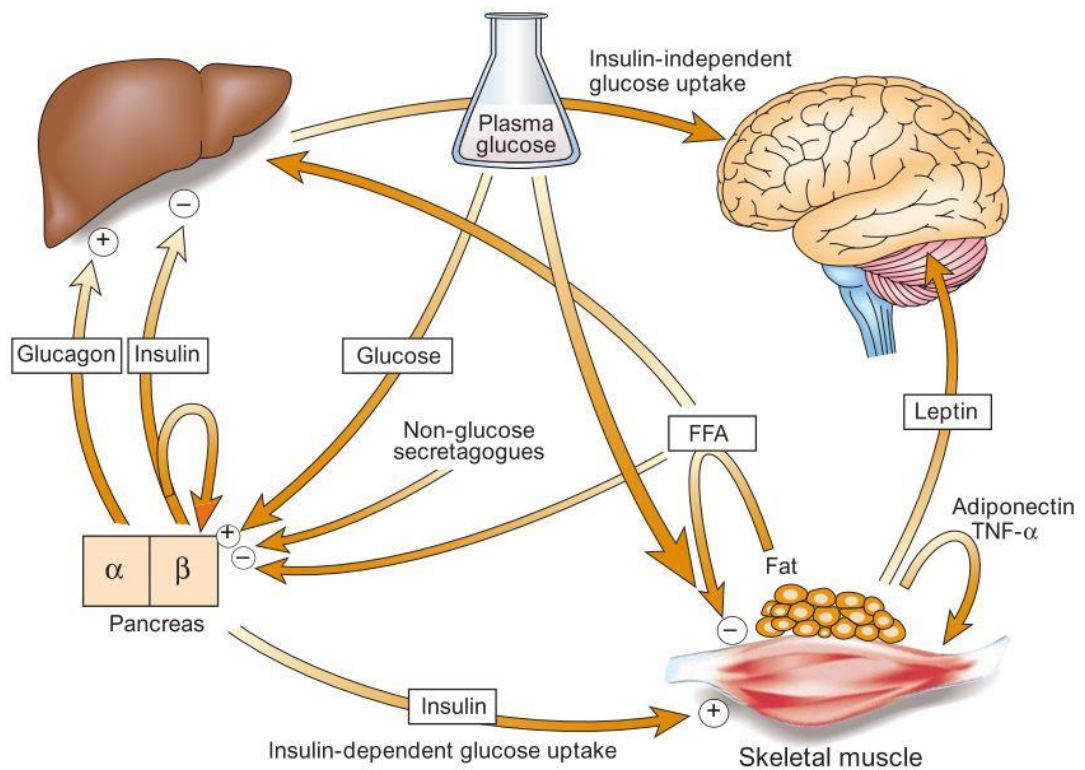


Figure 4: Crosstalk of insulin-sensitive tissues in the body (Source: (31), FFA = Free Fatty Acids)

1.3.1 Insulin resistance and skeletal muscle

The skeletal muscle has been estimated to carry out approximately 80% of total body glucose uptake in response to insulin secretion (32). In obese normal glucose tolerant patients, there is marked insulin resistance in skeletal muscle compared to lean, age- and sex-matched individuals (32). Animal, as well as, human studies have shown a direct correlation between increase in body mass and skeletal muscle insulin resistance, suggesting that skeletal muscle dysfunction may be a the primary defect in the development of insulin resistance and type 2 diabetes (32,33).

The reason for this increased insulin resistance in skeletal muscle is partially due to increased free fatty acid (FFA) levels in the circulation of obese and morbidly obese patients, as

reported previously(32,34). The reasons for the increased levels of free fatty acids in the circulation of obese patients was originally hypothesized by Randle et al. (35) to be due to the increased mass of the adipose tissue of obese individuals which in turn causes higher levels of circulating FFAs, which then interfere with glucose metabolism by overriding normal energy metabolism towards fatty acid oxidation instead of glycolysis, therefore causing build-up of glucose and worsening of insulin resistance (35,36). These fatty acids, which have been shown to increase insulin resistance after infusions in experimental models (32,33), are thought to act through the activation of inhibitory protein kinases such as JNK and Protein Kinase C which inhibit IRS-1 function in the insulin signalling pathway (32).

1.3.2 Insulin resistance and the liver

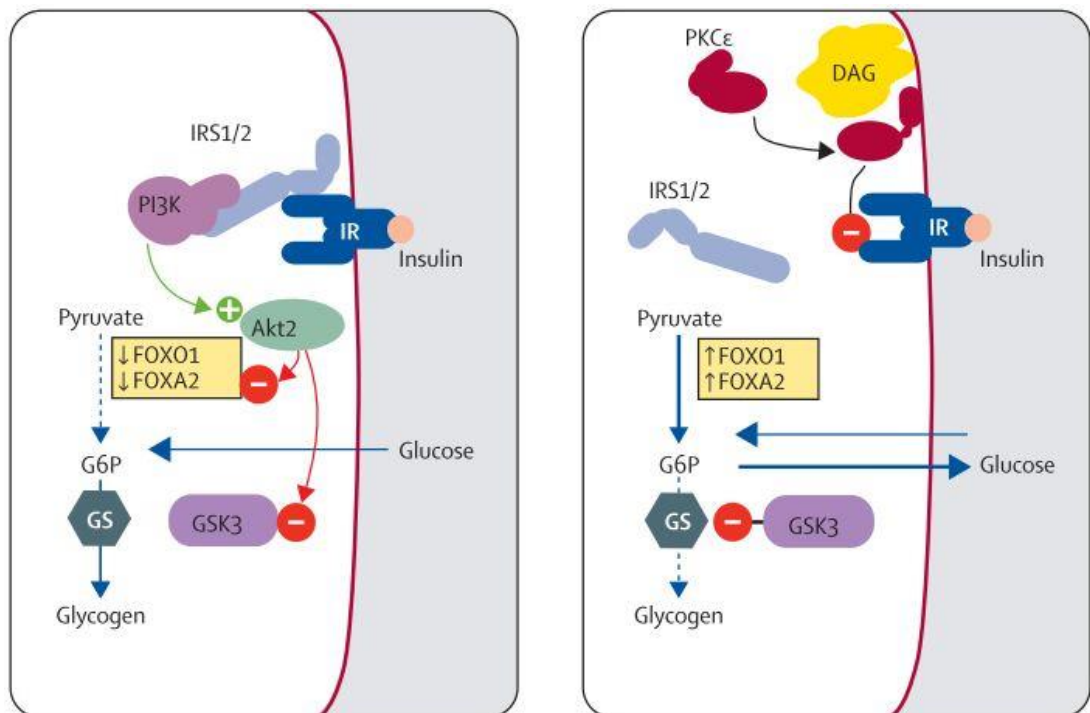


Figure 5: Insulin resistance in the liver. (Left: insulin sensitive liver. Right: Insulin resistant liver) (Source:(37))

Insulin resistance in the human liver is closely associated with raised intracellular fatty acid levels, which could allow the emergence of the previously discussed non-alcoholic fatty liver

disease, or NAFLD. This coupled with evidence of elevated hepatic lipid levels in mice with specific deletions of vital insulin-responsive genes, such as the GLUT4 glucose transporter (37), has led to the suggestion that insulin resistance in obesity could be the main cause of NAFLD, through impaired signalling of the insulin receptor by protein kinase C activation (as shown in Figure 5) by free fatty acids (specifically diacylglycerols) associated with heightened caloric intake during obesity (37,38). This in turn is exacerbated by the heightened levels of circulating glucose which are then thought to be converted into a greater amount of fatty acids by the liver through de novo lipogenesis, which in turn further increases insulin resistance in the organ itself (39). This is shown by studies illustrating the activation by insulin of SREBP-1c, a transcription factor responsible for the activation of lipogenesis genes (37,38). The activity of this gene will be discussed later in this introduction.

Since the liver is considered a very important organ in IR, changing levels of liver enzymes involved in lipid metabolism which occur due to the modulation of intracellular signalling, specifically in enzymes like alanine aminotransferase (ALT) are being proposed as part of metabolic syndrome due to their readily detectable changes in a clinical setting, as well as direct analysis of the ratio of circulating fatty types as an indicator of fatty acid accumulation in the liver (40) for indication of liver insulin resistance and cardiometabolic syndrome onset in obesity and morbid obesity.

1.4 Insulin resistance and the adipose tissue

1.4.1 Adipose tissue: an endocrine organ

Being directly involved with its expansion in the onset and exacerbation of obesity in response to overfeeding, and the main organ involved in long term energy storage, the adipose tissue is seen as a central player in the onset of the various comorbidities associated with obesity itself (41). It is also recognized as being an important participant in the metabolism and homeostasis of glucose levels in the body (42), as well as an extremely diverse and important secretory organ, secreting a wide array of adipokines such as leptin, IL-6, adiponectin, MCP-1 and TNF- α (See Figure 6). These are known to have effects at the local tissue and systemic levels

(43). The biological activity and systemic effects of these adipokines have been extensively reviewed in various publications (41,43–45).

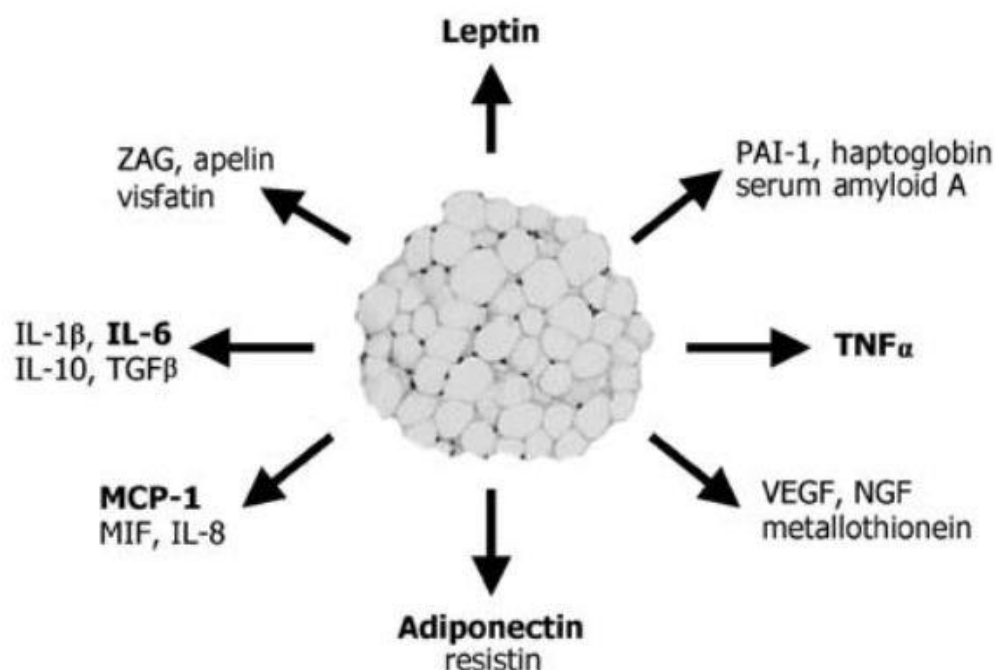


Figure 6: Adipose tissue adipokines (Source:(44))

The anatomical location of the adipose tissue and its expansion in different parts of the body can alter the secretory profile of these adipokines, with visceral depots having a more pro-inflammatory secretory profile in humans (41), and are able to modulate the function of immune system cells such as T-cells at a local and systemic level (46). The expansion of this depot specifically in the obese state is thought to promote greater metabolic risk in humans (43). Nevertheless, its central role as a secretory organ and metabolic hub of energy expenditure makes it a vital organ for the study of insulin resistance in obesity.

1.4.2 Adipose tissue remodelling and insulin resistance in obesity: Hypertrophy vs. hyperplasia

Adipose tissue undergoes expansion during excessive caloric intake, leading to its necessary remodelling. It has been hypothesized that impairments in the ability of the adipose tissue to generate new cells through differentiation of pre-adipocytes in the process of adipogenesis (hyperplasia) could be linked to the development of insulin resistance and diabetes mellitus (43), and that the enlargement of adipocytes associated with excess caloric intake (hypertrophy) is

correlated with necrosis of the adipocytes themselves, a heightened local inflammatory state and the recruitment of monocytes of the immune system as a response (47,48).

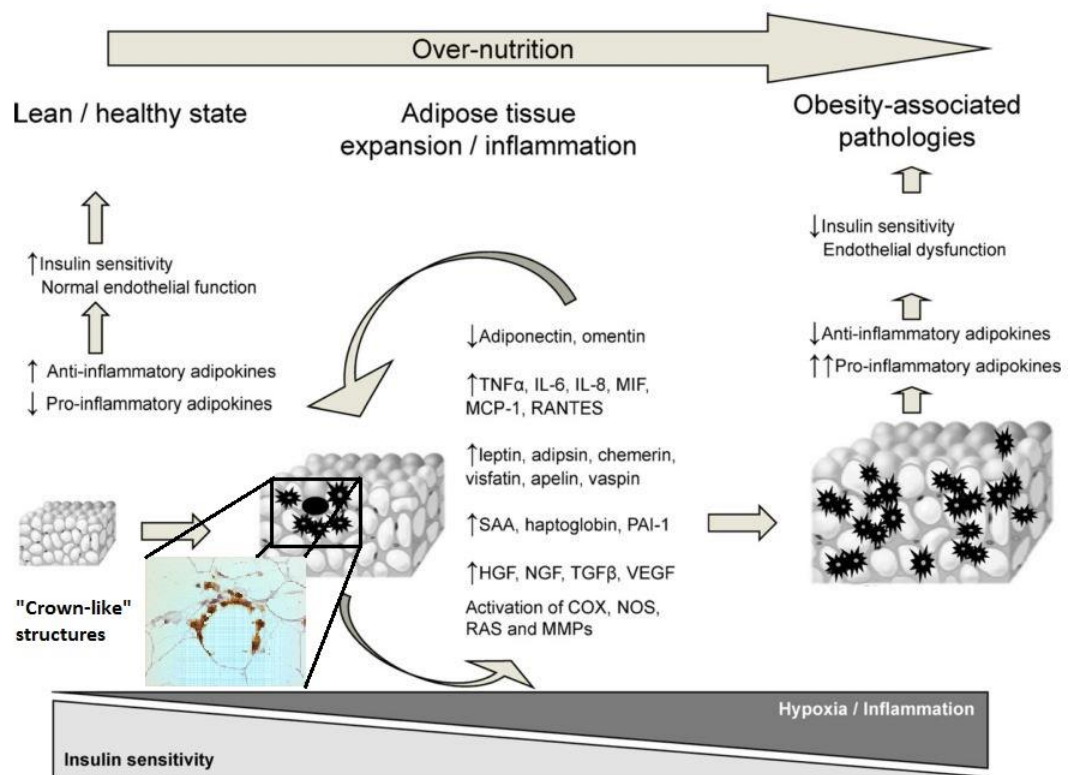


Figure 7: Adipose tissue hypertrophy and its local effects in obesity (Source: adapted from (43)) Note: black "dots" represent infiltrated monocytes in the adipose tissue

The evidence showing that adipocyte inflammation signalling caused by the presence of macrophages in the adipose tissue is linked to insulin resistance (49) has led to a proposed model for the change of adipose tissue function as a response to over nutrition is illustrated in Figure 7, where in a lean, healthy state adipose tissue is insulin sensitive, with a secretory balance focused towards a less inflammatory profile. In the occurrence of over nutrition and forced adipose tissue expansion, the hypertrophied adipocyte shifts its secretory balance towards a more inflammatory profile, with less anti-inflammatory adipokines like adiponectin secreted and more inflammatory cytokines such as interleukin-6 (IL-6) and Monocyte Chemotactic Protein 1 (MCP-1) being more readily secreted and present at a local level. This

causes the recruitment of adipose tissue macrophages which in turn focus around necrotic adipocytes (48) and cause yet more heightened inflammation.

This can lead to escalation in insulin resistance, endothelial dysfunction, hypoxia and inflammation in the adipose tissue as the number of tissue macrophages and hypertrophied adipocytes increase. The mechanisms through which the macrophages are initially recruited are thought to be various: The macrophages are hypothesized to respond to the presence of necrotic adipocytes in the adipose tissue due to increased hypoxia after adipocyte hypertrophy, to the presence of increased local levels of FFAs that may “leak” from hypertrophic adipocytes due to their efficiency limitations in the re-esterification process after lipolysis during fasting states.

These are thought to activate and polarize inflammation levels of macrophages through toll-like receptor 4 (TLR4) activation (49,50), in a phenomenon recently dubbed as “metaflammation” (51), which is also thought to be a primer for the increased inflammation levels and macrophage recruitment seen in dysfunctional adipose tissue.

Metaflammation may also be a result of endoplasmic reticulum (ER) stress, a phenomenon that occurs when the endoplasmic reticulum, in which all the secretory and membrane proteins are assembled into their secondary and tertiary structures, and where unfolded or mis-folded proteins are detected, removed and degraded by the 26S proteasome system (52) is subjected to an overload of unfolded proteins which results in the activation of an Unfolded Protein Response (UPR) to preserve ER function. This response, which can also occur due to metabolic overload in adipocytes and can be observed experimentally (53) by drug-induced impairment of ER function which mainly occurs through signalling pathways that inhibit insulin signalling such as the NF- κ B pathway (52,54), and promote an autophagic response, which if impaired (as can be seen in obesity (55)), may result in necrotic adipocyte death. Studies in mice show increased ER stress gene expression in diet-induced obesity, and the resulting inflammatory pathway activation in adipocytes (56), therefore suggesting a role for ER stress in insulin resistance and adipose tissue dysfunction.

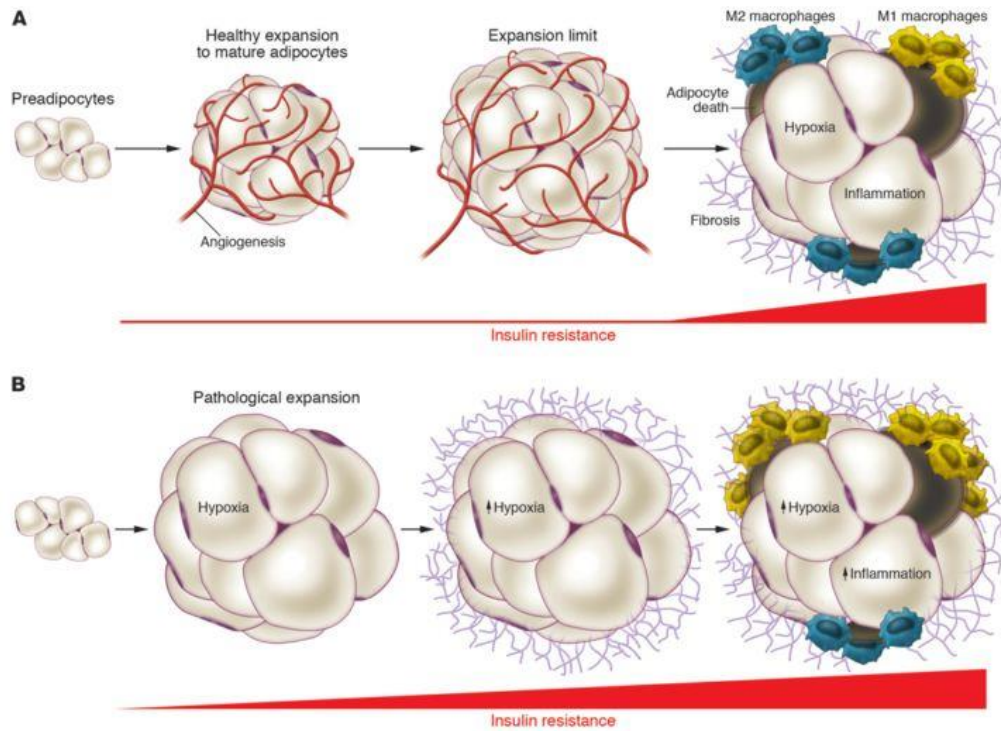


Figure 8: Adipose tissue remodelling in obesity (A: "healthy" expansion B: "pathological" expansion) (Source: (50))

The imbalance between adipocyte hypertrophy and hyperplasia, and the impairment in adipocyte turnover rate (57) favouring hypertrophy over hyperplasia (58) in the tissue has been implicated in the development of insulin resistance and a pathological development of obesity related comorbidities. This proposed dichotomy between "healthy" and "pathological" adipose tissue expansion (As shown in Figure 8), with the recruitment of new adipocytes and resulting beneficial angiogenesis is thought to be a central focus of the maintenance of insulin sensitivity, as opposed to the pathological expansion of the tissue involving adipocyte hypertrophy and poor remodelling of the tissue as a result of this (50).

The mechanistic cause for the choice of hypertrophy over hyperplasia in pathological adipose tissue expansion is still unknown. Although animal studies have suggested that factors such as macrophage recruitment into the adipose tissue, as occurs temporarily after significant weight loss, as well as the effect of lipolysis-inducing drugs such as β -adrenergic receptor

agonists in mice (50), the real mechanisms behind the choice of the adipose tissue to expand its existing adipocyte population rather than recruit new ones through adipogenesis from its pre-adipocyte population still remains unclear. The beneficial effects seen in the use of PPAR- γ (a nuclear receptor that has a major role in adipogenesis gene regulating) agonist drug family, the thiazolidinediones, in the treatment of insulin resistance could also show the importance of hyperplasia over hypertrophy (59).

As also referred to by Figure 8, the recruitment of specific types of macrophages in the two different models for adipose tissue expansion, an already extensively observed phenomenon (60) could be an important aspect to consider when observing the different ways the tissue can expand, including a pathological expansion type.

Macrophage polarity in tissue remodelling, namely looking at subtypes of the cells which can be observed according to activation state (61). M1 (a more pro-inflammatory form of macrophage, actively secreting pro-inflammatory cytokines and antigen-presenting molecules) and M2 macrophages (a less inflammatory subtype which is associated more closely with tissue remodelling), is an aspect which is being extensively explored and characterised in adipose tissue as well. There are interesting results associated with activation states such as the association of more pro-inflammatory M1 macrophages with a hypoxic state of the adipose tissue (62), and the alteration of the more anti-inflammatory M2 macrophage phenotype following adipocyte necrosis (63).

The mechanisms behind the shifts in polarity are still being characterised, with the aforementioned hypoxic state, the necrosis of surrounding adipocytes and a specific lipid profile also being explored as a possible contributing factor (64) to polarity shifts, which could be correlated to the inflammatory differences observed in adipose tissue between the insulin resistant state and the healthy state of obesity.

Another aspect that has also been explored is the difference in angiogenic potential of the tissue itself, which has already been shown to be different between adipose tissue depots (50). Whether impaired angiogenesis could be a rate-limiting step in the expansion of the adipose

tissue or there may be “improper” vascularization of the adipose tissue occurring, as suggested by evidence showing omental adipose tissue in humans to have higher vascularization but more hypoxia (50), is still being investigated . Since there is direct evidence that hypoxia causes an increase in pro-inflammatory adipokine secretion, this is an important factor to consider when exploring adipose tissue remodelling (65). Nevertheless, the resulting insulin resistance caused by the improper function of the adipose tissue during obesity makes adipose tissue an important player in the development of obesity related comorbidities and the study of adipose tissue dynamics in obesity can give extraordinary insight to the metabolic problems arising from obesity and insulin resistance.

1.4.3 FFA and insulin resistance in adipose tissue

Obesity in humans is characterized by a greater amount of FFAs in the circulation (59), and the presence of heightened levels of FFAs as well as an impaired glucose metabolism in lean, healthy individuals with family histories of type-2 diabetes (59) suggests that there could be a vital role of FFAs in the development of insulin resistance. Their effects on skeletal muscle and liver insulin resistance have been discussed earlier in this report, and being the main long-term storage source of FFAs, the adipose tissue in this case yet again plays a central role.

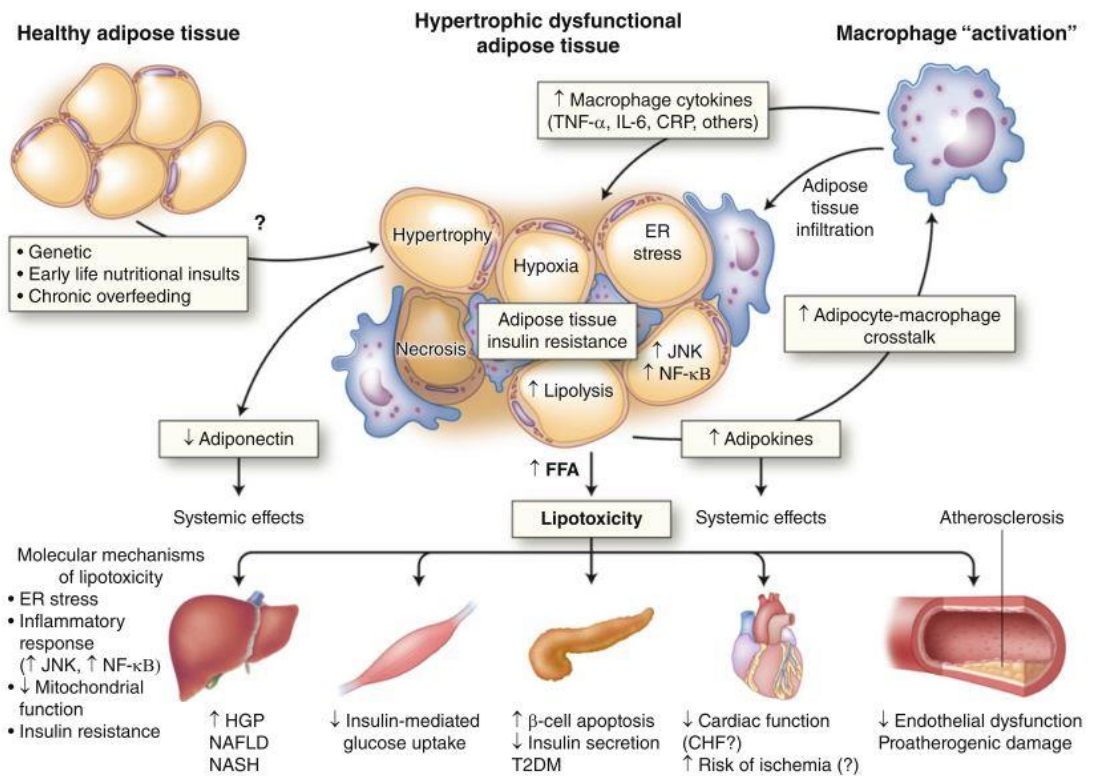


Figure 9: Role of lipotoxicity via adipose tissue FFAs in obesity (Source: (59))

The central role of FFAs in the development of insulin resistance (see Figure 9), again points to a pivotal role for adipose tissue, mediated by adipocyte hypertrophy, ER stress, necrosis and inflammatory signalling pathway activation leading to a change in the secretory profile of adipokines from less anti-inflammatory to more pro-inflammatory. Additionally, the development of resistance to the anti-lipolytic effects of insulin signalling causing heightened levels of local FFAs could also exacerbate macrophage infiltration due to TLR4 signalling activation (66). This in turn could exacerbate insulin resistance, causing a further increase of systemic FFA levels that are shown to affect other insulin-sensitive organs of the body, changing them to a more insulin-resistant state.

Therefore, an imbalance in the lipolytic potential of the adipose tissue could give rise to insulin resistance from a metabolic point of view, and not just that of an inflammatory phenomenon as the initial trigger for adipose tissue insulin resistance. Since the activity and regulation of fatty acid desaturase enzymes such as Stearyl-CoA-desaturase 1 (SCD1) that

convert saturated free fatty acids (SFA) to mono-unsaturated fatty acids (MUFA) in adipose tissue which are known to be less inflammatory (59,66,67) has also been associated with insulin signalling (67), the metabolic component of adipose tissue dysfunction becomes an extremely important aspect of obesity and the development of obesity related comorbidities.

1.4.4 Obesity or metabolism? The need to explore the heterogeneity of obesity

The dynamics and mechanisms of adipose tissue remodelling and dysfunction, inflammation, hypoxia and lipotoxicity in obesity have been explored mainly by comparing the adipose tissue from healthy, lean individuals to that of obese subjects, as the natural progression into the obese state via excess energy intake. The arising heterogeneity in insulin sensitivity (68) that have been observed in various obese and morbidly obese populations may point to the fact that metabolic syndrome is not a direct and inevitable consequence of excess energy intake, and that there are individuals that maintain a normal metabolic profile regardless of their morbid obese state (69). This could give precious insight not only into the subtle mechanisms that may come into play in the obese individual but also in lean, insulin resistant individuals and in the metabolism as a whole.

1.5 Heterogeneity of insulin resistance

1.5.1 Metabolically Healthy Obese (MHO) individuals

The importance of insulin resistance as a driving factor for the onset of obesity related comorbidities is significant, as previously described in section 1.4. However, the incidence of insulin resistance among obese and morbidly obese individuals is variable in different population groups (68) and groups of individuals, regardless of their obese or morbidly obese status that exhibit normal insulin responsiveness is apparent (69–72). These individuals, the “Metabolically Healthy Obese” (MHO), despite their obese state have favourable metabolic profiles with normal insulin responsiveness, lipid and inflammatory profiles and are normotensive. Conversely the majority of obese and morbidly obese individuals that develop

unfavourable metabolic profiles, insulin resistance and comorbidities have been referred to as the “pathologically obese” (PO) (69). A summary of MHO characteristics reported in various studies are shown in Figure 10.

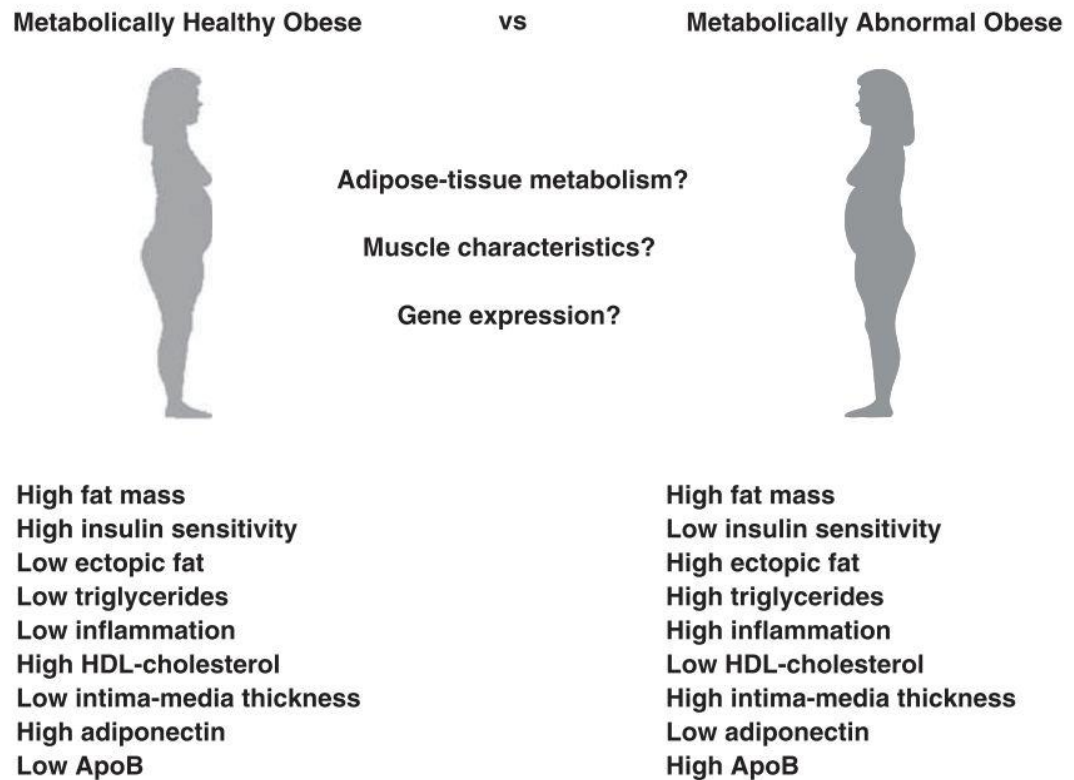


Figure 10: Profiles of MHO vs. MAO (PO) patients (Source: (73))

The reported prevalence of MHO depends, at least in part, on the stringency of the criteria used to describe the phenotype and varies from 10-40% (73). Even so, the evidence that there is such a phenotype, in diverse age ranges from 20 to 80 years suggests that the metabolic changes and this dichotomy is present, albeit changed in its proportions, in many populations that have been studied (74).

There is yet a consensus to be found as to how to characterize these individuals in patient populations, especially with respect to relevant diagnostic techniques and biomarkers. One reason for these discrepancies is that the gold-standard technique for the determination of insulin resistance, the euglycaemic-hyperinsulinaemic clamp, is too invasive, expensive and time

consuming a procedure to be considered for routine use in a clinical context, therefore increasing the need for finding easier, less invasive methods and biomarkers for characterizing the phenotype(73), especially since the incidence of these individuals may vary according to the criteria used to select them (75). Nevertheless, the overlapping criteria amongst most research groups studying the phenomenon are fasting plasma glucose and insulin levels, HOMA-IR index, and lipid profiles such a cholesterol and triglyceride levels (73). Using these criteria it is apparent that this metabolic heterogeneity is still present within the obese populations.

1.5.2 Implications of MHO individuals in the clinical setting

The acceptance of the existence of the MHO phenotype comes with practical consequences to clinical care. Is there such a thing as a metabolically healthy obese individual? Can he/she be described as healthy despite the obese state being described as sub-optimal to health? Is it worth treating these individuals in the same way as the other types of obese patients? The phenomenon is creating varying opinions with respect to treatment (76,77) from a practical perspective, but the general consensus about these assessments is that the lack of a common definition undermines the practical aspects of clinical care for these patients, especially with a lack of detailed longitudinal studies in exploring the long term effects of treatment in the MHO versus the PO.

The evidence of improvement in weight loss with respect to diet and exercise therapy on insulin sensitivity is apparent (77), and studies have shown that exercise alone can improve insulin signalling and sensitivity in the tissues involved (78). However, data on the effectiveness of exercise and diet for improving insulin sensitivity in MHO individuals is scarce. There are studies that show an increase in insulin sensitivity after weight loss in PO individuals, as opposed to a slight worsening of insulin resistance in the MHO population, showing that specific differences must be taken into account with respect to treatment for these individuals (79)., Another study by Shin et al. showed an improvement in inflammatory markers and lipid profiles of MHO women after weight loss, proving diet restrictions to be more effective in MHO women than PO women (80). Karelis et al. (81) showed that dietary/calorie restriction mediated weight

loss in MHO women led to a more unfavourable insulin resistance profile than with at-risk individuals. A positive change in insulin sensitivity and cardio metabolic risk factors was observed in Janizewski et al. (82) for both MHO men and women as opposed to previous findings after weight loss through diet or exercise. However, with only these few studies outlining the dynamics of weight loss in these MHO individuals it is not enough to come to a decision as to what is the most effective treatment for them (83). Therefore additional research needs to be carried out in order to see the differences with larger patient groups and with more follow-up data to prove whether weight loss is the most effective means to manage the continued status of MHO individuals and prevent worsening of the metabolic profile.

Surgically assisted weight loss has become one of the most effective ways of managing morbid obese patients in the developed world, and bariatric surgeries have been steadily increasing in the UK to about 6520 per year for both men and women (4). The proof of its effectiveness at 'treating' type 2 diabetes in morbidly obese populations is documented (84), as well as reducing overall mortality in morbidly obese patients (85,86). Its effectiveness at improving an MHO metabolic profile is much less studied: with only a single study reporting 6 month follow-up information regarding an MHO/PO population of morbidly obese patients carried out by Sesti et al. (87). This study showed that regardless of insulin sensitivity, which was supposedly better in the MHO individuals to begin with, the MHO subgroup of morbidly obese patients showed a significant weight loss and improvement in cardio metabolic risk markers compared to before gastric banding. At the same time, recent developments from the Swedish Obesity Study (SOS) in which 2,010 morbidly obese patients undergoing bariatric surgery were matched up to an equal population of patients receiving standard medical care, and the results indeed showed a reduced prevalence of cardio-metabolic abnormalities, although it was recognized that surgical benefits of bariatric surgery did not correlate with baseline BMI or post-operative weight loss, and the only predictive factor for cardiovascular events was fasting insulin levels suggesting that insulin resistance, and not obesity, being important for the development of cardiovascular comorbidity (88). Also, recent data from the American NHANES III study has

shown that despite the lack of a common definition for metabolically healthy obesity, by looking at commonly used diagnostic criteria for MHO status used more frequently, the varying MHO population still did not seem to exhibit the same all-cause mortality risk as the remaining unhealthy obese patients (89).

Therefore, the conclusion that can be drawn from these human studies is that healthy metabolic profiles, even in the morbidly obese, have less immediate benefit to gain from bariatric surgery than insulin resistant ones, and this could be a very solid reason to discern MHO patients from PO patients in a clinical context, in order to decide different therapeutic approaches for the two groups by also looking at how this group of patients avoid metabolic abnormalities across various BMI and age ranges. The varying evidence from this field of study is also a clear signal that more is needed to understand the phenomenon and learn from the different metabolic profiles of the patients in order to target specific mechanistic differences involved in the onset of the PO phenotype.

1.6 Mechanistic causes for MHO vs. PO differences

1.6.1 Adipokine profile differences

The differences in the secretory profile of adipose tissue with respect to its expansion could suggest an inherent difference in the levels of specific circulating adipokines such as resistin (associated with increased insulin resistance), adiponectin (known to be an endogenous insulin sensitizer) and TNF- α (associated with insulin resistance), all of which have been seen to be altered in the presence of insulin resistance in humans (90). Since these and other adipokines, like IL-6, all have autocrine and paracrine effects on glucose metabolism, lipolysis and insulin sensitivity (43) they could be different between MHO and PO in their levels and effects on insulin resistance and local inflammation. A difference in secretion levels of these adipokines could also be used as a biomarker for the onset of insulin resistance and the metabolic syndrome, which makes quantification of these adipokines and their metabolic effects important. Ratios of adiponectin to HOMA-IR index have already been used as a predictive tool for metabolic

syndrome in humans (91), and adipokine levels have been observed during weight loss (92), making the need for a biomarker that could distinguish MHO/PO patients important.

1.6.2 Inhibition of Adipogenesis

The possible mechanisms for the differences between the MHO and PO phenotype are being explored at the molecular level. Adipocyte hypertrophy has been reported in the subcutaneous adipose tissue of human patients as being predictive for type 2 diabetes (93). Similarly adipocyte hypertrophy has been shown in certain ethnic groups such as Pima Indians (58) and South Asian populations more prone to insulin resistance (94). Also hypertrophied, older adipocytes had been associated with insulin resistance and adipogenesis-associated genes are more poorly expressed in the adipose tissue of type-2 diabetic compared to non-diabetics (95,96). This inhibition of adipogenesis in insulin resistant adipose tissue is worthy of further exploration.

However data from various studies are inconclusive: some confirm the hypothesis that MHO patients have smaller adipocytes in various depots (yet with the omental being the only depot to be significantly correlated to the metabolic syndrome (97)), with lower expression of adipogenesis-inhibiting genes such as preadipocyte-factor 1 (PREF-1) in MHO patients. These data suggest an inhibition of adipogenesis in PO adipose tissue (98). Other studies point towards smaller adipocytes in both depots, despite impaired adipogenesis, as the possible cause of the difference between MHO and PO individuals. The emergence of studies also pointing towards lower PPAR γ expression in adipocytes either caused by inflammatory cytokines (99), or even xenobiotic molecules present in western diets such as naringenin (100) shows that a variety of factors can affect healthy adipocyte turnover and that the exploration of this difference is important to understanding metabolic variability. Also, an association between smaller adipocyte size and heightened local inflammatory signalling has been observed in some studies (101,102). This is contrary to the suggestion that inhibition of adipogenesis, adipocyte hypertrophy and necrosis could lead to local inflammation (48). These differences in data could arise from the different criteria used to select patients for the two groups, MHO and PO, therefore making the need for a common definition ever more important.

1.6.3 Dysfunction in the regulation of SREBP Proteins and the lipogenic/lipid homeostasis pathway

Lipogenesis and cholesterol homeostasis stimulated by insulin signalling in adipose tissue appears to be mediated by the transcription factor Sterol Regulatory Element-binding Protein 1-c (SREBP-1c) (103). This factor is a member of a family of three transcription factors, with the most prevalent one in adipose tissue being SREBP-1c. The SREBP-1c transcription factor is responsible for transcriptional activation of the entire monounsaturated fatty acid synthesis pathway (103), and is also activated during the adipocyte differentiation process (104). The regulation of SREBP-1c is complex and involves steps at the transcriptional and post-translational levels with initial transcripts encoding a membrane-bound precursor protein kept anchored to the endoplasmic reticulum via Insig proteins. When sterol depletion ensues the Insig proteins dissociate from SREBPs, allowing them to translocate to the Golgi apparatus where they are cleaved by proteases, and the N-terminal fragment of the SREBP is cleaved from the membrane and can finally translocate to the nucleus to regulate gene transcription (105), which involves several genes involved in fatty acid metabolism (see Figure 11). Regulation of SREBP levels by insulin signalling is supported by various pieces of evidence. Rat hepatocytes express higher levels of SREBP-1c after insulin treatment, as well as decreasing SREBP-1c levels after streptozotocin-induced diabetes in rat hepatocytes (106). Insulin also induces liver X receptor which in turn is known to activate SREBP-1c transcription (107), therefore linking insulin and insulin resistance to the possibility of improper lipid homeostasis, specifically with cholesterol levels (108).

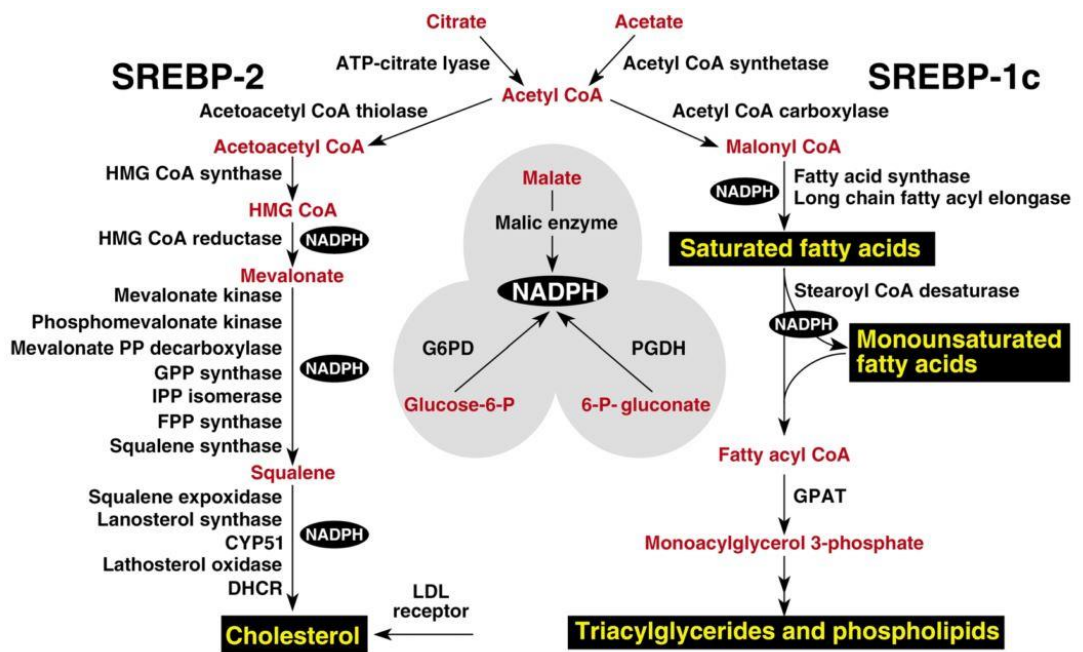


Figure 11: Genes regulated by SREBP activity in cholesterol and fatty acid synthesis pathways (Source:(105))

The discovery that dietary fatty acids such as ω -3 and ω -6 polyunsaturated fatty acids (PUFAs) are responsible for the down-regulation of the SREBP transcription factors in mouse livers (109), as well as the evidence showing that overexpression of SREBP-1c in mouse white adipose tissue led to an insulin-resistant phenotype of hypertrophied adipocytes in the adipose tissue of mice (110) suggest that a possible difference in metabolic regulation of lipid homeostasis maybe due to diet or genetic factors, leading to adipocyte hypertrophy due to excess lipid accumulation, and inhibition of adipogenesis by SREBPs as well as its target lipid metabolism genes like SCD1.

1.6.4 The need for a biomarker

As previously mentioned, studying and gaining an understanding of the differences in the local functioning of the adipose tissue can also be useful for determining a viable and detectable biomarker for the recognition of specific metabolic profiles. Despite the previous studies cited, there is still a difference in opinions as to whether the actual use of high molecular weight adiponectin or other adipokines such as C-reactive protein can give an indication of metabolic

status (111). Other types of biomarker types, namely neurotransmitters like epinephrine (112), are under study for their effects on the function of the adipose tissue and will be discussed in the next section of this thesis, or specific circulating serum microRNA types (113) which have been observed to be altered during the onset of insulin resistance and type 2 diabetes (114), and of which the signalling properties are only just being explored in these past years. Once a common definition for MHO is agreed upon and a common biomarker found, the process of discrimination could allow for a more stratified and accurate approach to the clinical treatment of obesity.

1.7 Sympathetic nervous system activity and metabolism

1.7.1 The sympathetic nervous system in breathing and blood pressure control

Blood pressure (BP) in humans is regulated by two concerting factors: vascular resistance and cardiac output. Both are directly controlled by the autonomic nervous system through specific mechanisms which not only determine the initial “set point” for basal pressure levels but also react to changes in the external environment that require homeostatic regulation (115). One of the most studied parts of the autonomic nervous system, specifically due to its activity regarding the regulation of blood pressure and its relevance in hypertension is the sympathetic portion, the SNS (116). The SNS controls the level of blood pressure in the body via three main types of neurons activated by different stimuli, barosensitive, thermosensitive and glucosensitive, which innervate the circulatory system, the heart, the kidneys and the adrenal medulla. Barosensitive sympathetic neurons are under the control of arterial baroreceptors in the carotid body. This large group of neurons is chiefly responsible for both short-term and long-term BP regulation and its level of activity at rest is thought to be the most important parameter for long-term BP control (116).

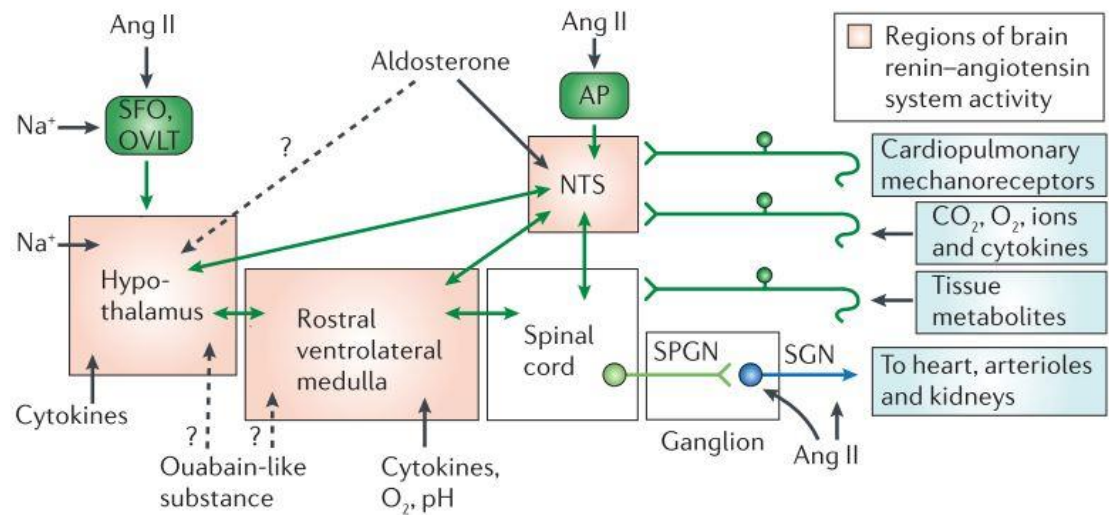


Figure 12: Sympathetic control of BP in humans.

Black arrows indicate external factors, green arrows interactions in the network. SFO = Sufornical organ OVLT = organum vasculosum lamina terminalis NTS = nucleus tractus solitarius AP = area postrema Ang II = Angiotensin II SPGN = sympathetic pre-ganglionic neuron SGN = sympathetic ganglionic neuron (Source: (116))

The core sympathetic network responsible for BP control in the human body is summarized in Figure 12, which comprises of three main neural control networks (all responsive to various types of circulating hormones): the Hypothalamus, the Nucleus of the Solitary Tract (NTS) and the Rostral Ventrolateral Medulla (RVLM). These are responsible for relaying external inputs (mainly from the renin—angiotensin system which will be discussed later in this introduction) and responding via the spinal cord ganglionic neurons in eliciting the change in blood pressure via the control of heart rate, vascular contraction or sodium retention by the kidneys (115,116). Elevated SNS activity concerted with hypertension has been observed as a common occurrence for decades (117), and dysfunction in sympathetic tone appears to be caused by other obesity-related comorbidities such as obstructive sleep apnoea (21). This correlation between sympathetic nervous system activity, obesity and hypertension makes the study of how brain stem control mechanisms in general are affected in the obese state, and the onset of obesity-related comorbidities extremely important.

1.7.2 The sympathetic nervous system and adipose tissue

Adipose tissue is innervated by the sympathetic nervous system, which is responsible for the stimulation of lipolysis in the tissue during fasting and exercise conditions (118,119). The presence of sympathetic neuron fibres in adipose tissue has been observed histologically and via in situ hybridisation for quite some time (120), and the main neurotransmitters responsible for lipolysis stimulation, namely adrenaline and noradrenaline (NA), have effects on adipose tissue lipolysis via adrenoceptors present on adipocytes (121).

The lipolytic pathway is mediated by the expression of these adrenoceptors as previously shown by studies carried out by Langin and Lafontan (118), with β_2 adrenoceptors being the lipolytic mediator of noradrenaline signalling whereas α_2 adrenoceptors act in an anti-lipolytic fashion.

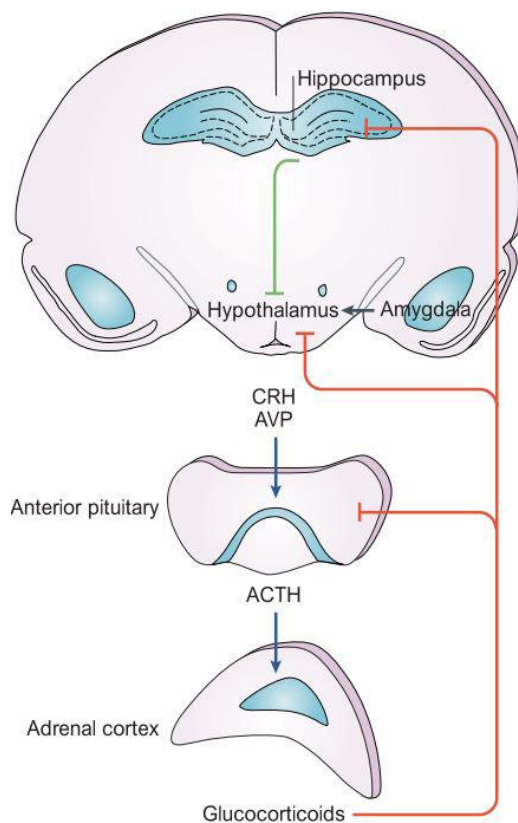


Figure 13: The HPA axis. CRH = Corticotropin releasing hormone, AVP= Vasopressin, ACTH = Adrenocorticotrophic hormone (Source: (122))

The presence of sympathetic neurons also appears to co-localise with other neuropeptides in the adipose tissue, such as neuropeptide Y. The correlation between SNS activity and

metabolic function observed through the innervation and the activity of the SNS during the stimulation of lipolysis leads to many questions regarding a possible link between stressors, metabolism and the Hypothalamic-Pituitary-Adrenal (HPA) axis, shown in Figure 13.

The reason why these questions make the HPA axis so important is due to its differential function in obesity and visceral obesity (123–125), and its direct link with gluconeogenesis mediated by the liver (126), which could be altered by chronic stress levels and other mediators of chronic SNS activity in stress, such as neuropeptide Y.

The HPA axis is the main endocrine pathway responsible for the stress response consisting of CRH release from the hypothalamus, which in turn causes ACTH release from the pituitary and ultimately the release of glucocorticoids from the adrenal cortex. Since glucocorticoids affect adipose tissue as mediators of lipolysis via the activation of lipolytic enzyme activity such as Lipoprotein Lipase (LPL) (127), levels of circulating glucocorticoids (and other mediators of stress and SNS activity) mediated by chronic stress are a link between the HPA axis, metabolism and the obese state. Therefore circulating glucocorticoids could be important in the understanding of metabolic differences between individuals in an obese or morbidly obese population.

1.7.3 Direct effectors of the SNS: catecholamines and adrenoceptors

Catecholamines such as noradrenaline are the neurotransmitters of the SNS. The synthesis of these catecholamines are carried out by a number of enzymes such as tyrosine hydroxylase (TH) in SNS neurons which can be histologically stained to reveal innervation in tissues, including adipose tissue (128,129).

The effects of catecholamines on adipose tissue lipolysis has been extensively studied, especially in WAT (130). The signalling pathway involved in the regulation of lipolysis is summarised in Figure 14.

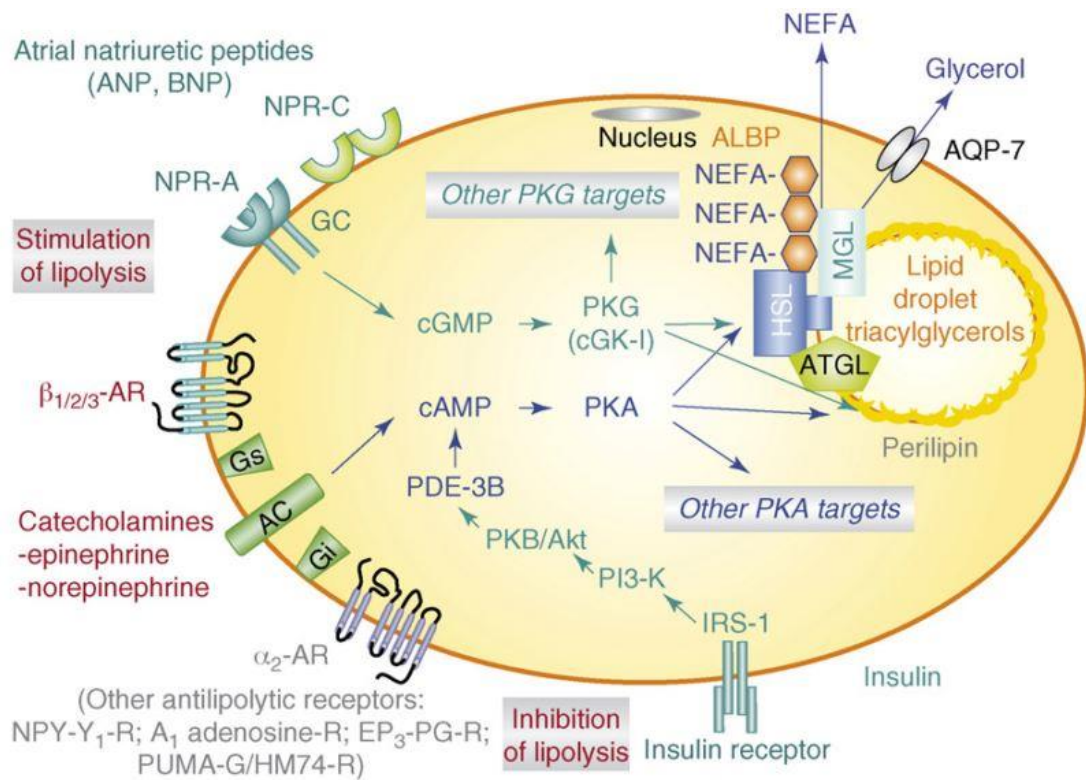


Figure 14: lipolysis pathway.

AC = adenylyl cyclase, cAMP = cyclic AMP, PKA = protein kinase A, HSL = hormone-sensitive lipase, TG = triglyceride, DG = diglyceride, MG = monoglyceride, AMPK = 5' AMP activated protein kinase, ATGL = adipose triglyceride lipase (Source: (131))

Noradrenaline binds to the β -adrenoceptors of the adipocyte through the activation of the G-protein coupled receptors responsible for adenylyl cyclase activation, resulting in a build-up of cytosolic cyclic AMP and the resulting activation of protein kinase A, which in turn phosphorylates hormone-sensitive lipase (HSL) activating the enzyme responsible for triglyceride breakdown, which results in the release of non-esterified (free) fatty acids and glycerol into the circulation. Within the cell the triglycerides are stored in the cytoplasm in lipid droplets surrounded by phosphorylated perilipin (118,127). This regulation of lipolysis denotes a direct effect of the SNS on the adipose tissue, and shows an important link between nervous system function and metabolism.

1.7.4 The role of astrocytes in the sympathetic nervous system

Since their shift in recent years from simple structural and maintenance-related cells of the nervous system to active participants of nervous system function, astrocytes have now become important players in neurology, with their role as metabolic suppliers to neurons and mediators of long-term potentiation (LTP), as well as integral parts of synaptic transmission maintenance, to the point where the theory of a “tripartite synapse” composed of the astrocyte as well as the classical two pre- and post-synaptic neurons is becoming widely accepted (132–135).

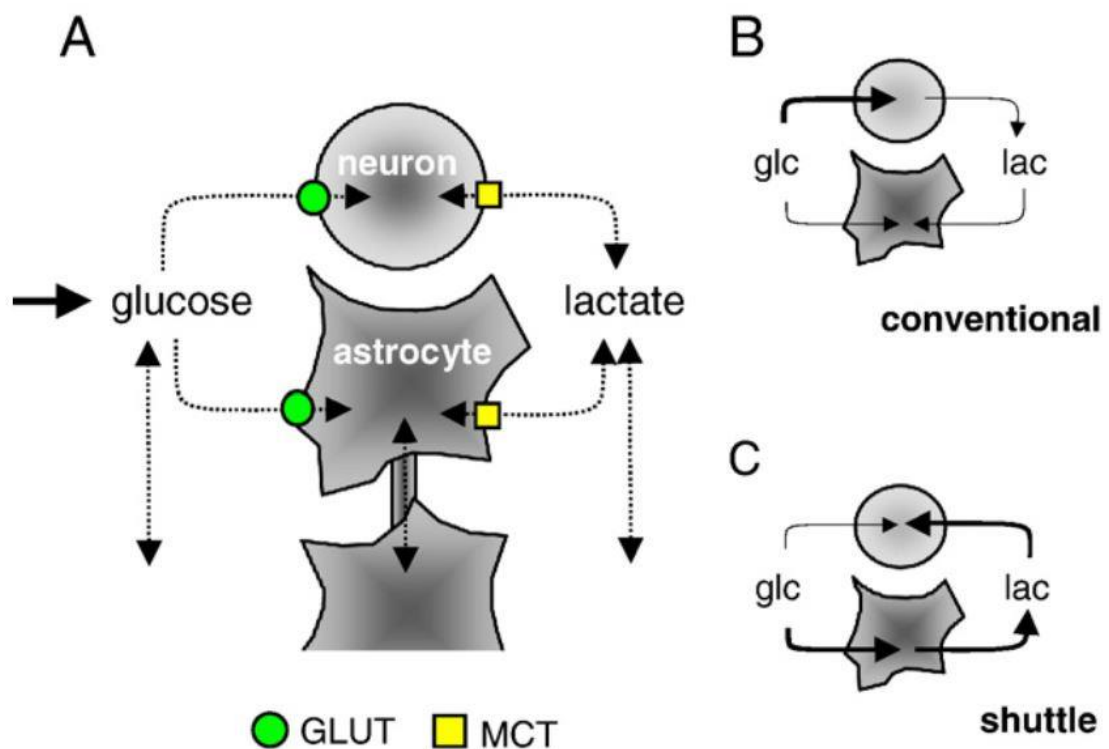


Figure 15: Models of metabolic coupling in the neuron/astrocyte interaction (source: (136)).

The metabolic role of the astrocytes, since the discovery of the highly capable glycolytic potential of the cells and the presence of specific lactate and glucose transporter proteins (GLUT family for glucose, MCT family for astrocytes both shown in Figure 15A) both involved in the supply of glucose and lactate involves two theories: a conventional model, (shown in Figure 15B) of neuronal energy supply which is thought to involve the direct use of glucose by the neuron

(therefore presuming a predominantly glycolytic metabolism in the astrocyte) and the resulting uptake of lactate as a waste product by the surrounding astrocytes or a “lactate shuttle” model (Figure 15C) by which the astrocyte shuttles lactate into the neuron (allowing a neuronal metabolism centred more towards the TCA cycle) after carrying out its own glycolytic cycle to produce lactate for the neuron (135,136). Glycogen stores previously described in astrocytes (137) are degraded into lactate directly inside the astrocyte during hypoglycaemia and noradrenaline stimulation (138), and experiments have linked synaptic activity to lactate uptake in the neurons via MCT2 lactate transporter proteins (136).

The opinion of the scientific community with respect to the astrocyte’s role in the neural circuitry of the CNS dramatically changed with the discovery of oscillatory intracellular calcium responses to specific neurotransmitters like glutamate (139), as well as the communication of astrocytes and neurons via these calcium oscillations (140). Further, the discovery of molecules secreted by the astrocytes that would affect synaptic function, dubbed “gliotransmitters”(141), solidified the hypothesis that this cell type was more than just “structural scaffolding” for the other components of a neural circuit, but was much more involved in the function of the synapse as well as brain circulation and blood supply in the blood brain barrier (141). Intracellular Ca²⁺ oscillations occur through a variety of stimuli that the astrocytes are subjected to, from mechanical stress to specific hormone responses elicited by receptors that are expressed on the cell membrane such as peptide receptors (142), as well as purinergic ATP receptors (143).

Oscillatory patterns in these astrocytes also are amplified by the interconnected nature of the cells themselves with neighbouring cells of the same type, since astrocytes are known to propagate the calcium oscillation “waves” via the expression of gap junction proteins such as connexins Cx30 and Cx43 (144), as well as metabolites such as glucose which has been observed as moving in between cytoplasms via connexin channels in hypothalamic astrocytes (145). This intercellular signalling is beginning to be studied for its possible control over neural networks responsible for central nervous system functions, such as breathing control. studies show (146)

cyclical activation of astrocyte calcium signalling, preceding inspiratory movement in the pre-Botzinger complex (an area of the ventrolateral medulla involved in breathing patterns during sleep) which regulate inspiratory neuronal output.

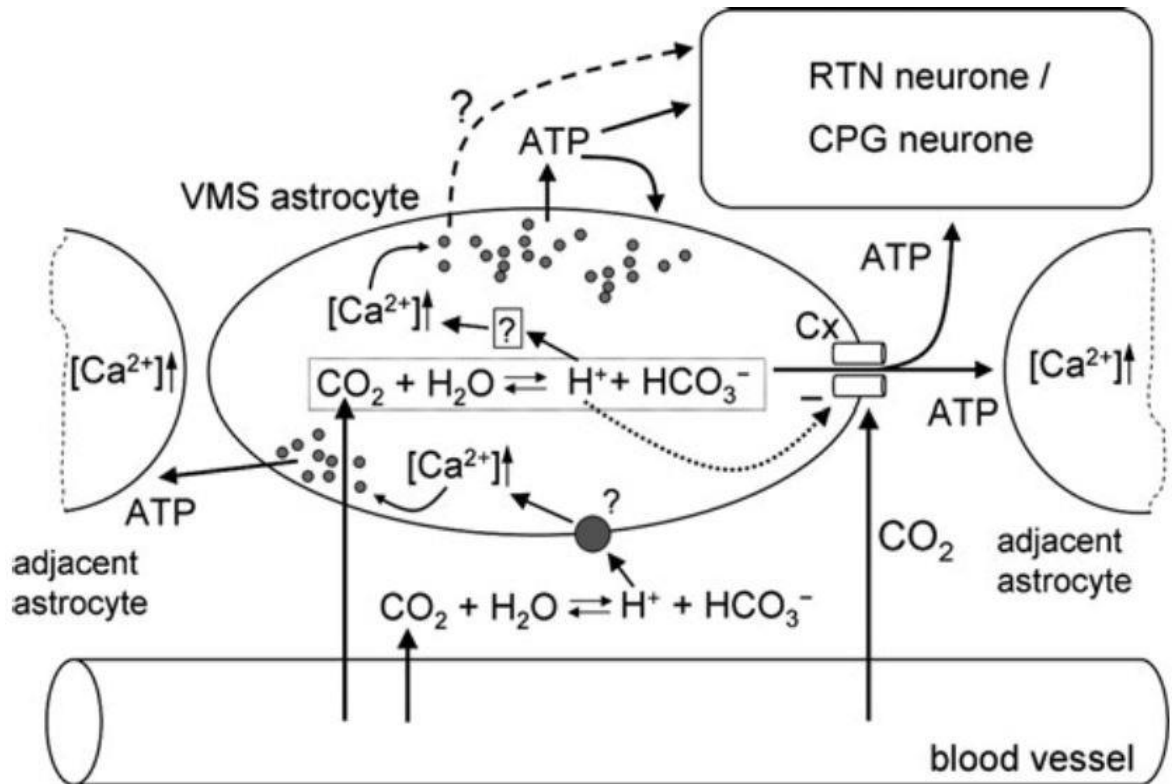


Figure 16: Possible pathways of astrocyte chemo-detection in the ventral surface of the medulla oblongata (VMS).

Cx = connexin hemichannel, RTN = retrotrapezoid nucleus, CPG = central pattern generator (Source: (134))

These data Gourine et al. (134,143) suggest that astrocytes have a very important role in the chemo detection of changes in CO_2 content of the blood, and do so in an independent manner compared to neuronal activity of the brain stem. The putative way that astrocytes of the brain stem do so is shown by Figure 16, where changes in blood acidity caused by a rise in circulating CO_2 , are detected in a resulting acidification of the cell's surrounding environment,

and is detected by the astrocytes (134), causing the opening of connexin hemichannels that release ATP in adjacent astrocytes. If the hypercapnic conditions persist, intracellular calcium is released after connexin hemichannels close and ATP release persists via exocytosis which acts in an autocrine and paracrine manner spreading Ca^{2+} excitation and enhancing ventilation by activating chemosensory neurons (RTN and CPG neurons). ATP may not be the sole player in the mechanism since other gliotransmitters are known to be released in response to Ca^{2+} oscillations (140), and may affect respiratory networks in a long-term stimulatory change, so their role in central nervous system regulation of breathing appears to be in need of elucidation.

Another interesting aspect surrounding astrocyte regulation of neuronal networks is the possible link between peripheral hormone secretion of organs such as the adipose tissue, with the release of leptin being important in the homeostatic CNS regulation of feeding stimuli in humans and the presence of astrocyte activity in response to leptin (147,148) in CNS areas responsible for the control of food intake such as the hypothalamus. This allows for possible hypotheses regarding the excitability and long-term plasticity of neuronal networks in response to peripheral hormones and the effects of peripherally secreted molecules in the functioning of the CNS itself, past the current understanding of the concept.

The role that chemosensing astrocytes could be playing in the regulation of higher functions of the CNS at the level of the medulla oblongata is clear. However, what the inherent signals from peripheral organs could be using to influence the RVLM to steer it away from its normal function are still to be elucidated, and were studied as part of this project.

1.7.5 Neuropeptide Y and the sympathetic nervous system

Neuropeptide Y or NPY is a 36 amino acid peptide and a sympathetic nervous system co-transmitter which was discovered over 30 years ago when originally isolated from porcine brain in 1982, studied chiefly for its role in the promotion of prolonged vasoconstriction in various vascular beds (149–151). The study of NPY later focused on its characteristics as a potent stimulator of appetite and feeding neuronal circuitry, but the aspect of its secretion being linked to the activation of the SNS is poorly understood. However, its levels are correlated with

heightened SNS activity (evident by higher circulating catecholamines) in many studies linking SNS-related pathologies to high NPY levels, such as Post Traumatic Stress Disorder (PTSD) (152), obstructive sleep apnoea (OSA, a typical comorbidity associated with obesity) (153) and stress-related adipose tissue accretion (154).

NPY is released after prolonged stimulation of sympathetic nerves. Long-term stimulation of the SNS (155), is commonly defined as stress on an organism. This type of release has allowed NPY to be studied in correlation with conditions of stress and stress responses, as well as being studied as a link between a long-term HPA axis activation due to increased levels of corticosteroids in the circulation in stress and high fat diets (156) and peripheral activity in organs such as adipose tissue and the vasculature, which also depend on the cleavage of the peptide into a shorter form by the enzyme DPP-IV which affects its receptor specificity in peripheral tissues. These recent findings have shown that NPY is important not only as a central feeding signal, but a signal that has peripheral origins and effects.

1.7.6 NPY and the periphery: adipose tissue npy receptors and adipose tissue function

NPY and its associated G-protein coupled receptor pathway has a documented range of effects on many different peripheral organs which has been extensively reviewed (155), but only relatively recently have the effects on metabolism been explored, specifically with respect to its activity in adipose tissue. Adipose tissue is known to produce NPY (157) as well as express NPY receptors 1 and 5 most abundantly (158). NPY signals may vary according to the activity of proteases such as DPP-IV that cleave NPY a specific sites, thus changing its receptor specificity, specifically changing it from neuropeptide receptor Y1 to neuropeptide receptor Y5, both commonly known to be expressed and most abundant in adipose tissue (159) . The main response exerted by the presence of NPY in the periphery is thought to be the inhibition of lipolysis (158) and the accumulation of fat mass through the stimulation of PPAR- γ expression in adipocytes, depending on the activity of DPP-IV which is also affected by insulin levels (159) . Adipogenesis also appears to be promoted by the presence of local NPY levels, and evidence

from in vitro models suggest that NPY receptor activation causes an impairment in the translocation of insulin-sensitive glucose transporter 4 (GLUT4) from the cytoplasm to the cell membrane (160), possibly via uncoupling of the mechanisms behind insulin-responsiveness of the adipocytes in individuals with higher locally secreted levels of NPY. These data allow for the formulation of the hypothesis that circulating NPY levels could be affecting not only adipocytes at the local tissue level, but also the regular function of the brain stem RVLM.

Another interesting aspect of NPY and adipose tissue interactions between the CNS and peripheral organs comes with the known involvement of central NPY signalling in the hypothalamus and its effect on the development of brown adipose tissue (BAT). BAT is an adipose tissue variant initially thought to be solely present in animal models and recently characterised as present also in humans (161) chiefly responsible for the dissipation of energy in the form of heat through the use of mitochondrial proton gradient disrupting proteins such as UCP1.

Brown adipocyte development has also been shown to be inducible from white adipose tissue cells and mesenchymal stem cells by signalling pathway regulation (162), and therefore achieved importance as a possible therapeutic target for abnormal energy expenditure in obesity. With evidence also showing that the knockdown of NPY gene expression in the hypothalamus causes an increase in the development of brown adipose tissue in rats (163), and the direct link between noradrenergic signalling and brown adipose tissue development and trans-differentiation (161), it becoming more and more clear that NPY could be an even more important player in the field of adipose tissue biology and a possible therapeutic target in obesity.

1.8 Hypothesis and aims of the study

1.8.1 Hypothesis: NPY as a possible link between periphery and CNS

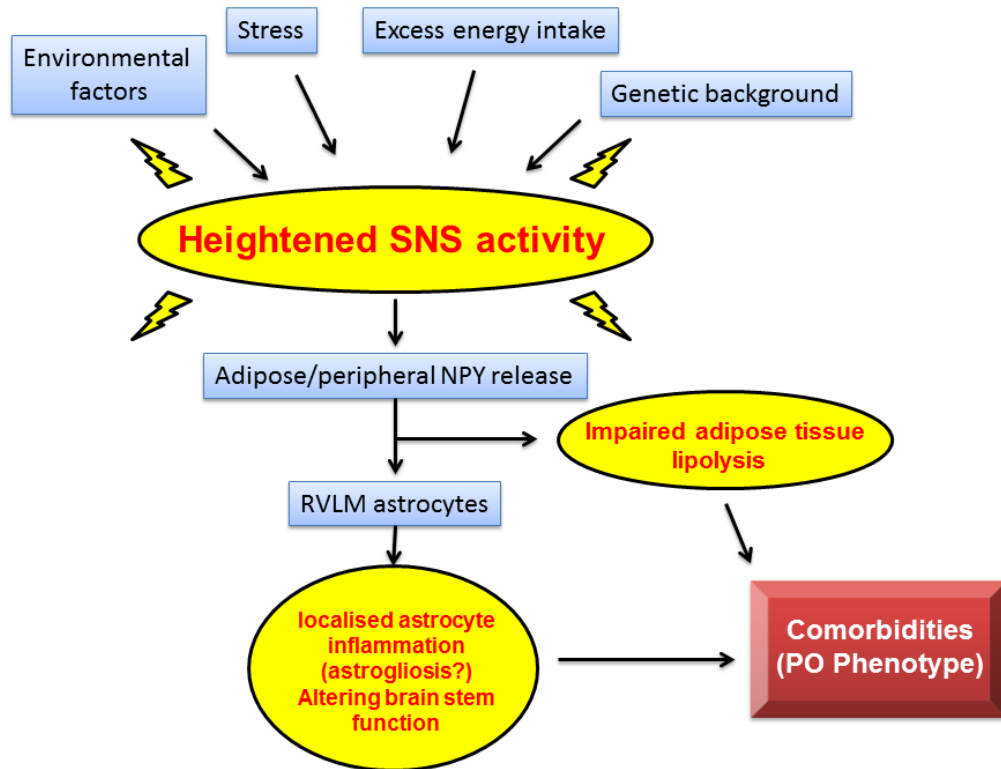


Figure 17: Possible hypothesis for SNS interference with energy homeostasis and BP regulation

Emerging evidence of NPY as a mediator of a variety of effects on peripheral organs, as well as on the central nervous system (155) has led to the hypothesis that there is a direct effect of elevated peripherally (adipose tissue)-derived NPY, perhaps consequent to increased stress-associated activity of the SNS, on the functioning of the CNS, mediated by astrocytes of the RVLM. This effect is summarised in Figure 17. Further, it was postulated that the astrocytes, through the modulation of intracellular signalling pathways, mediated the functioning of the neuronal circuits of the brainstem. This is in keeping with observations that obesity-related comorbidities, such as obstructive sleep apnoea (OSA), are associated with increased levels of circulating NPY (153,164) in the presence of greater SNS activity (20). This is supported by data

that peripheral NPY increases with stress and affects adipose tissue metabolism and vasculature (165), and that chronic elevation in circulating NPY impairs baroreflex sensitivity, as seen in human OSA cases (21,166). This could indicate a direct involvement of peripheral NPY on the normal function of brain stem astrocytes.

Hypothesis

That the presence of heightened NPY levels secreted from the central nervous system and peripheral tissues of an obese organism could be an additional mechanism partly responsible for the differences in comorbidities associated with the morbidly obese state between PO and MHO individuals

To be studied by the following aims:

1.8.2 Overall aims

1. To identify a normoinsulinemic/insulin sensitive morbidly obese Caucasian patient cohort
2. Compare differences in NPY levels, in the circulation and adipose tissue, between the normoinsulinemic and hyperinsulinemic subjects
3. Explore the hypothesis that elevated circulating peripheral NPY causes metabolic and/or inflammatory abnormalities in an *in vivo* rat model or *in vitro* model of primary human fetal brain stem chemo-sensing astrocyte cell line.

1.8.3 Patient recruitment and characterisation

The differences between MHO and PO individuals of the same ethnicity were explored in a clinical setting and described according to already described criteria used in the literature. This was carried out in order to identify a normoinsulinemic/insulin sensitive morbidly obese Caucasian patient cohort and to investigate the effect of weight loss in this normoinsulinemic group versus hyperinsulinaemic groups. This characterization was then further used for more detailed studies at the tissue level.

1.8.4 Assessment of adipokine differences and search for possible biomarkers

These characterised groups were also used to compare differences in secreted adipokines, including NPY levels, in the circulation and adipose tissue. They were quantified to determine differences in their levels in the two groups of patients in order to find other possible candidates as a readily detectable marker for the phenotype.

1.8.5 Differences in Morphological and local secretory function between subcutaneous (SC) and omental (OM) adipose tissue

Histological and secretory differences (organ cultures) in the adipose tissue between the two groups of patients as an indication of the proposed variation in tissue secretory and lipolytic function were examined.

1.8.6 Adipogenic/metabolic gene expression differences

As markers of tissue remodelling, the aim was also to determine the expression of selected adipogenic genes in the tissue, between depots of the same patients (SC and OM) and between patient groups such as MHO, PO and diabetic morbidly obese individuals. mRNA expression of metabolically significant genes, such as SCD1, as a marker not only of the level of SREBP-1c signalling inside the adipocytes, but also of possible dysfunction in lipid homeostasis of the adipose tissue. Furthermore, the levels of NPY receptor in the tissue were also determined.

1.8.7 Circulating NPY levels

Circulating NPY levels were measured as a biomarker for SNS hyperactivity in the metabolically unhealthy (pathological obesity).

1.8.7 Effects of NPY/NA levels simulating heightened SNS activity on human astrocytes

By using noradrenaline and NPY, alone and in combination, the rationale was to re-create conditions of stress and chronic SNS activation on human brain stem astrocytes. The function of the astrocytes was determined by measuring their release of inflammatory cytokines and lactate, as well as changes in intracellular signalling molecules (pSTAT3, cAMP and Ca²⁺).

Chapter 2

Materials and Methods

2.1 Clinical method protocols

2.1.1 Patient Recruitment

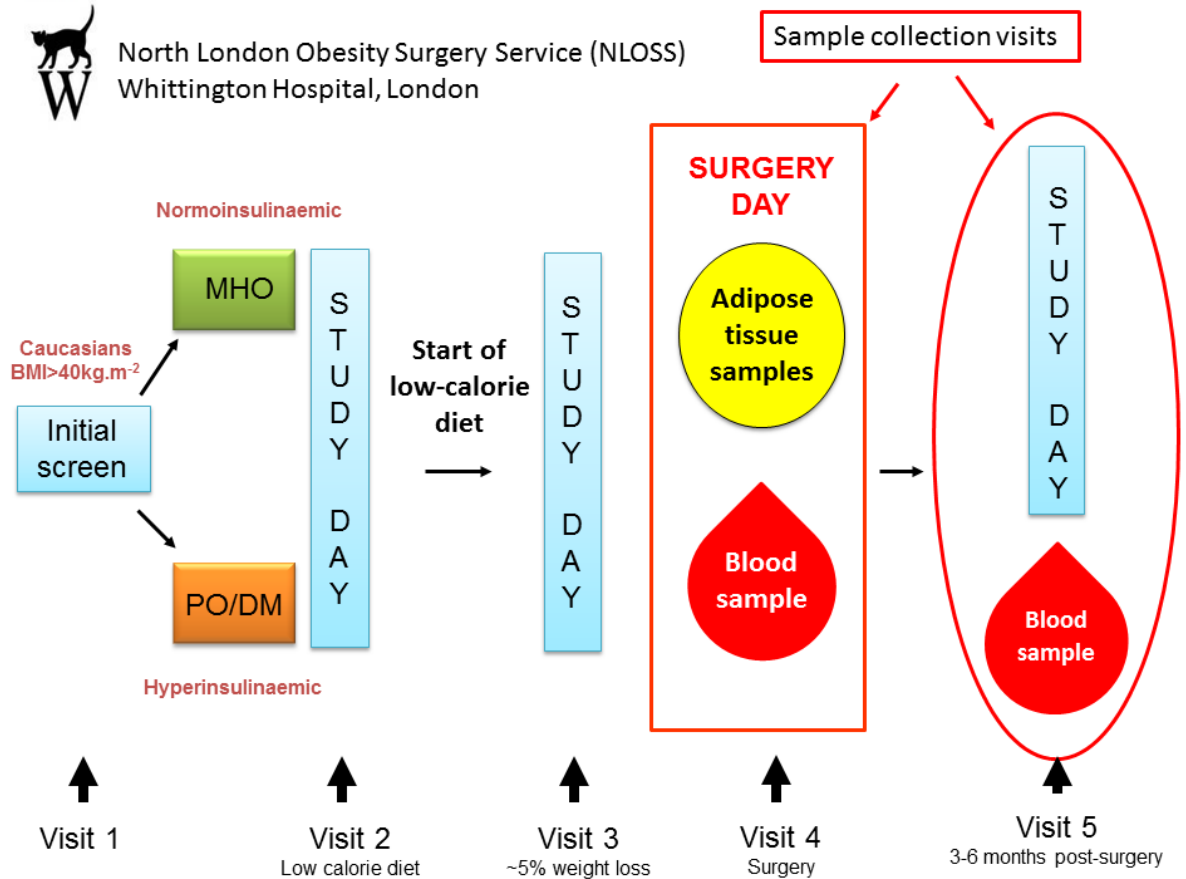


Figure 18: Clinical study structure

Patients of Caucasian background were recruited from the North London Obesity Surgery Service of the Whittington Hospital, London, UK while awaiting surgical weight reduction surgery. The method of recruitment was carried out in parallel with the regular clinical protocol for bariatric surgery eligibility assessment (as shown in figure 18), with hospital nutritionists monitoring the weight loss of the patients before undergoing assessment and leading up to surgery. Anthropometric and clinical data as well as data regarding medication taken by the patients prior to surgery (with respect to the exclusion of patients taking medication from the

MHO group) were all recorded from patient clinical notes. Prior to surgery fasting blood samples were taken from all patients. During surgery an abdominal subcutaneous (SC) and omental (OM) adipose tissue sample (2-5 gms) was obtained. All patient data was stored on an IBM SPSS Statistics 20 for Windows (IBM, USA) database file, and kept in compliance with protocols safeguarding patient privacy. All patients gave written informed consent. The study was approved by the National Ethical Committee.

2.1.2 Blood samples

Serum, plasma and sodium fluoride samples were taken from each patient on surgery day as well as on follow-up visits 3-6 months after surgery in a fasting state, and all centrifuged at 3000rpm for 15 minutes with supernatant collected and stored at -80°C for long-term storage. Plasma glucose concentration was assayed with glucose oxidase reagent (Beckman, USA Cat no. 472500). Serum insulin levels were determined by ELISA (Merckodia, UK Cat no. 10-1113-01). Serum triglycerides, total, low density lipoprotein (LDL-) and high density lipoprotein (HDL-) cholesterol were assayed with commercial reagents with total-cholesterol and triglycerides tested (Roche Diagnostics, UK). LDL-cholesterol was calculated using the Friedwald formula. All lipid assays were performed by Dr David Wickens (Chemical Pathology, Whittington Hospital, London UK). Insulin resistance was calculated using the homeostatic model assessment where $HOMA = (\text{glucose in mmol/L} \times \text{insulin in mIU/L}) / 22.5$.

2.1.3 MHO/PO characterisation criteria

The patients, after being matched for age and BMI, were considered MHO based on the presence of the following criteria:

- No metabolic disorders including T2DM, dyslipidaemia and hypertension
- Systolic blood pressure at < 140 mmHg, diastolic blood pressure at <85mmHg
- Absence of cardiovascular disease
- Fasting plasma glucose of <6.8 mmol/l and insulin <6.5 mIU/ml

2.2 Histology protocols

2.2.1 Histology sample preparation

A 0.2-0.3g sample from subcutaneous and omental adipose tissue was excised for histological purposes and incubated in neutral buffered formalin (VWR International, USA Cat no. 16004-126) for 24 hours and then transferred to 50% Ethanol (Sigma, UK) and stored at 4°C until processing.

2.2.2 Hematoxylin and Eosin staining

Slides from paraffin processed samples were placed in Gill's 1X Hematoxylin solution (Sigma, UK Cat no. GHS1128), rinsed with tap water for 5 minutes, Then placed in an acid ethanol solution (1%HCl in 70%ETOH, Sigma UK) for 2-3 times, rinsed with tap water for 3-5 minutes and then dunked 5-6 times in ammonia water solution (1mL NH₄ OH in 1L H₂ O), and then rinsed with tap water again for 3-5 minutes. The slides were then placed in Eosin Y (Sigma, UK Cat no. E4009) for 1 minute, rinsed in tap water once more and then washed in 3x 95%, 3x 100% ETOH, 50:50 Xylene-ETOH (Sigma, UK), and 3x 100% Xylene as the final steps before applying a cover slip.

2.2.3 NPY/CD68 Immunohistochemistry

Slides were washed in Tris buffered saline for 2 min and blocked at room temperature for 5 min in DAKO peroxidase blocking solution (Dako, Denmark Cat no. S2023) followed by 10% horse serum in Tris buffered saline for 10min. Primary antibody (1 in 200 dilution of affinity purified rabbit anti human NPY Y1 or Y5 receptor polyclonal antibody: Sigma, UK Cat no. HPA029903 and HPA013790, or CD68 affinity purified rabbit anti human polyclonal antibody Dako, Denmark Cat no. M0876) was added and incubated for 60 min at room temperature and secondary antibody (1 in 1000 dilution of anti-rabbit IgG peroxidase conjugated antibody: Sigma Cat. No. A0545) for 45 min. Detection was by standard Avidin Biotin Complex (ABC)/DAB method.

2.2.4 Adipocyte size calculation

Blinded to the metabolic status of the patient samples, for each slide (1 per depot of each patient) 3 images were captured using the bright field setting at 20x magnification on a microscope attached to a CCD camera on H&E stained slides.

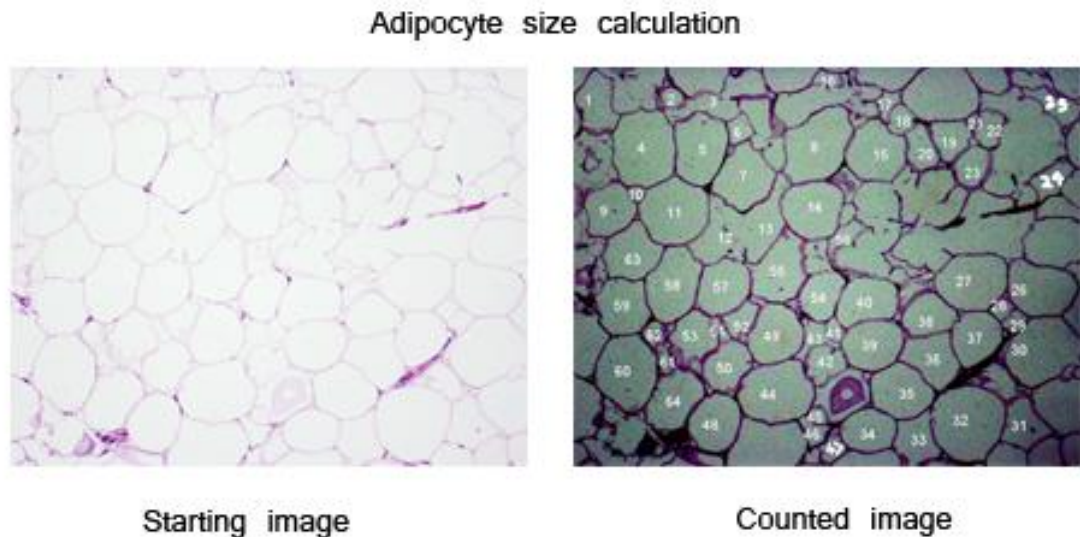


Figure 19: adipocyte size calculation method

Images were equally sized, non-overlapping and taken at random locations on each slide. For each image, after increasing contrast, all completely visible and completely circular cells were manually counted and traced and the area calculated in pixels through the “area” function in Image-J (National Institute of Health, USA) as shown by Figure 18. The pixel areas were then pooled according to MHO/PO status and statistical analysis was carried out on the two groups.

2.2.5 Quantification of CD68/NPY receptor DAB stain

Blinded to the metabolic status of the patient samples, for each slide (1 per depot of each patient) 10 images (5 in the case of the NPY immunohistochemistry) were captured using the bright field setting at 20x magnification on a light microscope (Nikon, Japan) attached to a CCD camera. Images were equally sized, non-overlapping and taken at random locations on each slide. Each image was processed in the same manner, however in order to emphasize the DAB

staining, each photograph was de-convoluted using the appropriate function (H DAB Colour de-convolution) in ImageJ and given an appropriate threshold value. This value was different for each picture. This method gave arbitrary values of zero for the images taken from the slides which had negative staining; and removed as much background signal as possible without compromising the positive staining. Once each image was processed the number of pixels was counted and recorded as an arbitrary value which represented a degree of valid staining for that particular image. The pixel values were then recorded and statistical analysis carried out.

2.2.6 NPY blood vessel image analysis

Blinded to the metabolic status of the patient samples, for each slide 3 images of blood vessels were captured, using the same criteria as above. To quantify the staining of the blood vessels, each vessel was graded as small, medium or large. The size allocated was determined by which size square the vessel fitted into best. The sizes are described in the table below:

Vessel size	Square dimensions (pixels)	Area (pixels)
Small	100 x 100	10000
Medium	150 x 150	22500
Large	200 x 200	40000

The individual vessel was cropped and the image modified to emphasize the brown staining. Each image was once again given an appropriate threshold value in the same way as the CD68 stain quantification. Once each image was processed the number of pixels was counted. This number was then expressed relative to the size of the vessel, by use of the following formula:

Arbitrary value representative of NPY staining of blood vessels

$$= \frac{\text{Pixels recored in the image of the vessel}}{\text{Area of square (pixels)}}$$

This would account for any differences in staining due to the vessel size *i.e.* a larger vessel would have an increased number of receptors, but not necessarily a greater concentration or density of receptors.

2.3 Adipokine protocols

2.3.1 Organ explant cultures

Subcutaneous and omental adipose tissue explants were excised ranging from 0.049g to 0.052g in size and incubated for 24 hours at 37°C and 5% CO₂ in 500µL CellGro Complete Medium (Mediatech, USA Cat no. 40-101-CV) + 1% Penicillin/Streptomycin solution (Invitrogen, USA Cat. No.15140122). Medium and tissue were stored at -80°C for long-term use.

2.3.2 Protein extraction

0.5g tissue samples were ground using liquid nitrogen, mortar and pestle and extracted using 800µL RIPA lysis buffer (Sigma, UK Cat no. R0278), vortex-shaking and a centrifugation step at 14,000 rpm at 4°C, collecting the supernatant and quantifying protein content using a Novagen BCA Protein Assay Kit according to supplier manual (Novagen, USA Cat. No.71285). The protein quantification assay was carried out according to user manual specifications and quantified using a Dynex Opsys-MR plate reader (Dynex Technologies, USA) at wavelengths specified by user manual. Samples were stored at -80°C for long-term use.

2.3.3 Circulating and local adipokine/NEFA levels

All circulating adipokines were tested in the serum or EDTA plasma samples taken and measured by ELISA (R&D Systems (UK), according to manufacturer's instructions. NPY levels in serum were assessed by ELISA (Millipore, UK Cat no. EZHNPY-25K) as per protocol. Final absorbance was read on a Dynex Opsys-MR plate (Dynex Technologies, USA) at wavelengths specified by supplier manuals. Circulating non-esterified fatty acid (NEFA) levels were assayed using a reactive colorimetric assay (Wako Diagnostics, USA Cat. No. 999-34691, 995-34791, 991-34891, 993-35191 and 276-76491) according to supplier manual, and analysed on a Dynex Opsys-MR plate reader (Dynex Technologies, USA).

2.3.4 Induction of IL-6 secretion by IL-1 β

0.05 to 0.06g explants of subcutaneous fat from a total of 12 patients were taken in 5 aliquots from an excised tissue sample, and incubated in 2mls of DMEM + 10%FBS + Penicillin/Streptomycin at 37°C and 5% CO₂ (Gibco, USA Cat no. 11965-084). Medium was changed at 24, 48 and 65 hours from start of incubation. After 65h the medium was finally changed to 2 ml CellGro + Penicillin/Streptomycin in wells 1 and 2 as a control and 2ml of CellGro + Penicillin/Streptomycin + 10ng/ml of IL-1 β in the remaining three for 8 hours (Mediatech, USA Cat no. 40-101-CV). The medium was collected after the final incubation and IL-6 levels secreted after the final 8 hours assessed (Quantikine HS Human IL-6 ELISA, R&D Systems).

2.4 RNA and gene expression analysis protocols

2.4.1 RNA extraction

Explants of approximately 0.5g from the tissue gathered on the day of surgery were preserved in RNAlater solution (Life Technologies, UK Cat no. AM7021) and stored at -80°C for subsequent extraction. RNA was extracted using Trizol (Invitrogen, UK Cat no. 15596-018) in a Trizol-chloroform extraction protocol, carried out as follows: 0.8 ml of Trizol was added to

dissolve the tissue and then re-suspended in a vortex shaker for 5 seconds X 10, and left to sit for 5 seconds on ice in between spins. The Trizol reagent was then removed from the sample avoiding any pelleted debris and transferred to a new cold tube. The volume was recorded and fifth of the recorded volume of chloroform (Sigma, UK Cat no. 496189) was added. The sample was re-suspended in a vortex shaker for 15 seconds and left on ice for 5 minutes. The sample was then centrifuged for 15 minutes at 14,000 rpm and 4°C, and the aqueous phase collected and an equal volume of isopropanol added (Sigma, UK Cat. No. I9516). The samples were left at -20°C for 1.5 hours and then centrifuged again for 15 minutes at 14,000 rpm/ 4°C. The supernatant fraction containing the precipitated RNA removed very carefully and pelleted. The pellet was washed twice with 0.8 ml of 75% ethanol (Sigma, UK Cat no. E7023) and centrifuged for 5 minutes at 14,000 rpm/ 4°C. The ethanol was then carefully removed from tube and the pellet dried on ice for 10 minutes to remove the remaining trace amounts of ethanol. After a final re-suspension of the pellet by adding 45µl of RNase-free H₂O (Life Technologies, UK Cat. No. 4387936) the sample was assayed for concentration and purity from contaminants by recording 260nm/280nm and 260nm/230nm absorbance wavelength ratios (NanoDrop ND-1000 spectrophotometer, Thermo Scientific, USA).

2.4.2 cDNA synthesis

For gene expression analysis, the isolated RNA from the samples in the previous section was used (500ng per sample), and the sample quantity adjusted for the amount of RNA sample taken. For reverse transcription, a TaqMan reverse transcription reagent kit was used (Applied Biosystems, UK Cat no. N8080234) and the proportions of reagents adjusted to the total reaction volume which varied per sample and the final reaction step was carried out on a Techne Genius FGEN05TP (Techne, UK) thermal cycler, incubated with settings as indicated by kit manual. Samples were kept long-term by storing in a -20°C freezer for repeat use.

2.4.3 Real-time PCR

Transcripts encoding for various genes from the cDNA samples created were measured by Real-time PCR on an Applied Biosystems ABI7900HT machine (Applied Biosystems, UK), using ABI

SYBR Green master mix (Applied Biosystems, UK Cat no. 4368708). Primers were obtained from Qiagen, (Crawley, UK Cat numbers variable according to specific gene used, consultable at <http://www.qiagen.com/products/catalog/assay-technologies/real-time-pcr-and-rt-pcr-reagents/quantitect-primer-assays>), and protocol was adjusted according to the instructions on the user manual. The control gene for every assay selected as a reference for the expression levels of the assayed gene was β -actin (Cat no. QT00094850), and total volume cDNA used was set at 1/40th of the original cDNA total reaction volume, with a total master mix/sample/primer solution of 25 μ L in each well. PCR protocol was carried out according to primer manufacturer specifications in the user manual. Software analysis of the resulting cycle threshold values was carried out on Sequence Detection Software 2.4 (Applied Biosystems, UK), and quantified as relative expression compared to the control gene using the Livak method (167) as also specified in the statistical analysis section in this chapter.

2.4.5 siRNA knockdown in adipose tissue

Following a method previously described by Puri *et al*, (168), 0.05 to 0.06 grams of subcutaneous adipose tissue (16 explants in total, 4 for each miR-146b siRNA type) were cut from an explanted sample of subcutaneous fat from a bariatric surgery patient. The pieces were then minced into 1-2 mm fragments and placed in cuvettes containing 200 μ L of sterile PBS containing 15nmols of the desired siRNA type (AllStars Negative Control – Cat no. SI03650318, MiScript Negative Control - Cat no. 1027272, mi-146b siRNA mimic – Cat no. SI05362297 and mi-146b inhibitor siRNA – Cat no. SI05362287 all obtained from Qiagen, USA). The electroporation experiment was then carried out in the cuvettes by subjecting the submerged pieces of adipose tissue to 16 shocks at 50V and 950 μ F on a BioRad GenePulser II electroporator (BioRad, USA) with shock duration of 30msec, square wave setting. The procedure involved shocking the tissue 8 times, then gently tapping the cuvette to mix the PBS/adipose tissue solution and the shocking another 8 times. After the final shocks the tissue solution was supplemented immediately with 1ml of DMEM + 10% CCS + Penicillin/Streptomycin solution, and taken to a tissue culture hood where it was transferred using sterile needles to a 24-well

plate and supplemented with an extra 1.5ml of DMEM, with medium changes occurring at 2h, 4h, 24, 48 and 65 hours after the start of the first incubation, reducing the total medium in the wells to 2ml instead of the previous 2.5ml after 24 hours. After 65h hours of incubation half the explants were incubated with CellGro + Penicillin/Streptomycin as a control, whereas half were incubated in CellGro + p/s with 10ng/ml of IL-1 β for 8 hours total, with the medium collected and stored at -80°C and the adipose tissue placed in RNAlater solution, stored at the same temperature at the end of the incubation. The resulting gene expression changes were examined via RNA extraction, reverse transcription and real time PCR with methods described previously in this chapter.

2.5 Astrocyte protocols

2.5.1 Astrocyte cell culture

Human primary brain stem astrocytes (ScienCell, USA Cat no. 1840) of foetal origin were cultured in a sterile tissue culture environment in T75 Flasks previously coated in a 50:50 distilled water/Poly-L-Lysine solution (Sigma, UK Cat no. P4707) with 15ml Astrocyte Medium supplemented with Astrocyte Growth Supplement, Penicillin/Streptomycin solution and 5% Foetal Bovine Serum (all supplied by ScienCell, USA Cat no. 1801, 1852, 0503 and 0010). T75 Flasks (BD Biosciences, UK Cat. No. 353136) were seeded with at least 1×10^6 cells after counting using a Neubauer haemocytometer (Hausser Scientific, USA Cat no. 3120), and incubated at 37°C and 5% CO₂. Passaging was carried out using 5 minute incubations with 5ml 2.5% Trypsin solution (Invitrogen, UK Cat no. 15090-046) which were then centrifuged at 1000 rpm and re-suspended in an equal amount of astrocyte medium for further seeding in pre-coated flasks. Cells were not used past passage 15 as specified by supplier manual, and passage number was recorded at every flask change. Medium was changed every 24-36 hours according to confluency of flask and rate of growth of the cells judged using an inverted light microscope (Nikon, Japan).

2.5.2 Astrocyte incubations

Passage 5-10 astrocytes grown in pre-coated T75 flasks at 37°C and 5% CO₂ in Astrocyte Medium (ScienCell, USA) supplemented with Astrocyte Growth Supplement, Penicillin/Streptomycin solution and FBS were passaged and evenly split after counting in the wells of a 6-well plate (Corning, USA Cat no. 3335), and grown in 1.5ml Astrocyte Medium supplemented with Astrocyte Growth Supplement and penicillin/streptomycin solution but without the addition of Foetal Bovine serum overnight (16 hours) in separate containing the various molecules (Human recombinant NPY from Tocris Bioscience, UK Cat No. 1153 and Noradrenaline from Sigma, UK Cat no. A7257, Leptin from Peprotech, USA Cat no. 300-27). The cells were then lysed to extract RNA/protein according to respective protocols described previously in this introduction. The levels of secreted IL-6 and MCP were all expressed as a percentage increase over the control levels of untreated baseline secretion by the astrocytes. All astrocyte incubations were adjusted for the volume of protein present in each well in order to avoid quantification errors that could arise from different growth rates in different wells.

2.5.3 Quantification of astrocyte pSTAT3, cAMP, IL-6 and lactate levels

Quantification of intracellular cAMP levels was carried out using cell protein samples extracted with RIPA buffer (Sigma, UK) (as described in the protein extraction section of this chapter) and tested on a cAMP complete ELISA kit (Enzo Life Sciences, USA Cat no. ADI-900-163). Intracellular pSTAT3 was also assayed via ELISA (Invitrogen, USA Cat no. KHO0481), as well as IL-6 levels secreted by the astrocytes in the medium (R&D Systems, UK). Released lactate levels were quantified using a colorimetric assay (Sigma, UK Cat no. MAK064). For the intracellular pSTAT3 and cAMP levels and the secreted IL-6 levels, sample preparation and actual assay were carried out as specified in the user manual, and analysed on specified wavelengths on a Dynex Opsys MR plate reader (Dynex Technologies, USA). The assay analysing secreted lactate levels in the medium was carried out according to manual and analysed on a FLUOstar Optima plate reader (BMG Labtech, Germany) according to manual-specified wavelengths and reagent proportions. All results were adjusted to total protein content after a BCA assay quantification of the sample as previously described.

2.5.4 Astrocyte Immunohistochemistry

The protocol for the staining of astrocytes cultured *in vitro* was followed according to the numerous protocols for immunohistochemistry present in the available literature, and was carried out as follows: after initial seeding of a passage 5-10 population of astrocytes grown in Astrocyte Medium (AM) with addition of growth solution, FBS and antibiotics (as specified previously in this section) onto cover slips bathed in Poly-Lysine solution (Sigma, UK) diluted in sterile distilled water (1 in 7.5 dilution) and coated overnight at 37°C. Upon reaching confluence, the cells were washed cells with Phosphate Buffered Saline twice for 5 min each and incubated with 4% Paraformaldehyde (Sigma, UK Cat no. P6148) for 15 minutes. The paraformaldehyde was then removed by washing PBS 2-3 times (10 min each time) and the cells were incubated in PBS + 15% Triton X-100 (Sigma, UK Cat no. X100) and 10% FBS (Invitrogen, USA Cat no. 16000044) for 30 minutes. After washing with PBS-T and 1% FBS for an additional 10 minutes, primary antibodies for NPY receptor 1 or 5 were added to the bathing solution (both antibodies from Sigma, UK), and the slides incubated in a oscillating shaker for 12-16 hours at 4°C. After primary antibody incubation (Sigma, UK) the cells were washed in PBS 3 times and 5 minutes each, and secondary and rabbit-Cy5 antibody (Invitrogen, USA Cat no. A10523) was added in PBS solution and the cover slips left to incubate for 1.5 hours. Finally, the cover slips were washed with PBS twice and mounted on slides using Citifluor mounting medium (Citifluor, UK Cat no. AF1) and sealed with nail polish. After sealing, slides were conserved in the dark at 4°C indefinitely. Photos of the stained astrocytes were taken at 40X magnification using an Olympus FluoView FV1000 Confocal microscope (Olympus, Japan).

2.5.5 Cytokine array

Quantification of cytokine levels in astrocyte protein extracts was carried out using a Human Cytokine Array Kit Panel-A (R&D Systems, UK Cat no. ARY005). The tested human cytokines were as follows:

C5a	IL-4	IL-32 alpha
CD40 ligand	IL-5	CXCL10/IP-10
G-CSF	IL-6	CXCL11/I-TAC
GM-CSF	IL-8	CCL2/MCP-1
CXCL1/GRO alpha	IL-10	MIF
CCL1/I-309	IL-12 p70	CCL3/MIP-1 alpha
ICAM-1	IL-13	CCL4/MIP-1 beta
IFN-gamma	IL-16	CCL5/RANTES
IL-1 alpha	IL-17	CXCL12/SDF-1
IL-1 beta	IL-17E	Serpin E1/PAI-1
IL-1ra	IL-23	TNF-alpha
IL-2	IL-27	TREM-1

Samples were concentrated according to user manual specifications and protocol followed as specified by the kit manual. Samples were analysed using an Epson 636U scanner (Epson, Japan) and digitally acquired using IrfanView open-source software (Available at www.irfanview.com). Protein density calculations were carried out on ImageJ software (National Institute of Health, USA) using the “Gels” function on the “Analyse” menu.

2.5.6 Astrocyte gene silencing

Passage 3 astrocytes cultured in T25 flasks were seeded in 6-well plates (at approximately 50,000 cells per well) and grown to 70% confluency in astrocyte medium with the addition of 2% FBS, Astrocyte Growth Supplement and penicillin/streptomycin solution as described in previous parts of this section. After sufficient growth was achieved in the plates, the plates were transfected (along with a un-transfected control) with SilencerSelect (Ambion, USA) custom-made siRNA molecules at 50µM specifically for human Leptin receptor (Cat. no. 4392420), GAPDH (Cat. no. 4390849) and a negative control (Cat no. 4390843). The siRNA molecules were dissolved in 1.5ml Gibco OPTIMEM reduced serum medium per well (Gibco, USA Cat no. 31985-062) and transfected with the same medium along with 0.2% Lipofectamine RNAiMAX (Invitrogen, USA Cat. No. 13778-075) transfection reagent. The cells were transfected with the siRNA + reduced serum lipofectamine medium at 37°C and 5% CO₂ for 24 hours, and after transfection a PBS wash in each well was carried out and the medium substituted with Astrocyte Medium + 2% FBS + Growth Solution + Penicillin/Streptomycin solution and incubated for an additional 24 hours. After another 24 hours the cells were washed with PBS once and RNA

directly extracted by addition of 1.5ml of Trizol reagent, following the RNA extraction protocol described in 2.4.1.

2.5.7 Astrocyte intracellular calcium imaging

Primary brain stem astrocytes at passage 5-10 were seeded on polylysine-coated cover slips (coated as previously described in 2.5.5) (VWR, Germany Cat. No. 631-0666), and grown to confluency in astrocyte medium supplemented with 2% FBS (ScienCell, USA). After growth, the astrocytes were stained by adding a solution of 0.5% Fluo-4 Ca²⁺ sensitive dye (Life Technologies, USA Cat. No. F-14201) along with 5µL of Pluronic surfactant for 1.5ml of total medium (Sigma, UK Cat. No. P2443) to facilitate entry of the dye in the cell. The cells were then incubated at 37°C and 5% CO₂ for 45 minutes before the cover slip was washed twice with Hank's Balanced Salt Solution (with no added Ca²⁺) and transferred to a slide mount on an inverted light microscope (Olympus, Japan) and captured and analysed using Andor iQ software (Andor Technology, UK). During an experiment, an initial phase of resting activity was recorded (usually 3-5 minutes) before adding any molecule to the medium. After recording of an exposure to a molecule, 10 cells were selected at random in the field of view and monitored for intracellular Ca²⁺ fluctuation. The data for the initial control phase was then used to normalise activity for the rest of the experiment, and normalisation was carried out using OriginLab Origin Pro 9 software (OriginLab, USA).

2.6 Statistical analysis

All statistical analyses were carried out using IBM SPSS Statistics 20 for Windows (IBM, USA). Parametric variables were tested using a paired sample *t*-test and are displayed as mean (standard deviation), while non-parametric variables were tested using the Wilcoxon-Mann-Whitney U test and displayed as median (interquartile range). Correlations were calculated using Pearson or Spearman's correlation coefficient test. RNA expression was calculated either as a ratio of the control gene threshold cycle value (Ct) or using the $-2^{-\Delta\Delta Ct}$ method (167). All graphs were presented and compiled either in SPSS Statistics 20 for Windows or in OriginLab Origin Pro 9.0 (OriginLab, USA).

Chapter 3

Results

3.1 Clinical recruitment

3.1.1 General patient characteristics

The basic characteristics for the patients recruited in the course of this study according to the criteria described in Chapter 2 are summarised in Table 1.

Category	MHO	PO + DM	p-value
<i>N</i>	29	106	
<i>Age(y)</i>	39.0(9.3)	44.7(11)	0.09
<i>BMI (kg/m²)</i>	46.0(6)	46.9(7.9)	0.10
<i>Systolic Blood Pressure (mmHg)</i>	125.3(20.4)	132.9(20.3)	0.40
<i>Diastolic Blood Pressure (mmHg)</i>	71.9(14.2)	76.6(12.8)	0.95
<i>Fasting Plasma Glucose (mmol/L)</i>	4.7(0.7)	5.6(1.8)	0.02
<i>Insulin (miU/ml)</i>	4.5(3.2-5.6)	13.7(7.1-16)	<0.001
<i>HOMA-IR</i>	0.9(0.6-1.2)	2.2(1.5-4.1)	<0.001
<i>Total Cholesterol (mmol/L)</i>	3.7(8.5)	3.9(1.2)	0.08
<i>LDL Cholesterol (mmol/L)</i>	2.1(0.8)	2.2(1.1)	0.20
<i>HDL Cholesterol (mmol/L)</i>	1.0(0.2)	0.96(0.3)	0.70
<i>Triglycerides (mmol/L)</i>	1.1(0.9-1.7)	1.5(1.2-2.1)	0.01

Data are shown as mean (SD) or median (interquartile range).

Table 1: Patient characteristics

Out of a total of 135 Caucasian patients (25 of whom were male and the remainder female) screened 106 fit into the insulin resistant or diabetic group (with 31 diagnosed type 2 diabetics) 29 (21.5% of total) were observed to be metabolically healthy according to the criteria used for our study. Despite no significant differences in age and BMI of the patients between the healthy and non-healthy obese groups, there was a significant difference in fasting plasma glucose, insulin levels and HOMA-IR index, with all values being greater for the non-MHO. Triglycerides were also observed to be significantly elevated in this group. Total cholesterol levels also

appeared to be slightly higher in the PO/DM group as well as systolic blood pressure, albeit both not to a statistically significant level.

3.1.2 Circulating adipokines

In a representative subset of the above patients systemic adipokines were determined as an index of adipose tissue function in the two groups, Table 2.

Category	MHO	PO/DM	<i>p</i> -value
<i>N</i>	23	85	
<i>Serum Leptin</i> (ng/ml)	33.6(15.6-49.8)	37.0(23.1-57.2)	0.20
<i>Serum IL-6</i> (pg/ml)	3.0(1.0-5.4)	2.3(1.5-3.8)	0.80
<i>Serum MCP-1</i> (pg/ml)	290.0(139.0-380.0)	179.4(136.9-381.1)	0.50
<i>Serum NPY</i> (pg/ml)	6.3(3.7-12.3)	11.4(5.4-18.2)	0.03
<i>Serum Adiponectin</i> (µg/ml)	6.1(3.4-9.7)	3.0(1.9-5.2)	0.005
<i>Serum NEFA</i> (mmol)	1.1(0.9-1.4)	1.2(1-1.5)	0.20

Data are shown as mean (SD) or median (interquartile range).

Table 2: Serum adipokines in MHO and PO patients.

Systemic NPY concentrations were significantly higher in the PO/DM group, while conversely adiponectin levels were significantly higher in the MHO. Circulating NEFA and leptin levels were higher in the PO/DM, but did not reach significance. Inflammatory molecules such as IL-6 and MCP-1 were not different in the two groups.

3.1.3 Locally secreted adipokines from adipose tissue explants

The levels of locally secreted adipokines from adipose organ cultures of samples taken at surgery from both depots and measured following 24-hour incubation in growth medium (as described in Chapter 2) was recorded in a sub-group of samples from the clinical study population.

Category	MHO	PO/DM	p-value
<i>N</i>	11	28	
<i>SC Adiponectin</i> (ng/ml)	79(49-109)	77.6(55.3-102.7)	0.9
<i>OM Adiponectin</i> (ng/ml)	60.0(44.8-91.1)	58.6(45.7-88.6)	0.8
<i>SC Leptin</i> (ng/ml)	1.5(0.9-2.4)	3.0(1.6-4.2)	0.02
<i>OM Leptin</i> (ng/ml)	0.2(0.1-0.8)	0.4(0.2-2.2)	0.3
<i>SC NPY</i> (pg/ml)	2.9(2.5-3.6)	3.2(2.6-3.8)	0.7
<i>OM NPY</i> (pg/ml)	13.0(4.0-28.8)	5.2(4.1-8.4)	0.08
<i>SC MCP-1</i> (ng/ml)	3.2(1.1-9.3)	5.2(2.0-11.3)	0.2
<i>OM MCP-1</i> (ng/ml)	2.0(0.3-8.9)	8.5(1.4-13.5)	0.08
<i>SC IL-6</i> (ng/ml)	1.4(0.5-13.6)	1.1(0.4-3.2)	0.6
<i>OM IL-6</i> (pg/ml)	2.6(1.9-6.3)	1.3(0.8-1.1)	0.6

Data are shown as mean (SD) or median (interquartile range).

Table 3: Adipokine secretion from tissue explants after 24h incubation

In this cohort, shown in Table 3, overall leptin and adiponectin were released to a greater extent from the sub-cutaneous, as opposed to the omental depot, while NPY was more abundant in the omental depot. Surprisingly there was no marked depot specific difference in the release of IL-6 or MCP-1 release.

There was no difference in the local production of inflammatory adipokines, IL-6 and MCP-1, between either depots of the PO/DM and the MHO population. Local abdominal adipose adiponectin secretion was also not different between the patients.

Only leptin was secreted in greater quantities by the subcutaneous adipose tissue of the PO/DM population.

3.1.4 IL-1 β induction of IL-6 secretion

In order to determine the viability and hormone responsiveness of human adipose tissue after explantation and further manipulation of inflammatory microRNAs such as miR-146b, the

capability of adipose tissue to be release IL-6 in response to IL-1 β after 65 hours of culture ex vivo from sample collection was investigated. The results of the experiment carried out on subcutaneous adipose tissue explants of 12 patients are shown in Table 4 and Figure 20.

Average IL-6 (ng/ml/mg of tissue)	
Control samples (n= 8)	140.4
10ng/ml IL-1 β (n = 12)	271.6
p – value	<0.001

Table 4: Average sub-cutaneous IL-6 secretion after stimulation with IL-1 β
The tissue had been in ex vivo organ cultures for upto 65h and then induced with IL-1 β for 8h (n = number patients in group, control group is incubation without added IL-1 β 65h post-explantation of tissue).

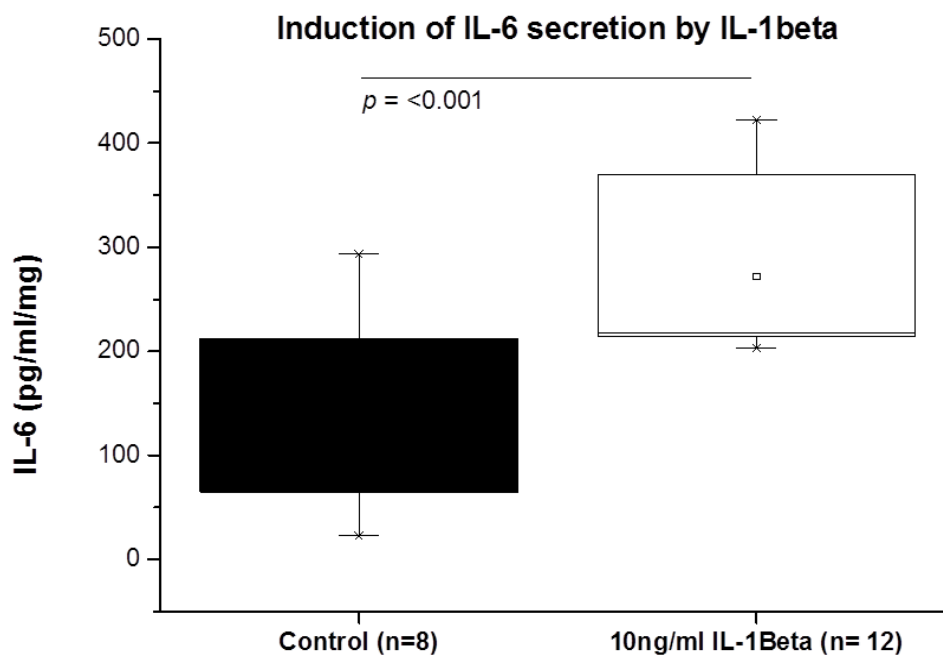


Figure 20: Secretion of IL-6 from subcutaneous adipose tissue after induction with IL-1 β . Black = control (untreated) tissue, white = tissue treated with both patient group explants were maintained ex vivo for 65h prior to induction with 10ng/ml IL-1 β for 8h. Error bars represent S.D.

3.1.5 Patient characteristics following surgical weight loss

A sub-group of patients (10 MHO, 13 PO) were monitored 3-6 months after the operation during a follow-up visit (see study structure in methods chapter) in order to discern any possible changes between the healthy and non-healthy obese patient groups in effectiveness of bariatric surgery on weight loss and metabolic parameters.

In order to assess the clinical consequences of bariatric surgery on the two different patient groups, a blood test on a subset of study participants was carried out on a period ranging from surgery day (“before” in Table 5) to 3-6 months after surgery (“after” in Table 5). The clinical parameters are shown in Table 4. The significant changes observed were a weight loss, shown by reduction of BMI, and circulating NEFA levels in both groups. There was an increase in LDL-cholesterol in the PO/DM group and serum adiponectin in both groups following surgery. HDL-cholesterol increased significantly in the PO/DM group, and Insulin levels and HOMA-IR index only decreased significantly in the PO/DM group. While levels of NPY decreased in both groups it did not reach significance. Fasting plasma glucose did not change after weight loss in either group, however total cholesterol increased in both groups significantly.

Category	MHO	MHO <i>p</i> against		PO/DM <i>p</i> against
		before	PO/DM	
<i>n</i> (after surgery)	10		13	
BMI (kg/m ²) Before	46(6)		46.9(7.9)	
BMI (kg/m ²) After	39.0(7.9)	<0.001	37.1(5.6)	<0.001
FPG (mmol/L) Before	4.7(0.7)		5.6(1.8)	
FPG (mmol/L) After	4.9(0.4)	0.9	5.0(1.1)	0.2
TC (mmol/L) Before	3.7(8.5)		3.9(1.2)	
TC (mmol/L) After	4.1(0.7)	0.01	4.8(0.9)	0.02
LDL (mmol/L) Before	2.1(0.8)		2.2(1.1)	
LDL (mmol/L) After	2.4(0.8)	0.3	3.1(0.7)	0.04
HDL (mmol/L) Before	1.0(0.2)		0.96(0.3)	
HDL (mmol/L) After	1.2(0.5)	0.2	1.2(0.3)	0.001
Triglycerides (mmol/L) Before	1.1(0.9-1.7)		1.5(1.2-2.1)	
Triglycerides (mmol/L) After	0.95(0.9-1.1)	0.5	1.3(0.9-1.6)	0.2
Insulin (miU/ml) Before	4.5(3.2-5.6)		13.7(7.1-16)	
Insulin (miU/ml) After	4.2(3.2-5.4)	0.9	7.4(4.1-9.8)	0.009
HOMA-IR Before	0.9(0.6-1.2)		2.2(1.5-4.1)	
HOMA-IR After	0.9(0.7-1.2)	0.7	1.6(0.9-2.1)	0.009
Serum Adiponectin (µg/ml)				
Before	6.1(3.4-9.7)		3.0(1.9-5.2)	
Serum Adiponectin (µg/ml)				
After	14.3(8.6-22.8)	0.01	6.0(3.7-13.3)	0.005
Serum NPY before (pg/ml)	6.3(3.7-12.3)		11.4(5.4-18.2)	
Serum NPY after (pg/ml)	3.9(1.5-9.6)	1	7.3(3.5-13.6)	0.07
Serum NEFA before (mmol)	1.1(0-9-1.4)		1.2(1-1.5)	
Serum NEFA after (mmol)	0.5(0.4-0.6)	0.02	0.5(0.3-0.6)	0.002

Data are shown as mean (SD) or median (interquartile range).

Table 5: Patient characterises following weight loss

3.2 Histology investigation

3.2.1 Adipocyte area

With evidence discussed in Chapter 1 (and analysed using the method described in the relevant chapter of this thesis) regarding adipose tissue remodelling and dysfunction underlying some of the differences in insulin sensitivity between the MHO and PO, the possibility of morphological changes in the subcutaneous and omental depots of the two populations was examined.

Subcutaneous	MHO	PO	P
<i>N (cells traced)</i>	849	571	
<i>Area (pixels)</i>	3400(1954-5275)	5309(3154-7684)	<0.001
Omental	MHO	PO	P
<i>N (cells traced)</i>	582	739	
<i>Area (pixels)</i>	5059(2665-7790)	6186(3025-9653)	<0.001

Data are shown as median (interquartile range).

Table 6: Adipocyte size of SC and OM adipose tissue

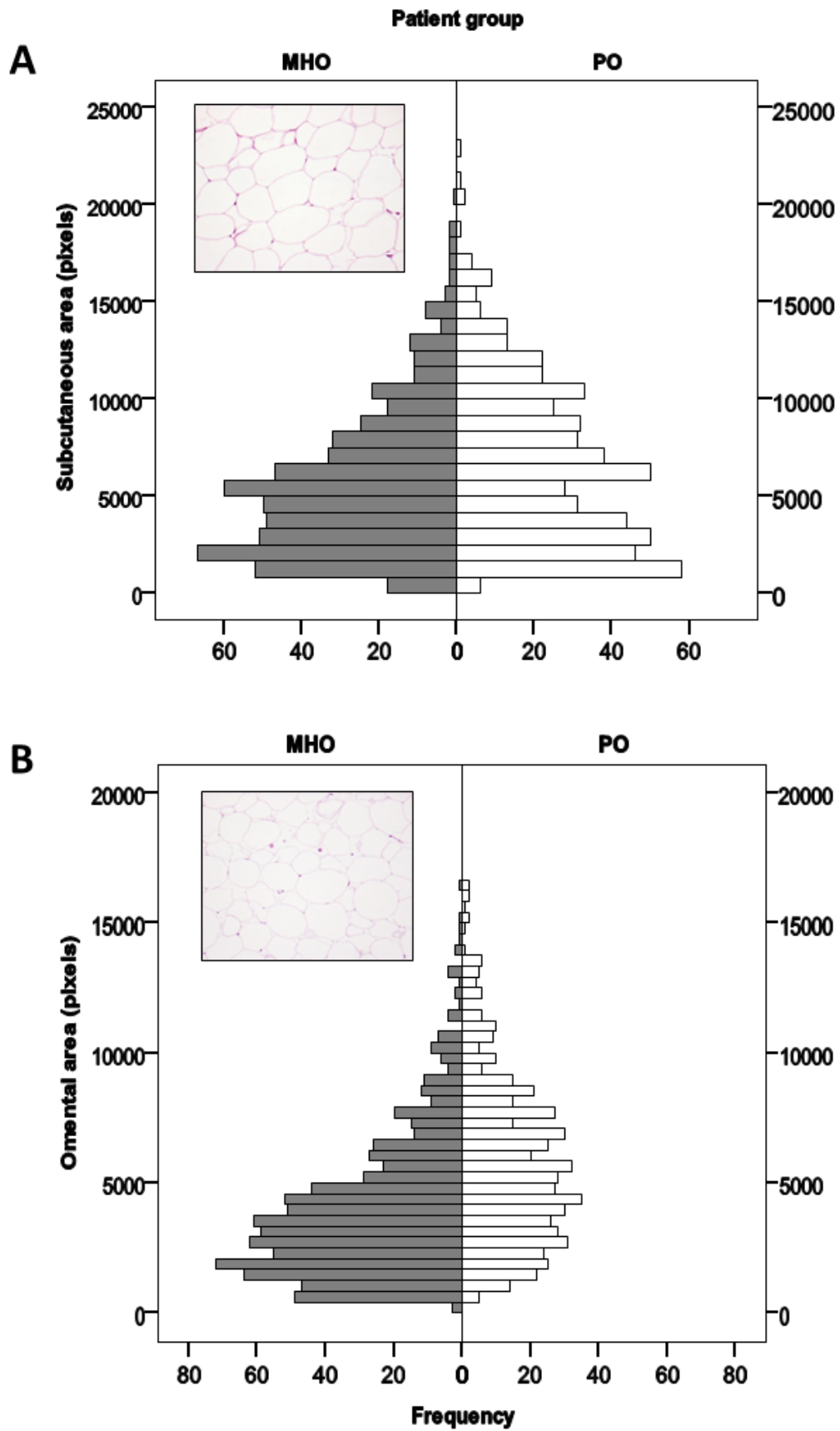


Figure 21: Distribution of adipocyte area. Frequency histogram based on data in Table 6 shows number of cells observed in the x-axis in a specific area range shown by the y-axis in pixels. Gray = MHO cells White = PO cells

(A: SC Adipocyte area frequency histogram [blue are MHO n=849, green are PO n=571] B: OM [blue as MHO n=582, green as PO n=739] adipocyte area frequency histogram)

Table 6 and Figure 21 show that both depots of the PO patients had significantly larger adipocytes compared to the MHO, as estimated by area. Figure 21 displays a shift in frequencies of the larger adipocytes in both the SC and OM depots of the PO individuals, while Table 6 that the overall size (area) of the adipocytes was larger in the PO compared MHO tissue.

3.2.2 Adipose tissue CD68+ cells

In order to gage inflammatory cell infiltration into the adipose tissue that putatively accompanies the adipocyte hypertrophy the presence of “crown-like structures” was investigated (48). These structures should contain CD68+ monocyte macrophages. However, no significant difference in CD68+ staining between MHO and PO patients (Table 7) were apparent. Despite the presence of crown-like structures in some patients this seemed independent of metabolic status (Figure 22A).

Group	MHO	PO	p value
<i>N (number of patients)</i>	4	9	
	1670.5	1717.0	
<i>SC DAB (pixels)</i>	(983.8-2558.5)	(1097.0-2862.0)	0.39
	2070.5	2075.0	
<i>OM DAB (pixels)</i>	(999.0-3260.0)	(1273.0-3172.0)	0.88
p value	0.12	0.52	

Data are shown as median (interquartile range).

Table 7: Histological quantification of inflammatory cell infiltration. CD68+ DAB staining in SC and OM adipose tissue of MHO and PO patients.

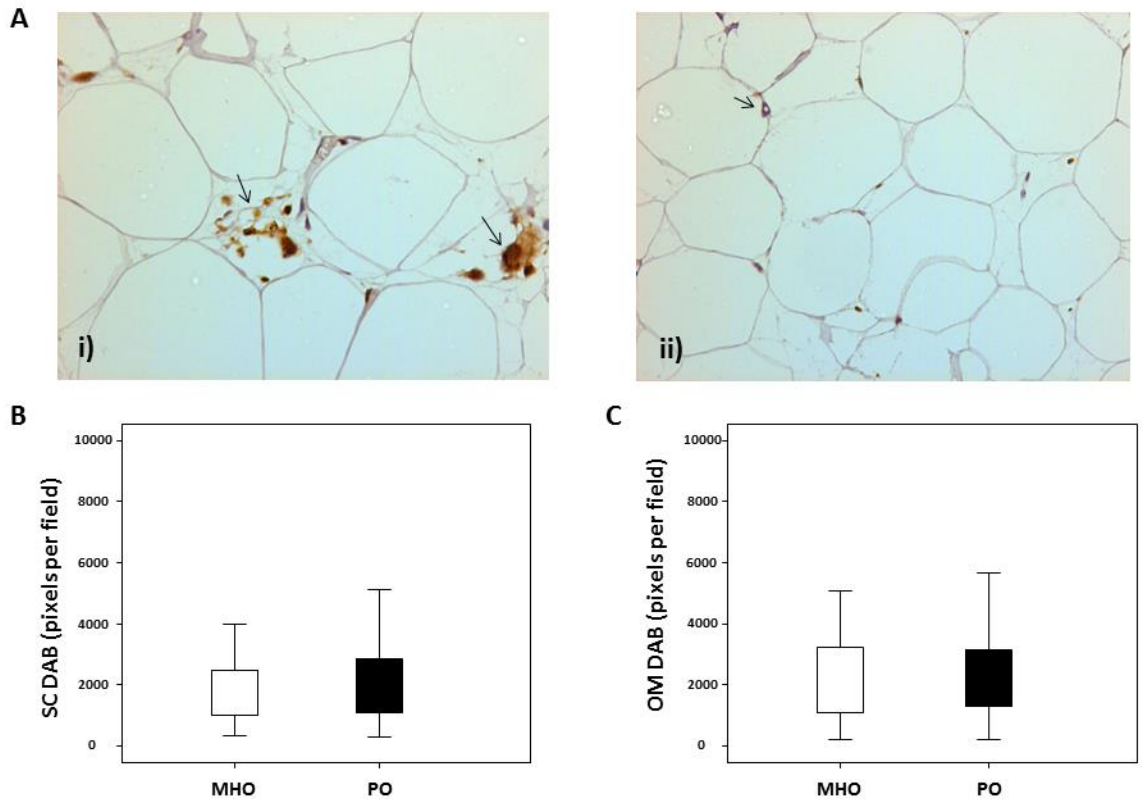


Figure 22: Inflammatory cell infiltration into adipose tissue.
(A) CD68+ staining in SC (i) and OM (ii) adipose tissue. Boxplots for SC (B) and OM (C) show no difference in DAB staining between MHO and PO patients. Error bars represent SD

3.2.3 NPY receptor staining in tissue

Systemic NPY is elevated in the PO/DM cohort (Table 2), along with local release of the peptide from both adipose depots (Table 3) and adipocyte hypertrophy. In order to investigate the direct effects of NPY in these depots in an autocrine/paracrine fashion the expression of NPY receptors were investigated, with NPY receptors 1 and 5 being specifically investigated in line with previous studies in the RNA expression of these receptors showing them to be detectable as well as previous studies in the literature.

NPY receptor expression was detectable on the adipocyte cell surface but this was not different between the depots or the groups (Table 8 and Figure 23).

<u>Tissue DAB stain (AU)</u>	MHO (n=4)	PO (n=8)	<i>p-value</i>
Y1 SC	6300.0 (4783.3-9823.3)	6132.5 (4193.7-7875.5)	0.44
Y1 OM	8836.5 (4681.3-18499.5)	7801.5 (6530.3-10205.3)	0.61
	MHO (n=4)	PO (n=8)	<i>p-value</i>
Y5 SC	6551.0 (2968.5-7242.0)	4940 (3826.5-6769.5)	0.80
Y5 OM	10207.0 (6787.0-7242.0)	8486 (6349.8-12068.3)	0.73

Data are shown as median (interquartile range).

**Table 8: NPY receptor expression.
Immunohistochemistry quantification in arbitrary units (AU) between MHO and PO
subcutaneous and omental adipose tissue**

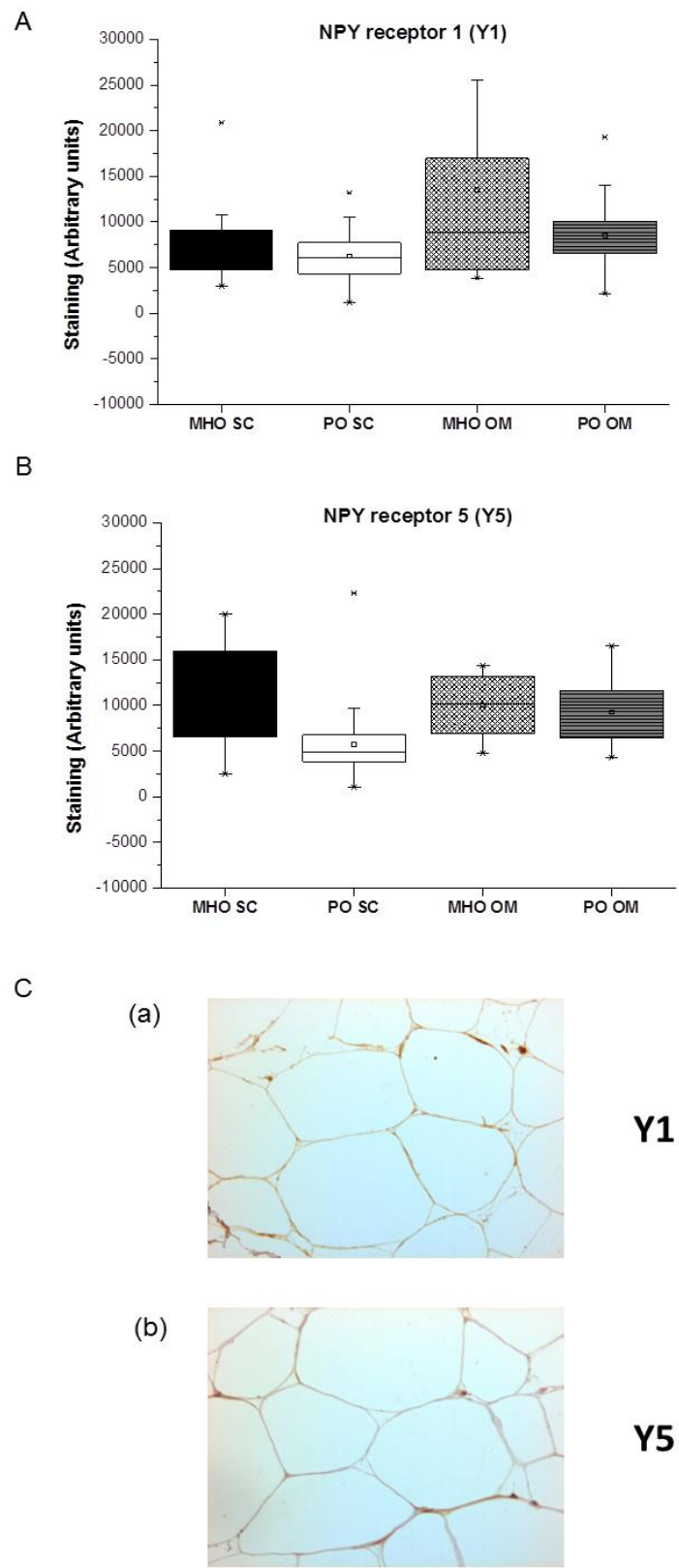


Figure 23: NPY receptors Y1 and Y5 in MHO and PO adipose tissue. (A = Y1 receptor density, B = Y5 receptor density, C = example staining in adipose tissue with (a) Y1 receptor and (b) Y5 receptor antibody. Error bars represent SD

3.2.4 Blood vessel-associated NPY receptor quantification

As NPY is a potent vasoactive molecule the expression of its receptors associated with the vasculature was further probed.

<u>Vessel DAB stain (AU)</u>	MHO (n=12 vessels)	PO (n=30 vessels)	p-value
Y1 SC	0.1198 (0.0989-0.1976)	0.1777 (0.1495-0.2297)	0.04
Y1 OM	0.1242 (0.1053-0.1485)	0.1353 (0.1155-0.1800)	0.37
p-value	0.64	0.03	
	MHO (n=6 vessels)	PO (n=21 vessels)	p-value
Y5 SC	0.1165 (0.978-0.1245)	0.1777 (0.1274-0.2426)	0.006
Y5 OM	0.1342 (0.1061-0.1923)	0.1973 (0.1576-0.2399)	0.02
p-value	0.35	0.66	

Data are shown as median (interquartile range).

Table 9: NPY blood vessel staining quantification

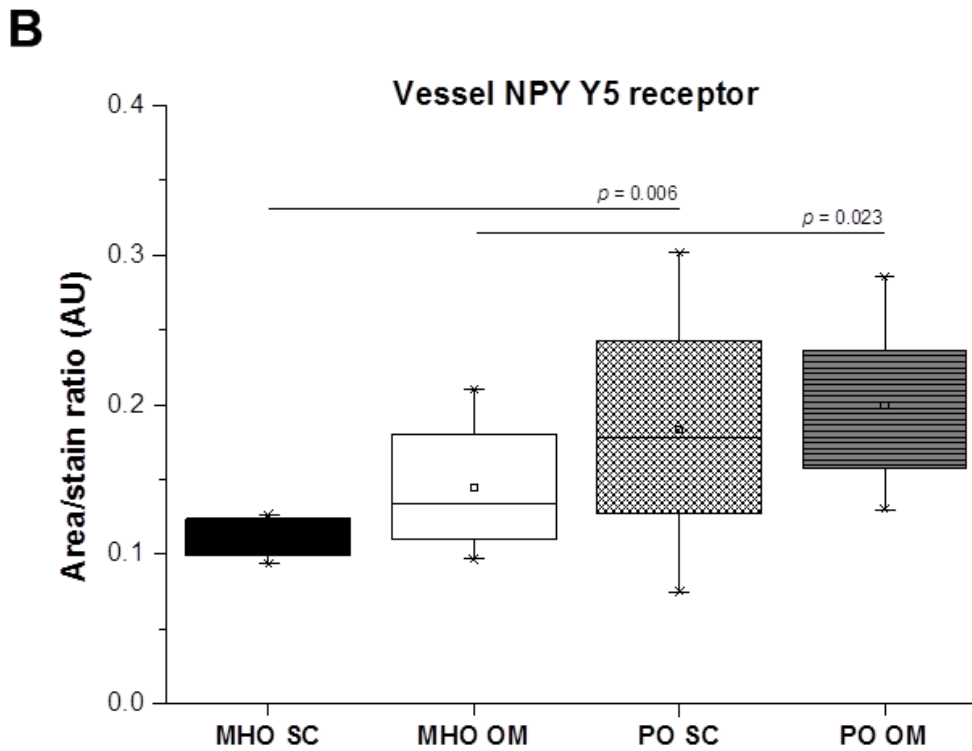
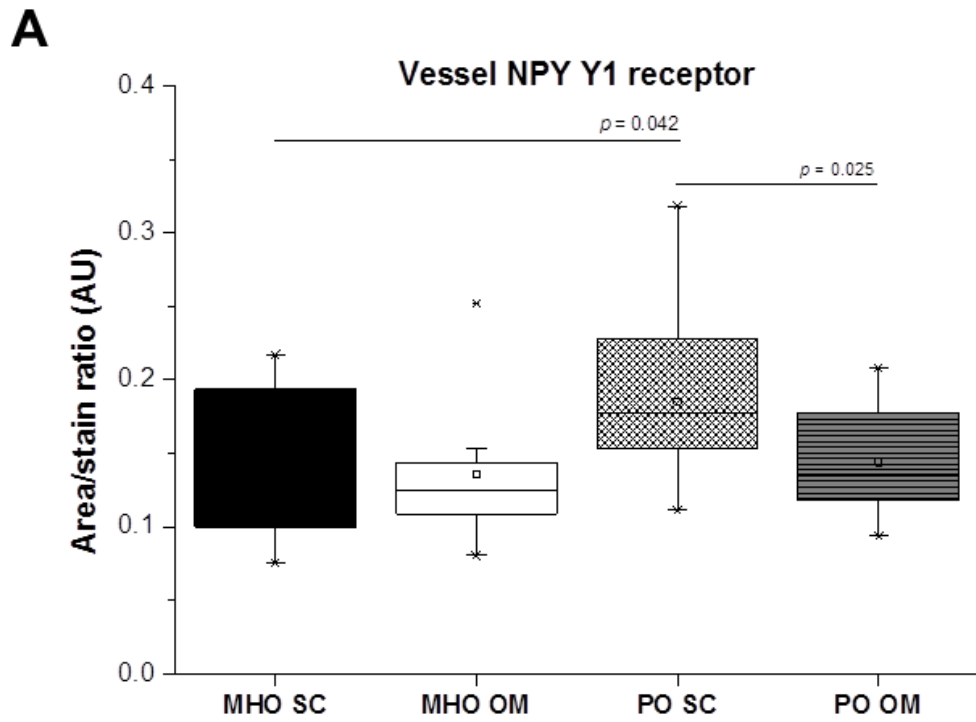


Figure 24: NPY receptor Y1 and Y5 staining associated with vessels in adipose tissue in the various patient groups from data described in table 9. (A = Y1 receptor, B = Y5 receptor). Error bars represent SD.

Overall much of the receptor expression was indeed associated with the vasculature. In the MHO both Y1 and Y5 were expressed equally in both depots. However, in the PO the sub-cutaneous depot had higher levels of Y1 compared to omental, but Y5 was comparable in the depots. Further, compared to the MHO, Y1 was higher in the sub-cutaneous of the PO, while Y5 was higher in both depots of these patients (Figure 24 and Table 9).

3.3 Adipose tissue transcriptional studies

The data in the preceding section showed hypertrophy of adipocytes in both the depots of the PO compared to the MHO. Hypertrophy may be indicative of inhibition in adipogenesis. Therefore the expression of key regulators of adipogenesis was examined in the whole tissue of these patients via total RNA extraction.

3.3.1 Adipogenesis: adipocyte PPAR γ expression

The expression of PPAR γ 2, considered to be the adipogenic “master switch” (169) was determined and the relative expression compared to the MHO group (Figure 25).

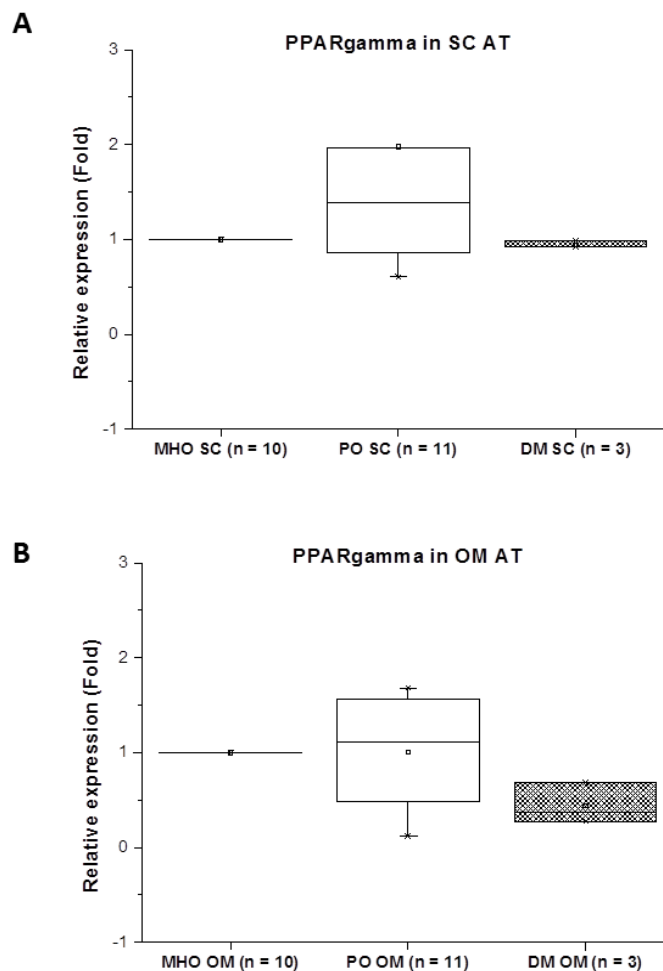


Figure 25: PPAR γ 2 expression in (A) subcutaneous and (B) omental adipose tissue. Error bars represent SD. Values of relative expression shown against control value of 1 for MHO group used as reference for other PO and DM groups.

The level of expression in the MHO patients was taken as 1 and expression in the tissue from the other groups shown relative to this.

The results did not show any significant differences between the groups or the depots. The SC adipose tissue showed a trend towards greater (0.5-fold) relative expression of PPAR γ expression in the PO compared to the MHO, with the type 2 diabetes group (DM) showing a comparable level. In the omental the expression was lowest in the DM (Figure 25). However, none of these changes were statistically significant.

3.3.2 Metabolism: adipocyte SCD1 expression

To probe for any change in regulators of cellular metabolism the expression of an important lipid homeostasis enzyme, Stearoyl-CoA desaturase -1 (SCD1), which is activated by the transcription factor SREBP-1c and is responsible for the conversion of saturated fatty acids to monounsaturated fatty acids (MUFA), was investigated. Expression of SCD1 may also reflect differences in local inflammation given the close link between MUFA levels and adipose tissue inflammation (170).

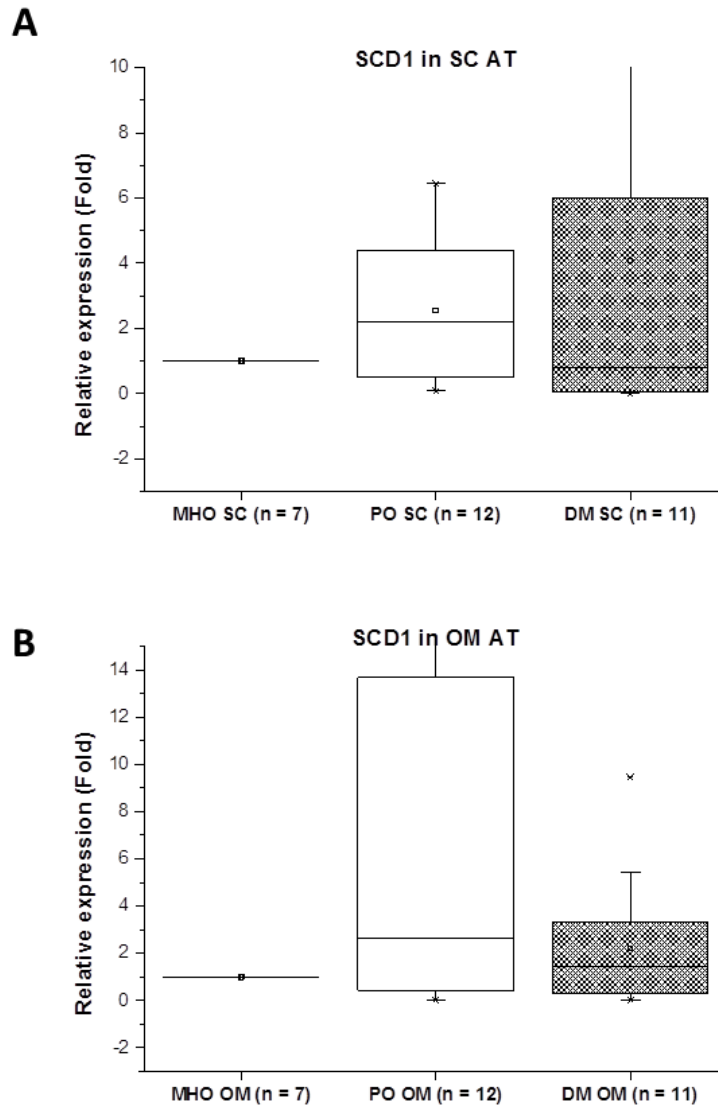


Figure 26: SCD1 expression in (A) subcutaneous and (B) omental adipose tissue. Error bars represent SD. Values of relative expression shown against control value of 1 for MHO group used as reference for other PO and DM groups.

The level of expression in the MHO patients was taken as 1 and expression in the tissue from the other groups shown relative to this.

There was a trend towards greater expression of adipose tissue SCD1 in both depots of the PO compared to the MHO group, with the omental depot showing the greatest difference. The DM group showed lower expression in the subcutaneous depot but greater expression in the omental. However, none of these changes were statistically significant (Figure 26).

3.3.3 Adipocyte NPY receptor expression

The mRNA expression of NPY receptors was investigated. Y1 and Y5 were the most abundant species.

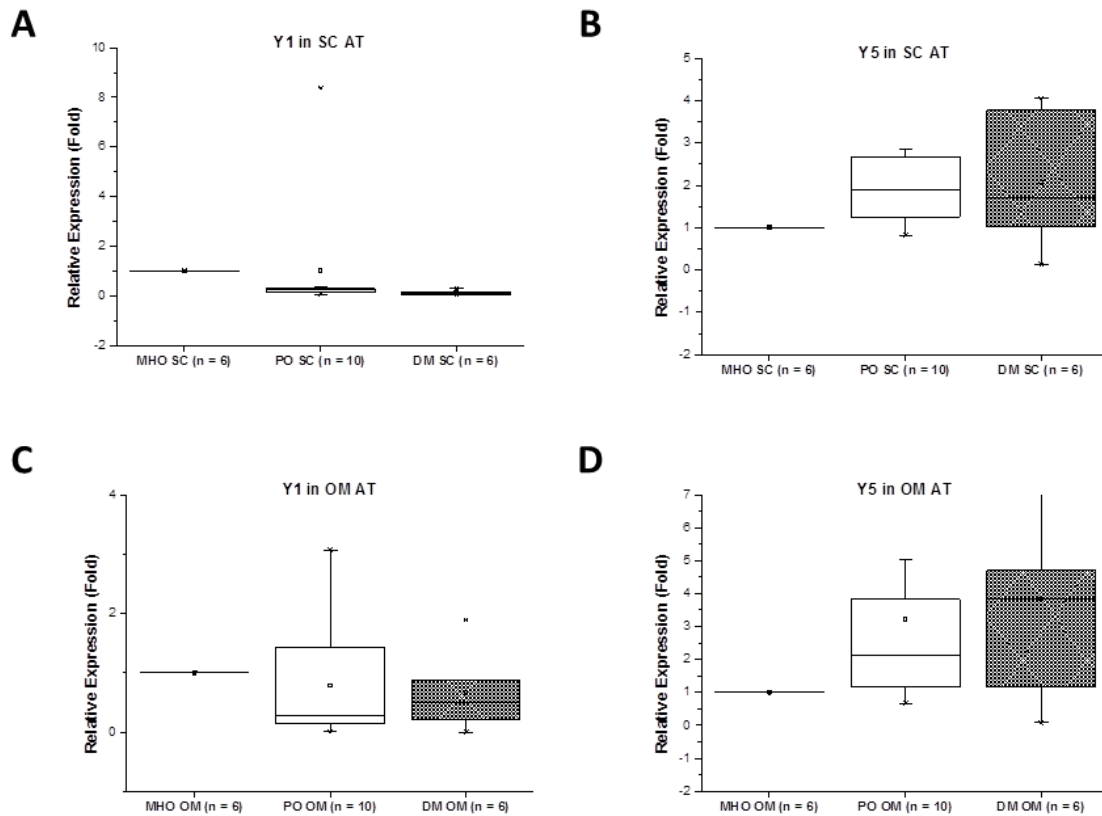


Figure 27: NPY receptor 1 (A, C) and 5 (B, D) RNA expression in subcutaneous and omental adipose tissue. Error bars represent SD. Values of relative expression shown against control value of 1 for MHO group used as reference for other PO and DM groups.

The differences in expression between the groups (Figure 27) was not statistically significant, although the trend showed a decrease in Y1 expression with worsening metabolic status compared to the MHO group in both depots. Conversely, Y5 appeared to increase in both PO and DM groups compared to the MHO control, showing a trend towards greater expression with worsening metabolic status.

3.3.4 Adipose tissue siRNA knockdown

As it was shown that the tissue remains responsive to cytokine stimulation for up to 65 hours, a pilot study was carried out to knock-down a specific microRNA, miR-146b, which may be responsible for the inflammatory response to IL-1 β in cells (171) and thought to be diversely modulated in inflamed (and therefore insulin resistant) adipocytes (172). Using the subcutaneous adipose tissue from a single patient microRNA was knocked down and IL-6 secretion measured with and without IL-1 β stimulation.

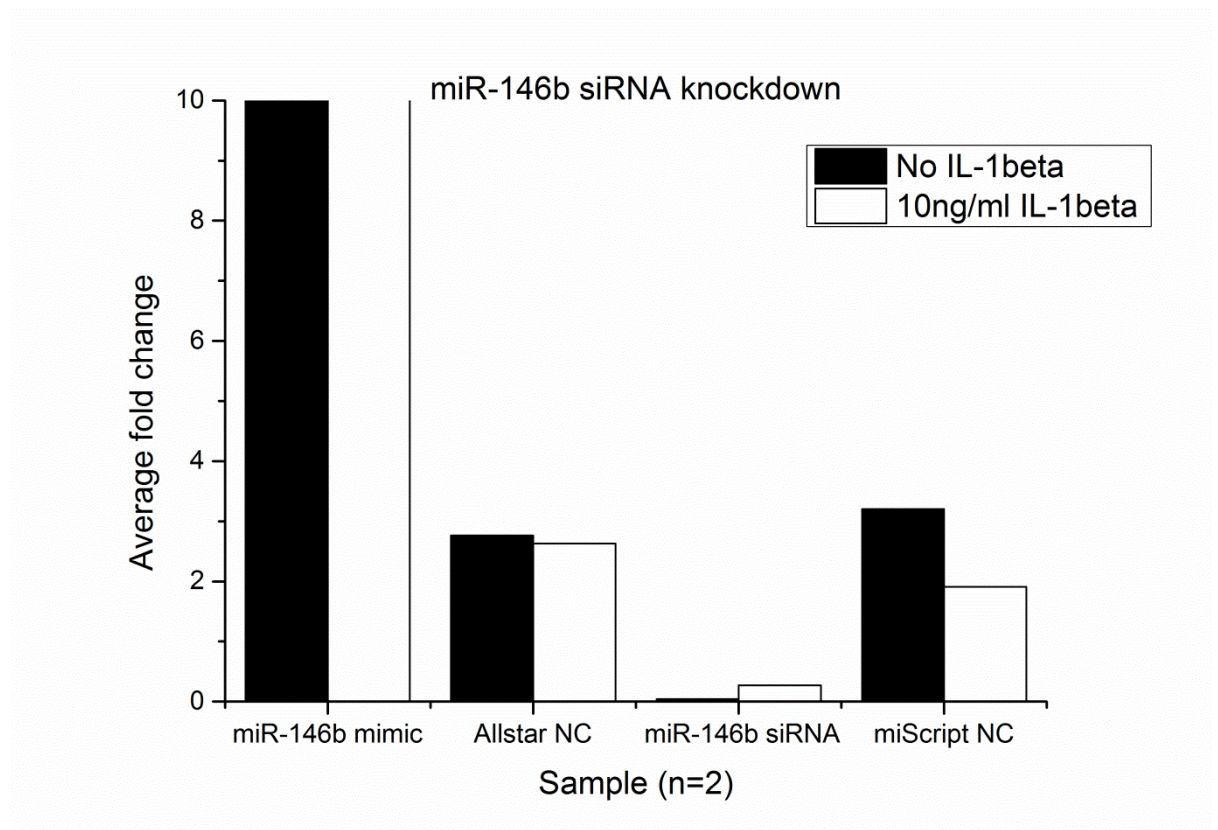


Figure 28: miR-146b expression knockdown in adipose tissue after electroporation and 65h incubation.

The miR-146b mimic caused an increase in the gene expression compared to the two negative controls, while the siRNA dramatically decreased the levels of detectable miR-146b in the subcutaneous adipose tissue (Figure 28).

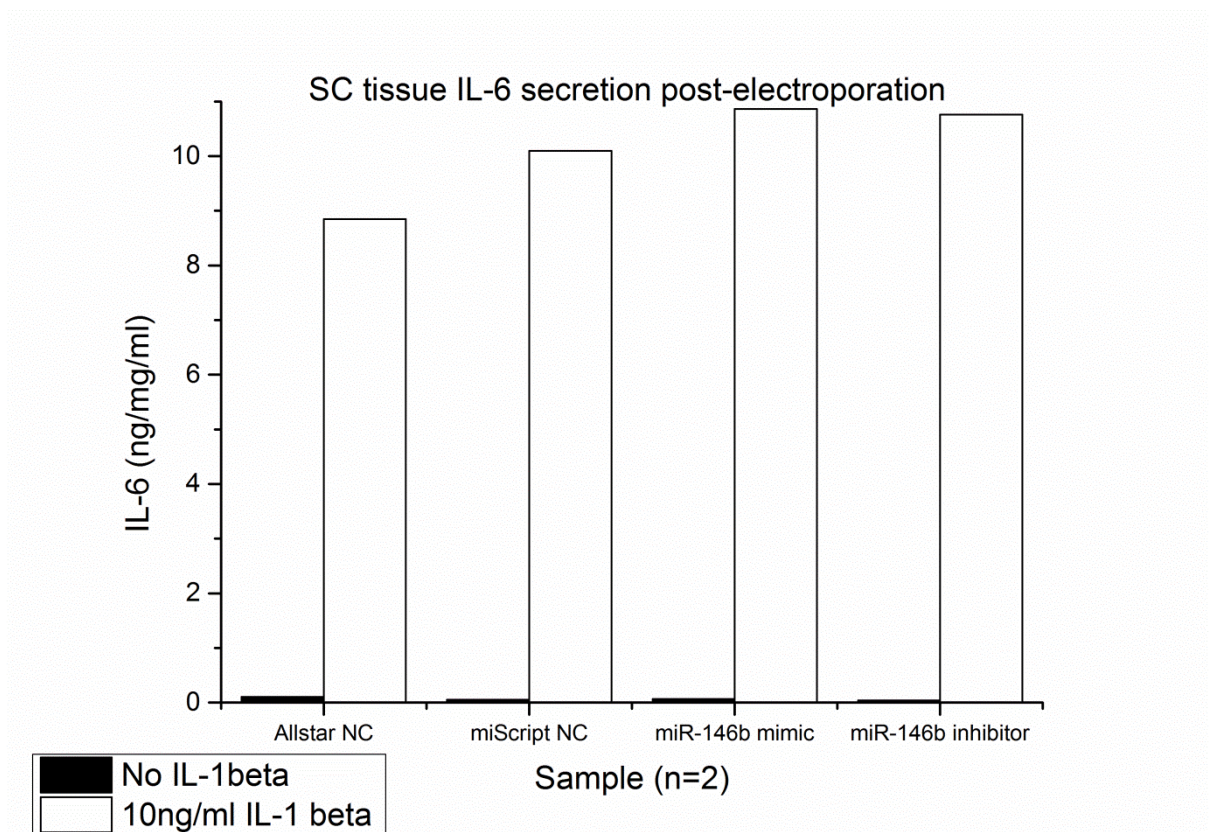


Figure 29: Subcutaneous adipose tissue IL-6 secretion following tissue electroporation and IL-1 β stimulation after 65 hours

However, despite the differences in miR-146b expression in the different samples the effect on IL-1 β -induced IL-6 secretion by the tissue was negligible (Figure 29). Thus miR-146b did not appear to modulate IL-1 β stimulation of IL-6.

3.4 Brain stem astrocyte in vitro studies

Circulating NPY was shown to be secreted by adipose tissue and was specifically elevated in the PO/DM cohort in whom both dyslipidaemia and hypertension was elevated. Thus it was decided to test the hypothesis that NPY could have an effect on cells of the central nervous system, specifically the brain stem, which mediates hypertension. This was investigated *in vitro* using a primary cell line of astrocytes of human foetal origin. Experiments were designed to simulate the effects of prolonged SNS activity on the chemosensory astrocytes.

3.4.1 Astrocyte NPY receptor immunohistochemistry

The expression of NPY receptors on the surface of the brain stem astrocyte cells was confirmed using immunofluorescence and confocal microscopy. The presence of Y1 receptor on the cell surface was ascertained (Figure 30A), and to a lesser degree that of the Y5 receptor (Figure 30B).

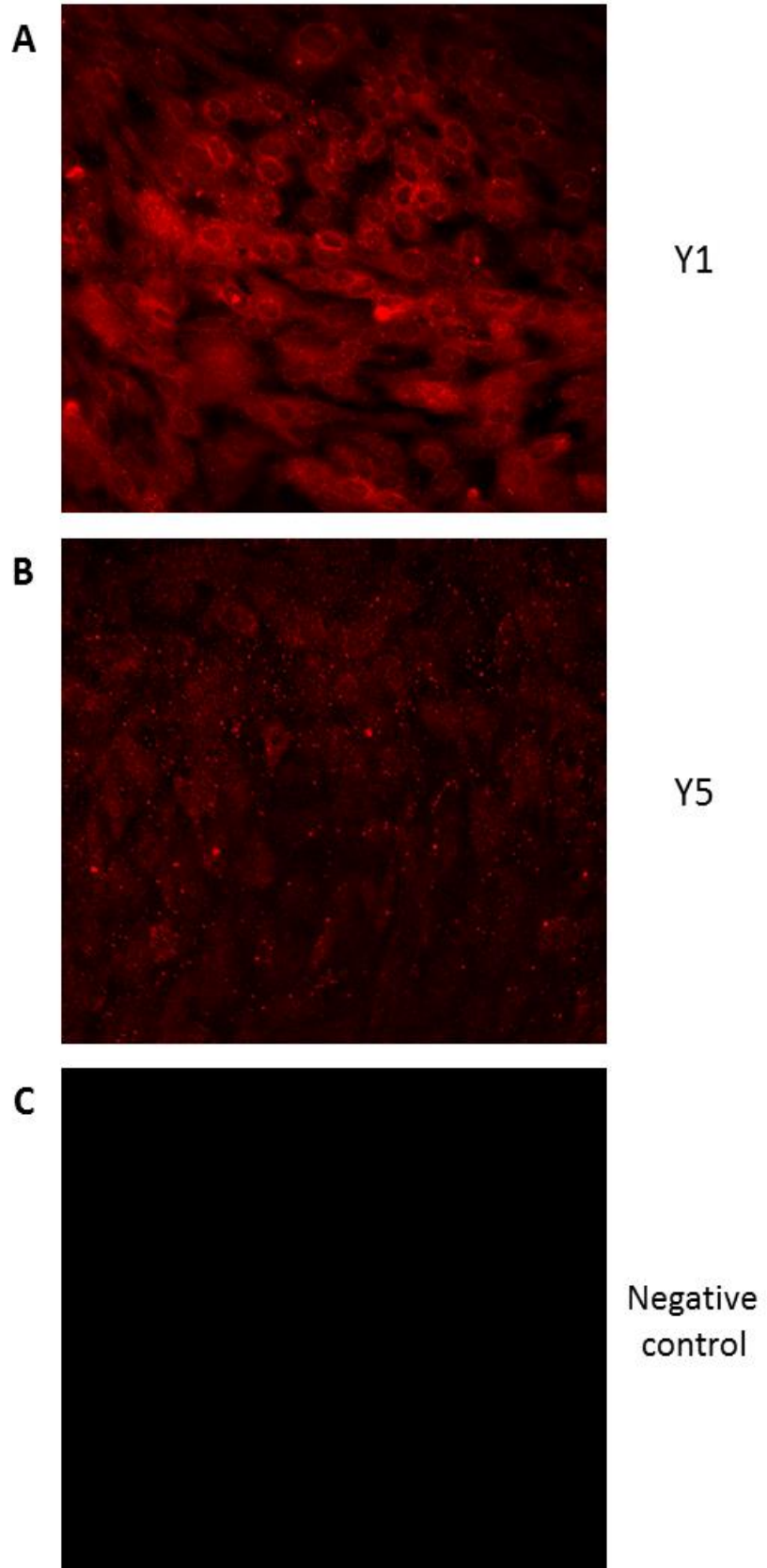
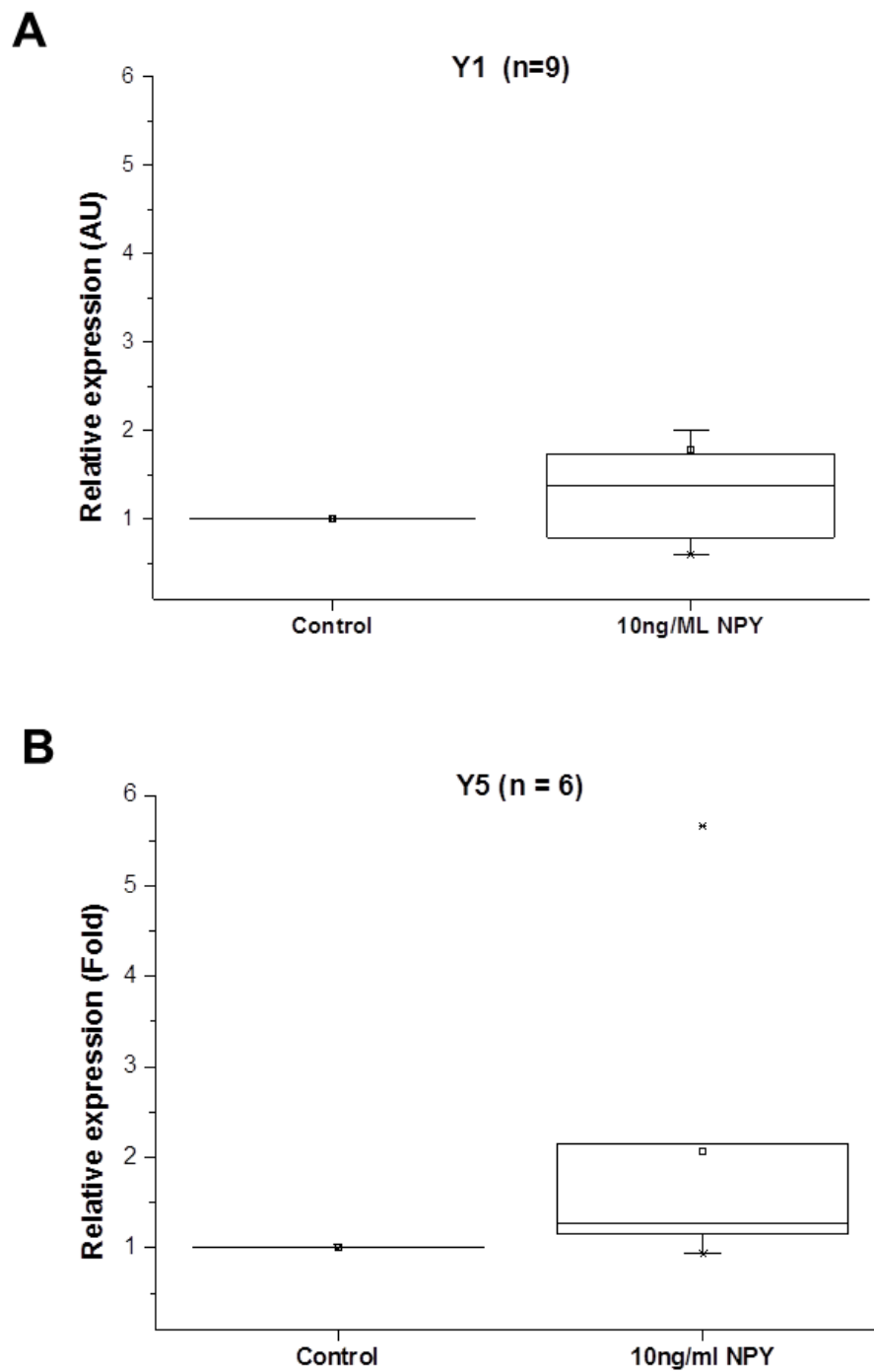


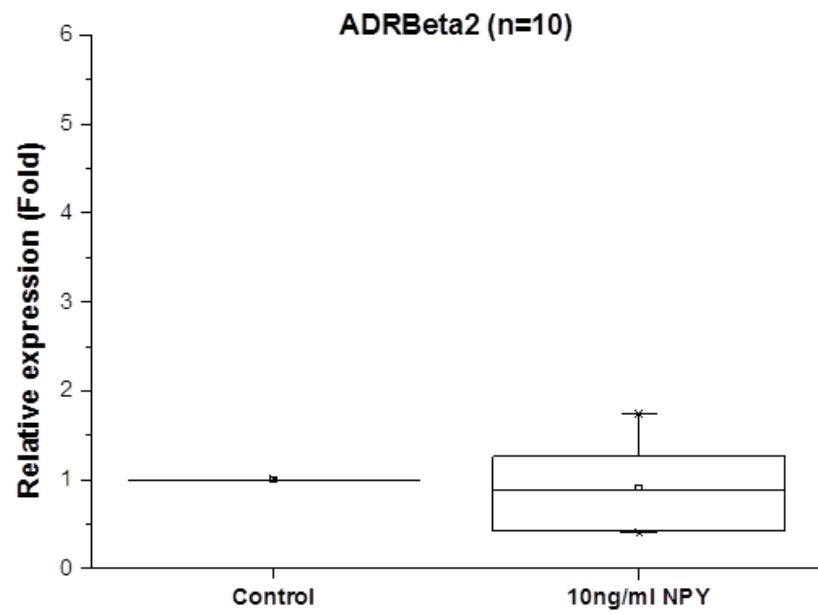
Figure 30: Astrocyte receptor Y1 (A) and Y5 (B) immunohistochemistry for detection of receptors on cell surface

3.4.2 Astrocyte NPY receptor transcription modulation in response to NPY

The modulation of expression of the NPY receptors in response to NPY was determined, along with those of other adipokine receptors, such as the leptin receptor, as well as the β 2 adrenoceptor. Further studies examined the effect of both NPY and leptin exposure.



C



D

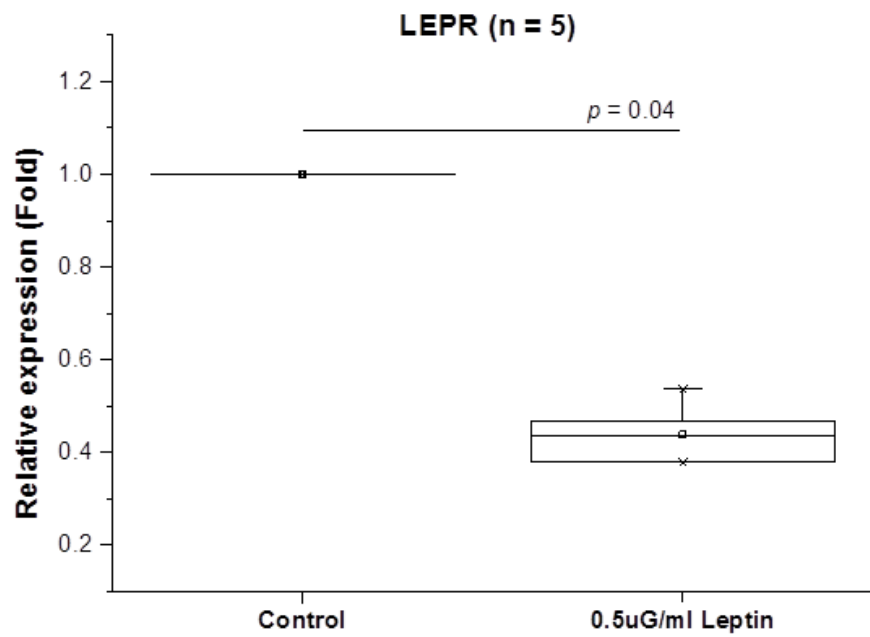


Figure 31: Astrocyte mRNA expression of (A) Y1, (B) Y5 and (C) Beta2 adrenergic receptors and (D) leptin receptor. Error bars represent SD

Response to NPY treatment (A-C) and leptin receptor expression in response to leptin treatment (D) were examined.

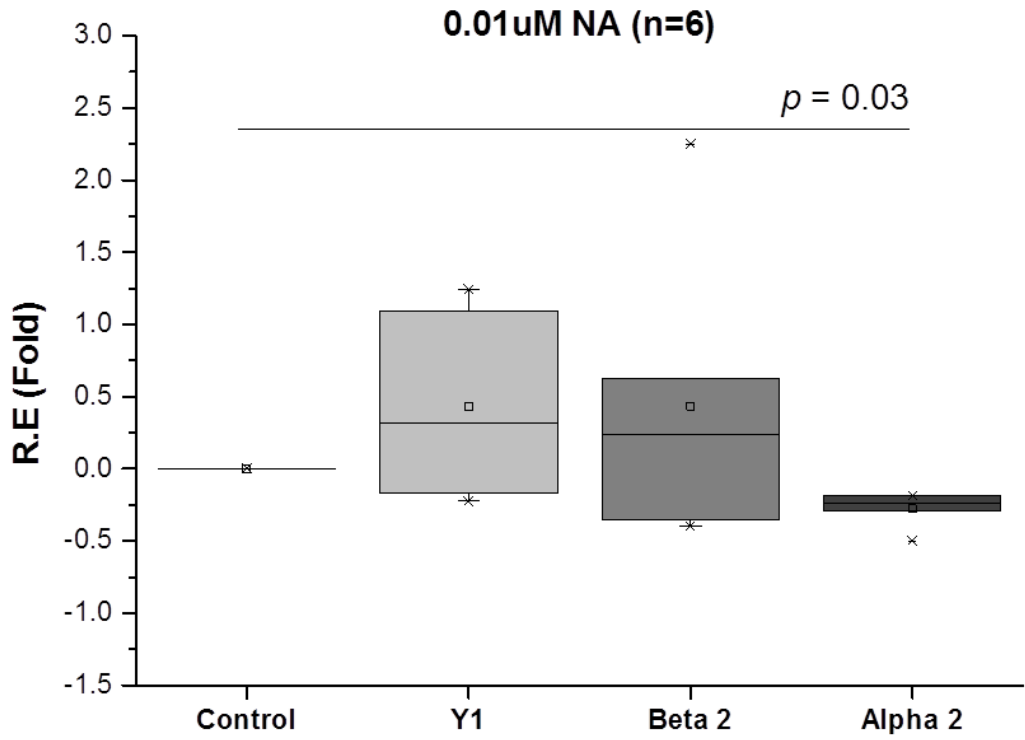
The Y1 and Y5 receptors were expressed at the mRNA level as confirmed by Figure 31A and Figure 31B, as well as the presence of adrenergic receptor β_2 , although expression did not seem to change after overnight NPY exposure. The astrocytes expressed human leptin receptor and modulation of expression occurred after exposure to 50ng/ml leptin overnight at a statistically significant level with an overall decrease in total expression to about half that of the control.

3.4.3 Astrocyte NPY/adrenergic receptor transcription in simulated SNS activity

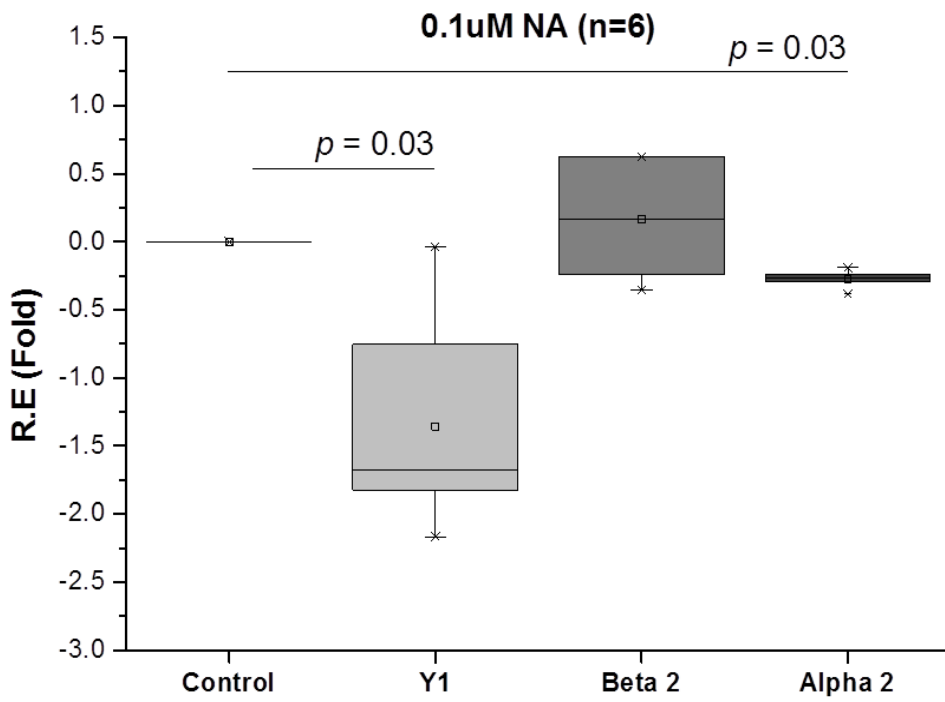
Due to the lack of modulation with NPY alone in the preliminary results, the next part of the investigation into astrocyte susceptibility to SNS activity was to determine the presence and the reactivity of receptors in the conditions of simulated SNS activity, with the presence of a neurotransmitter, noradrenaline, and NPY in combination. The expression of NPY receptor 1, which was more abundant in these cells, along with those of adrenoceptors β_2 and α_2 were investigated. Treatment conditions included the SNS neurotransmitter noradrenaline (at 0.01 μ M and 0.1 μ M concentrations) and/or recombinant human NPY (at 10ng/ml or 2.3mM), to simulate heightened activity.

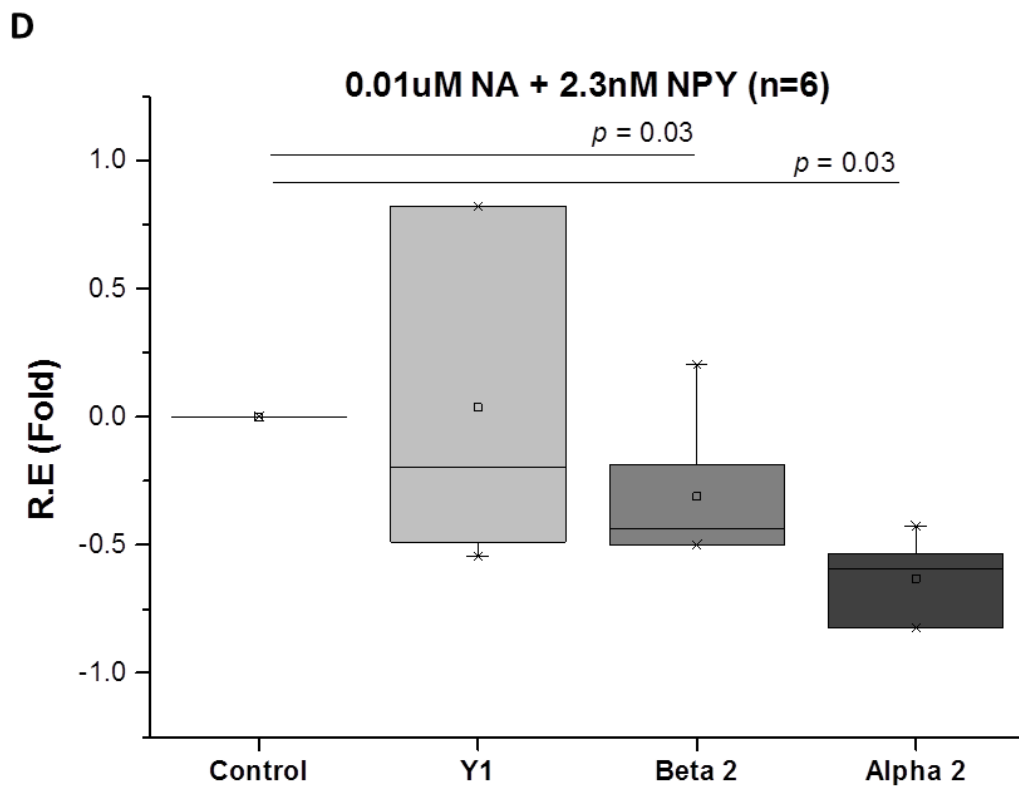
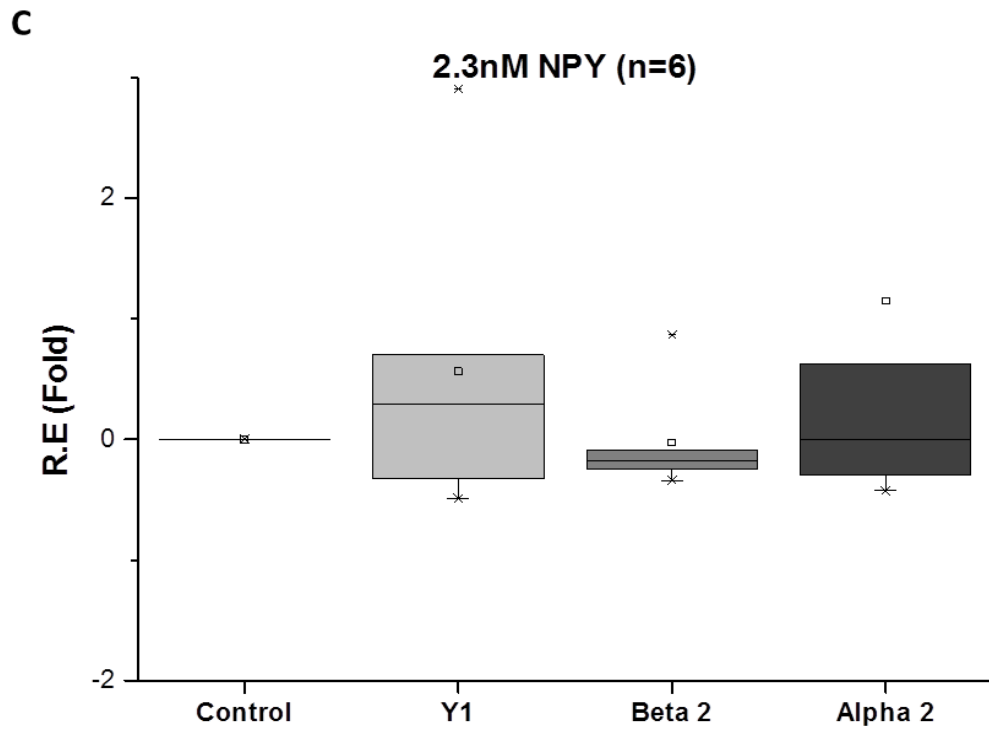
There was a slight, but statistically significant, decrease in adrenergic receptor α_2 expression after exposure to the lower (0.01 μ M) concentration of NA (Figure 32A). At higher doses of NA to 0.1 μ M (Figure 32B) Y1 receptor decreased significantly, along with the slight decrease in α_2 expression seen with the lower dose. NPY alone did not cause any significant changes in the expression of any receptors (Figure 32C). However in combination, lower NA concentration (Figure 32D) caused a statistically significant decrease in β_2 expression as well as the decrease in α_2 observed previously. Figure 32E showed the combination of molecules at the higher NA concentration, where there was a statistically significant increase in Y1 expression by 1.5-fold.

A



B





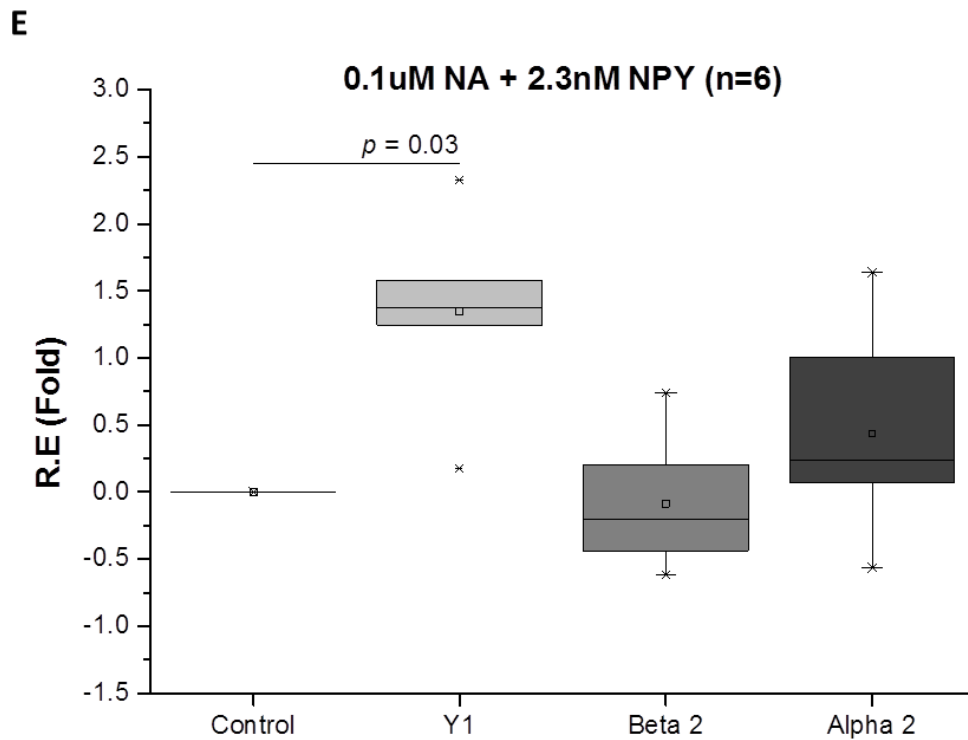


Figure 32: Relative mRNA expression in NPY receptor Y1 and adrenergic receptors β_2 and α_2 in the presence of NPY and/or noradrenaline
(A = 0.01 μ M noradrenaline, B = 0.1 μ M noradrenaline, C = 2.3nM NPY, D = 0.01 μ M noradrenaline + 2.3nM NPY, E = 0.1 μ M NA + 2.3nM NPY). Error bars represent SD

3.4.4 Astrocyte inflammatory mediator secretion

The effects of the combination of noradrenaline and NPY on the secretion of inflammatory mediators such as MCP-1 and IL-6 were investigated. This was done with the rationale that inflammation could compromise functionality of the brain stem astrocytes and damage their chemo- and baroreflex regulatory capacity.

Other than IL-1 β (positive control), only NPY (2.3nM) significantly induced MCP-1 release from these cells (Figure 33A). However NA (0.1 μ M), NPY (2.3nM) and the combination of NA (at 0.01 and 0.1 μ M) with NPY (2.3nM) all caused significant IL-6 release from astrocytes (Figure 33B).

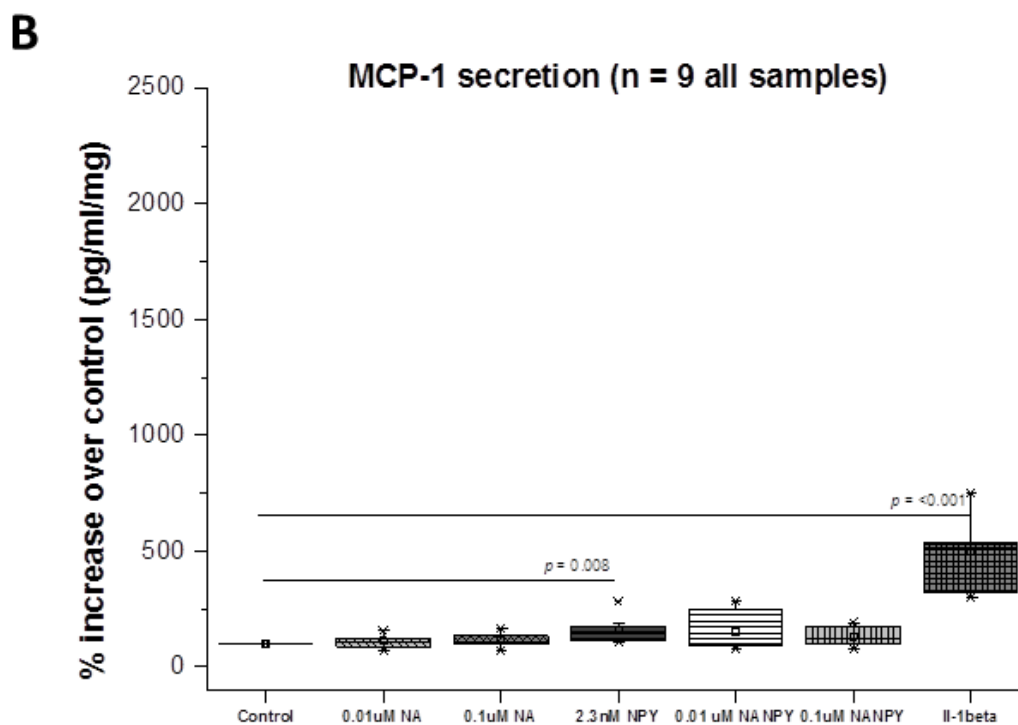
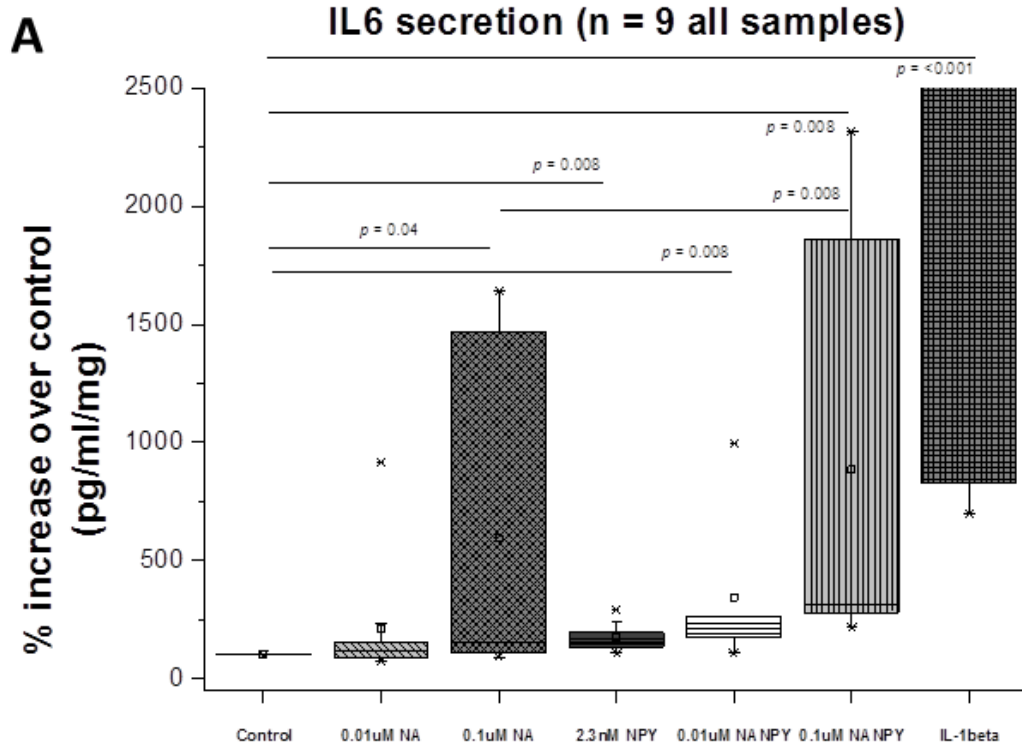
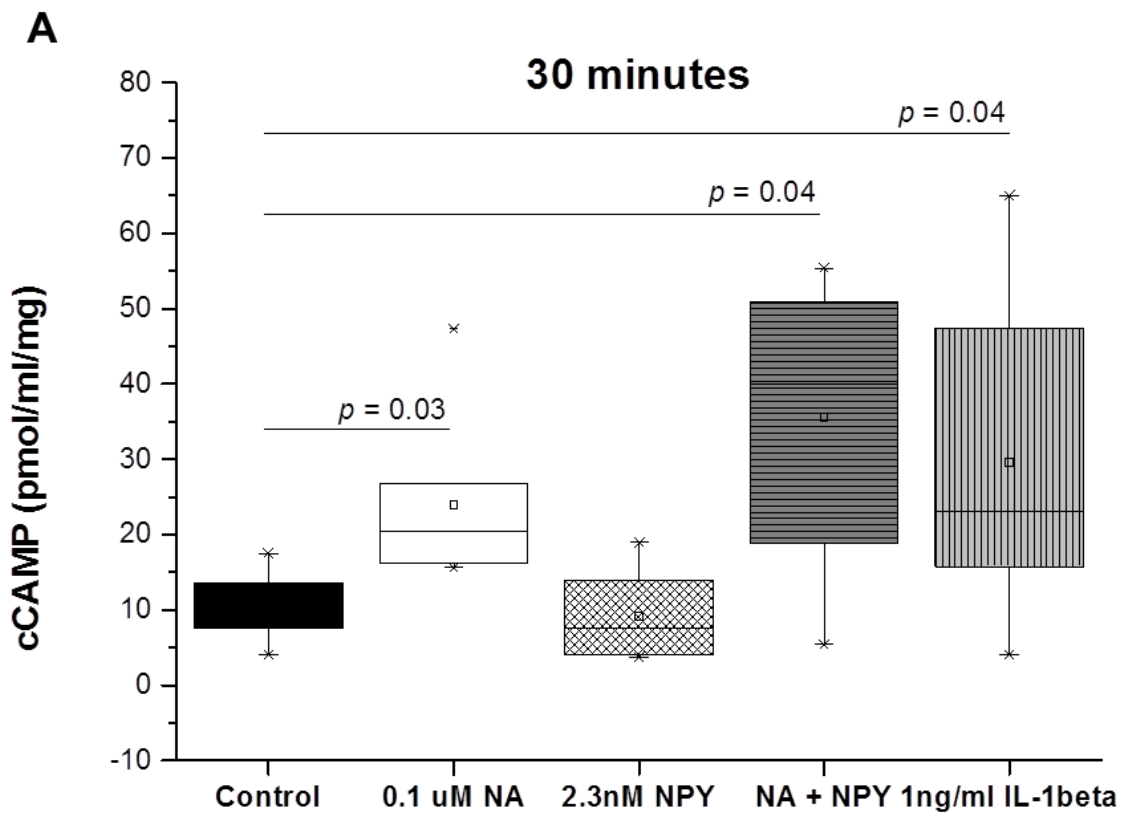


Figure 33: Astrocyte IL-6 (A) and MCP-1(B) secretion after overnight exposure to NA and/or NPY concentrations. Error bars represent SD

3.4.5 Intracellular signalling molecules and IL-6 secretion

In order to elucidate the intracellular signalling molecules that facilitate the NA and NPY mediated IL-6 release phosphorylated STAT3 (pY107) and intracellular cAMP levels were assayed following exposure to NA and NPY at three different time points. A rapid and sharp increase in intracellular cAMP was apparent after 30 minutes of exposure to NA, NA+NPY and the positive control (Figure 34). The remaining time points did not show significant differences



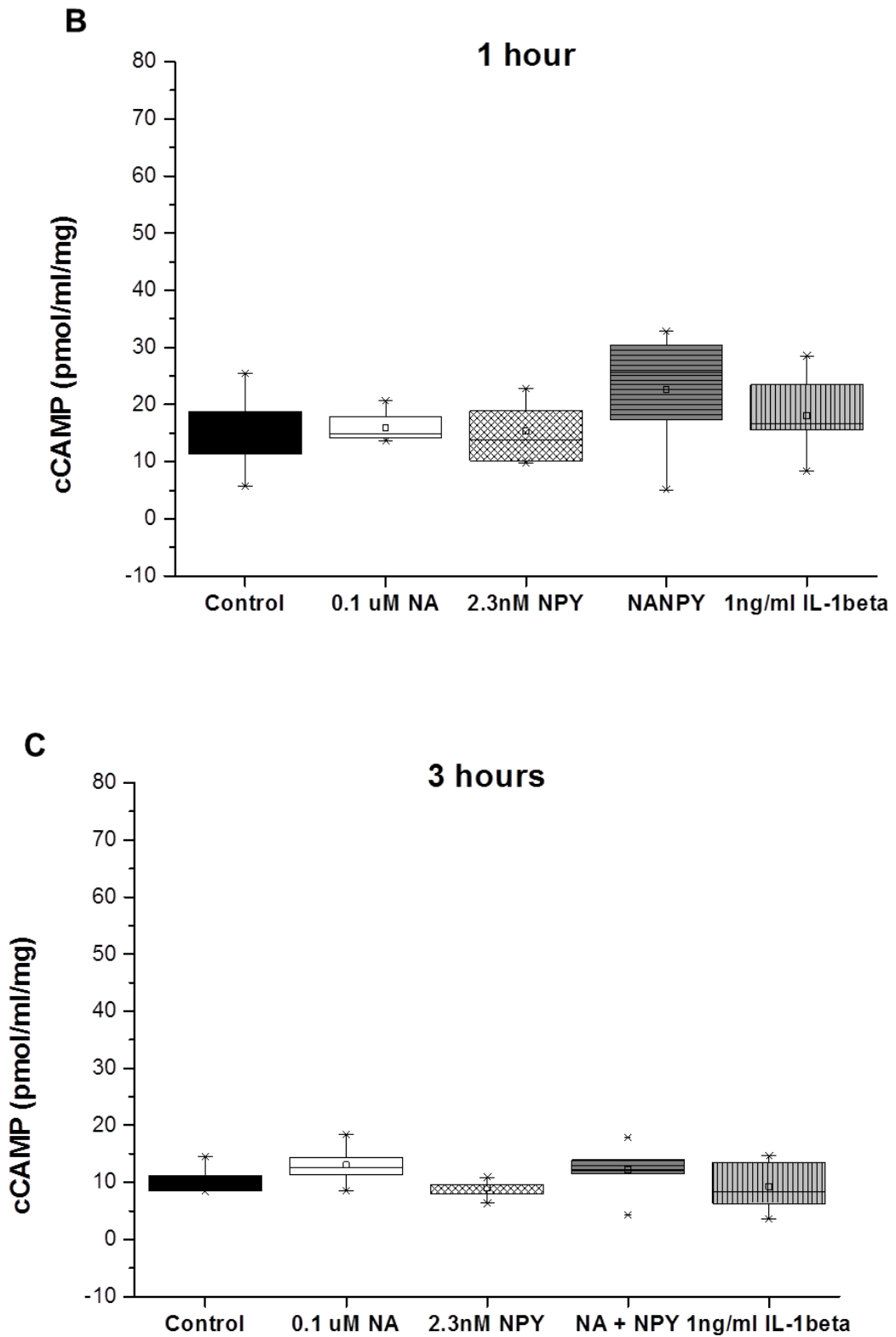
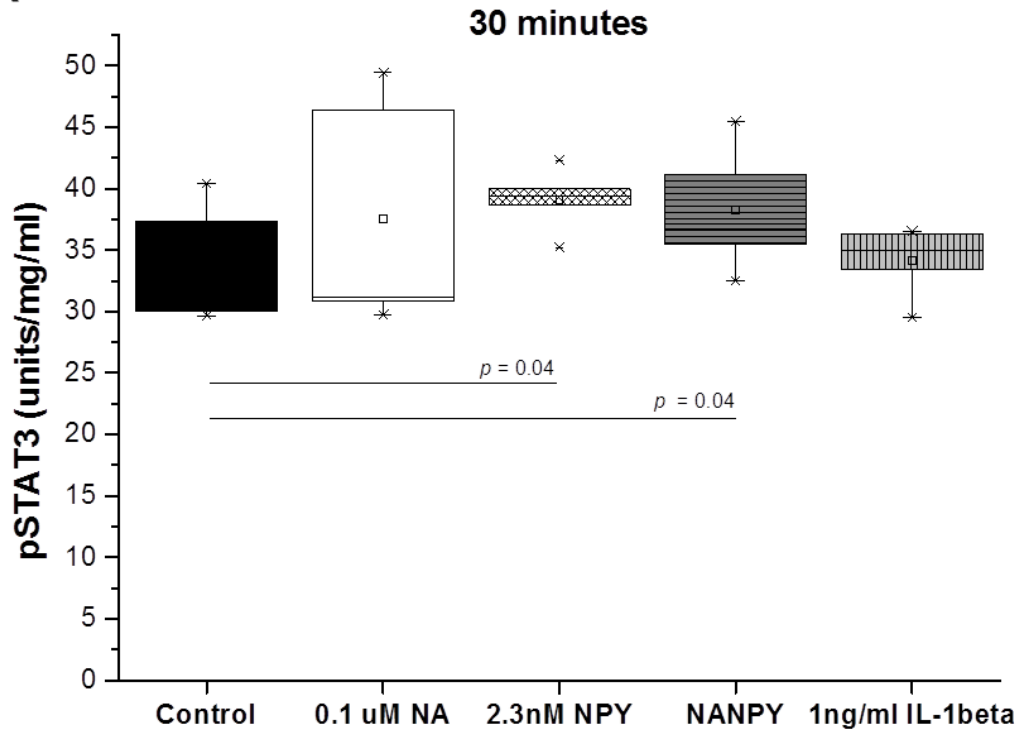
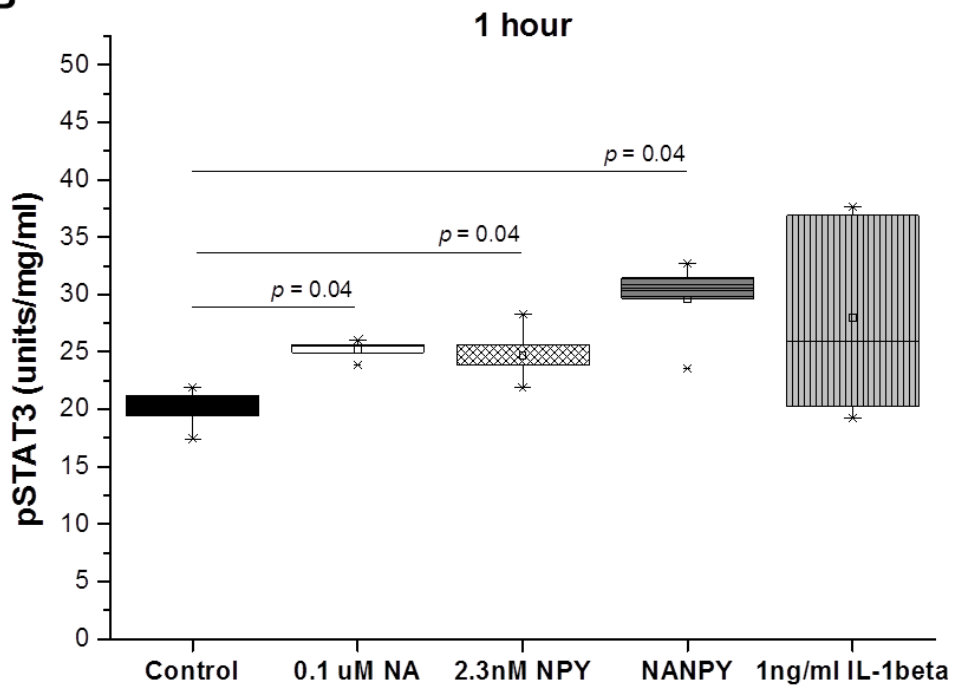


Figure 34: cAMP responses for NA and/or NPY at (A) 30 minutes (B) 1 hour and (C) 3 hours after start of incubation. IL-1 β used as a positive control. Error bars represent SD

A**B**

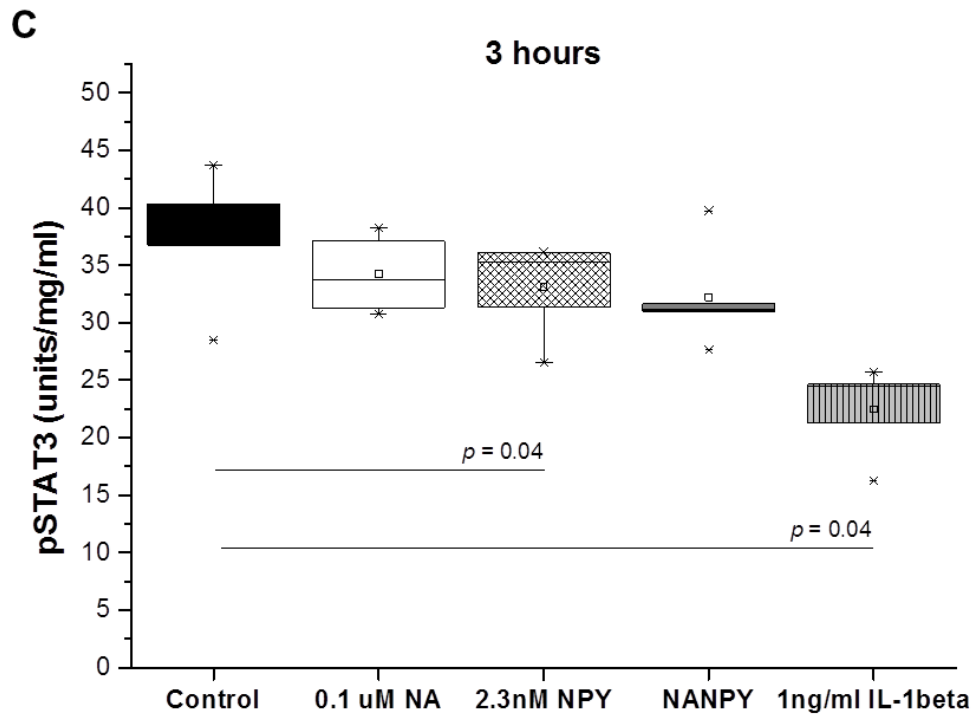


Figure 35: pSTAT3 responses for NA and/or NPY at (A) 30 minutes (B) 1 hour and (C) 3 hours after start of incubation. IL-1 β used as a positive control. Error bars represent SD

pSTAT3 was elevated after 30 min exposure to NPY and NA+NPY (Figure 35A) and at 1 hour (Figure 35B) and after exposure to NA, NPY and the combination. This response started to decrease after 3 hours (Figure 35C).

3.4.6 Intracellular secondary messengers and IL-6 secretion

A series of experiments were carried out to increase levels of intracellular cAMP using various drugs such as Forskolin (an adenylyl cyclase activator), 3-isobutyl-1-methylxanthine (IBMX, a nonselective competitive inhibitor of phosphodiesterases) and Dibutyryl-cAMP (dbcAMP, a cAMP analogue and also an inhibitor of phosphodiesterases) to confirm intracellular cAMP as the mediator of IL-6 secretion in astrocytes.

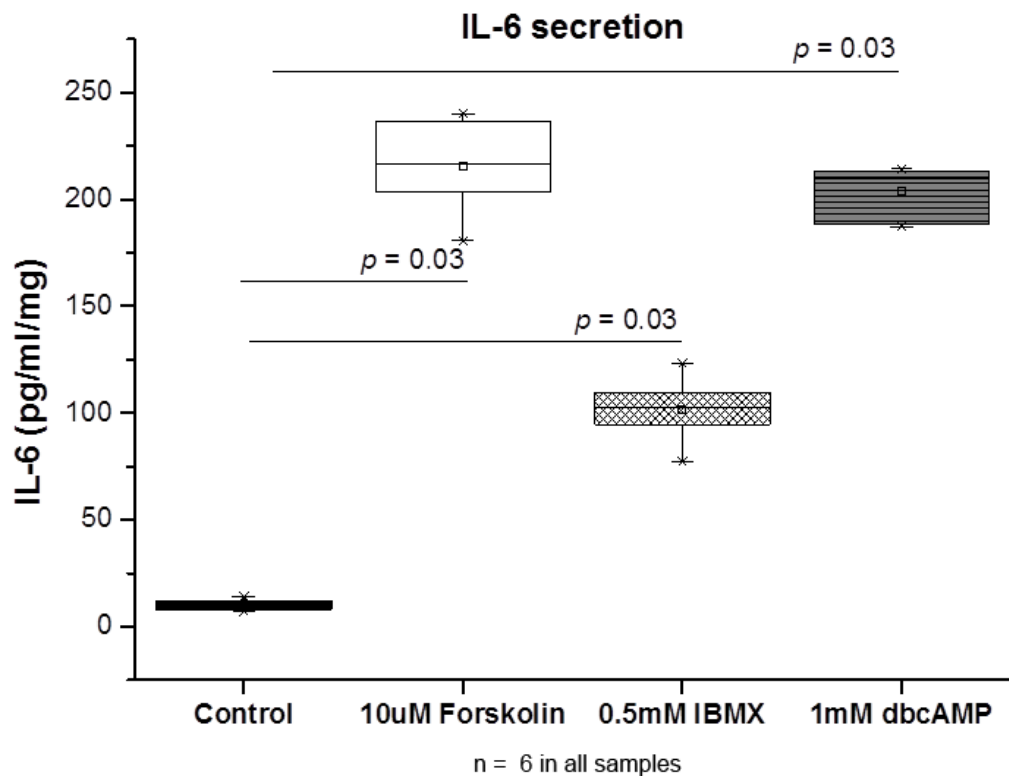


Figure 36: IL-6 secretion following overnight incubations with concentrations intracellular cAMP-boosting drugs. Error bars represent SD

All the agents used to boost intracellular cAMP resulted in significantly increasing IL-6 secretion, with Forskolin eliciting the highest rise. The control cells showed a basal level of IL-6 secretion which was comparable to the previous overnight incubations.

3.4.7 IL-6 incubation and astrocyte lactate release

Having observed the increase in IL-6 secretion caused by the heightening of intracellular cAMP levels, the next step in the investigation of the possible effects of heightened inflammation levels (such as the increased levels of IL-6 in local tissue) on the regular function of astrocytes was to examine one of the most important known functions of astrocytes, that of releasing lactate as an energy substrate to neighbouring neuronal cells, as well as having a possible signalling function towards long-term synaptic plasticity. The levels of secreted lactate from a population of *in vitro* cultured brain stem astrocytes were assayed in the presence of IL-6 at different time points.

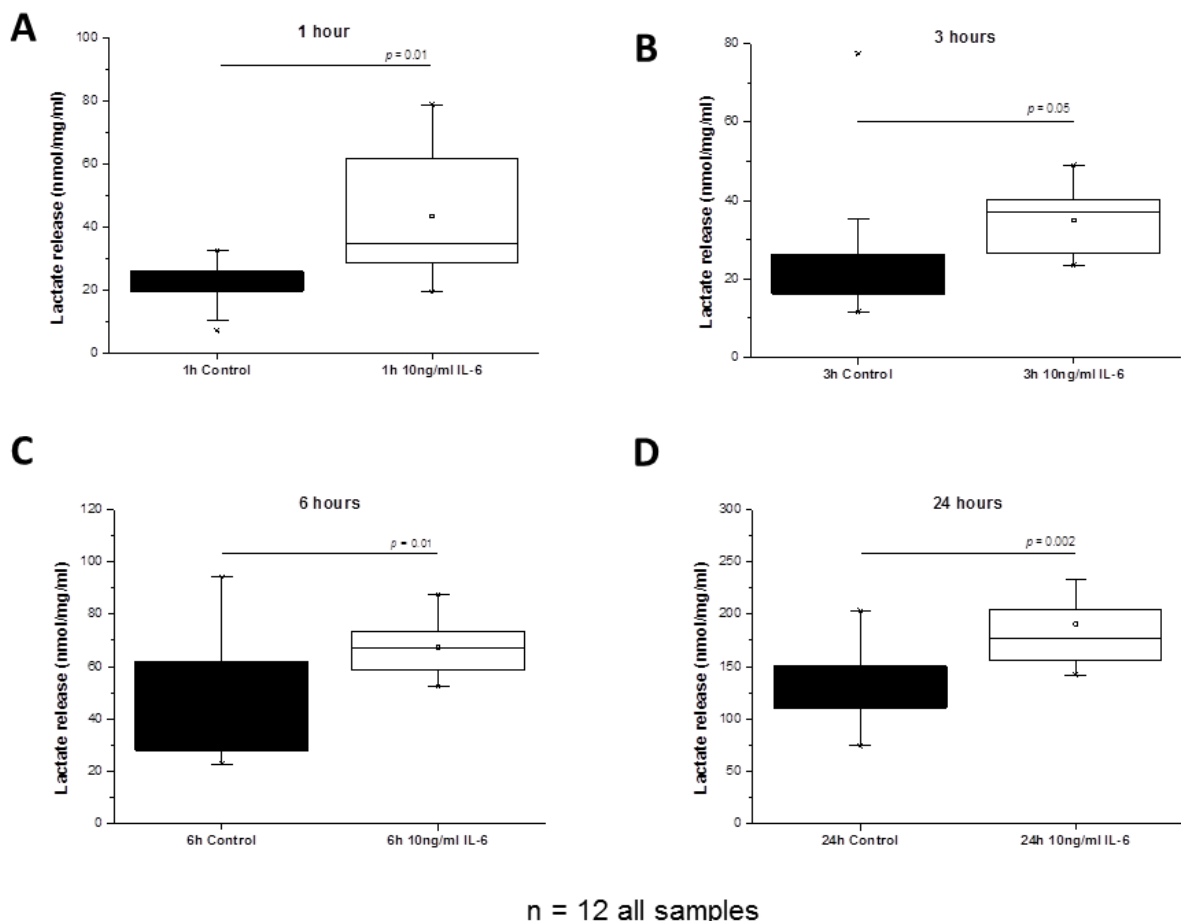
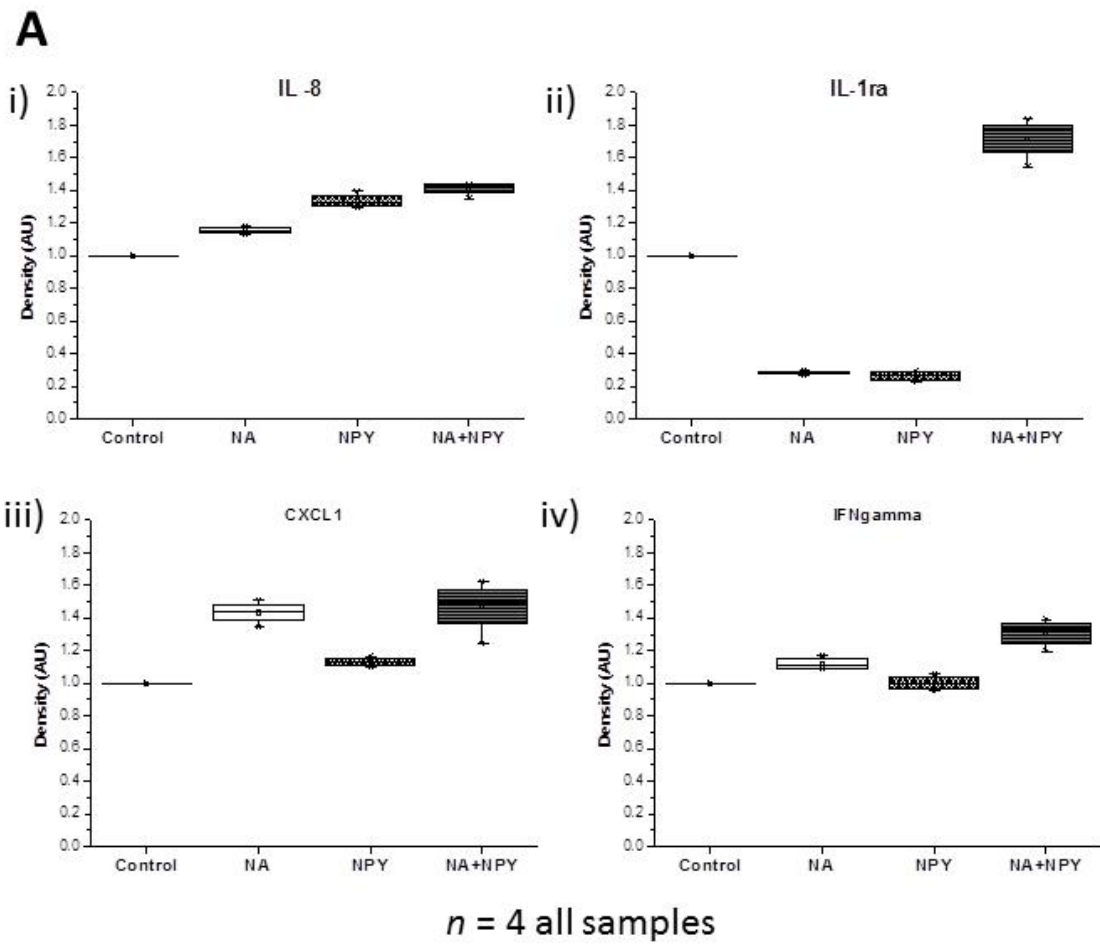


Figure 37: lactate release in astrocytes exposed to 10ng/ml IL-6 at (A) 1 hour, (B) 3 hours, (C) 6 hours and (D) 24 hours after initial exposure. Error bars represent SD

The results shown in Figure 37 show that in every time point observed, the quantity of released lactate (measured in picomoles and adjusted to protein content in each well measured) and is significantly higher from the control incubation and denotes an increased overall level of heightened secretion activity.

3.4.8 Astrocyte cytokine array quantification

Since the variation of IL-6 release and its effects on the regular secretion of lactate were verified, The levels of other intracellular cytokines produced by the astrocytes were also assayed with noradrenaline and NPY via the use of a cytokine panel array (Figure 38B, list of assayed cytokines can be consulted in the relevant methods section of this showing differences in a number of intracellular cytokines shown in Figure 38A, showing a clear variation in IL-1ra and IL-8 levels, as well as fluctuations in the levels of other cytokines such as CXCL1 and Interferon- γ .



B

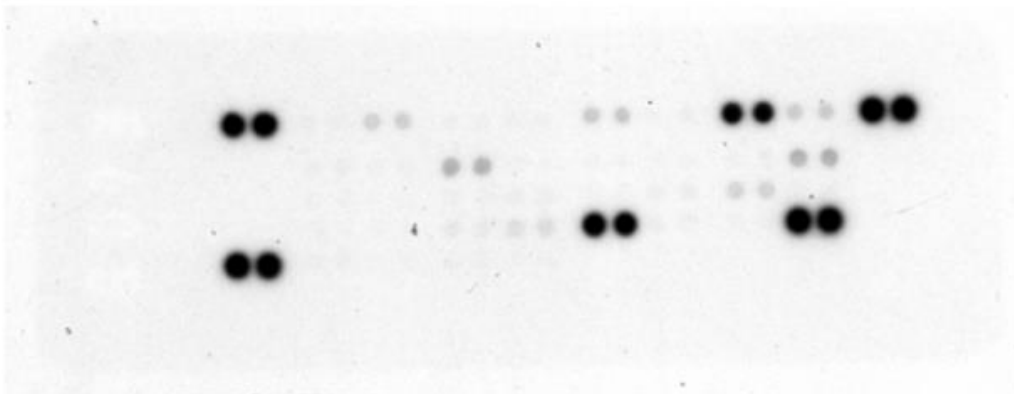


Figure 38: Astrocyte array densitometry (A) of secreted the cytokines (i) IL-8, (ii) IL-1ra, (iii) CXCL1 and (iv) Interferon-gamma from astrocyte incubation medium which appeared to change in concentration and sample array blot (B). Error bars represent SD

3.4.9 Astrocyte gene silencing

Attempts were also made to create a model of astrocyte manipulation of gene expression in order to mimic long-term changes in gene expression that occur with the prolonged activity of the SNS. An attempt was made with the leptin receptor, already established to be present and its transcription sensitive to the presence of the hormone (see section 3.4.2 in this chapter). SiRNA-mediated gene silencing was used to modulate human leptin receptor expression in astrocytes. The results shown in Figure 39.

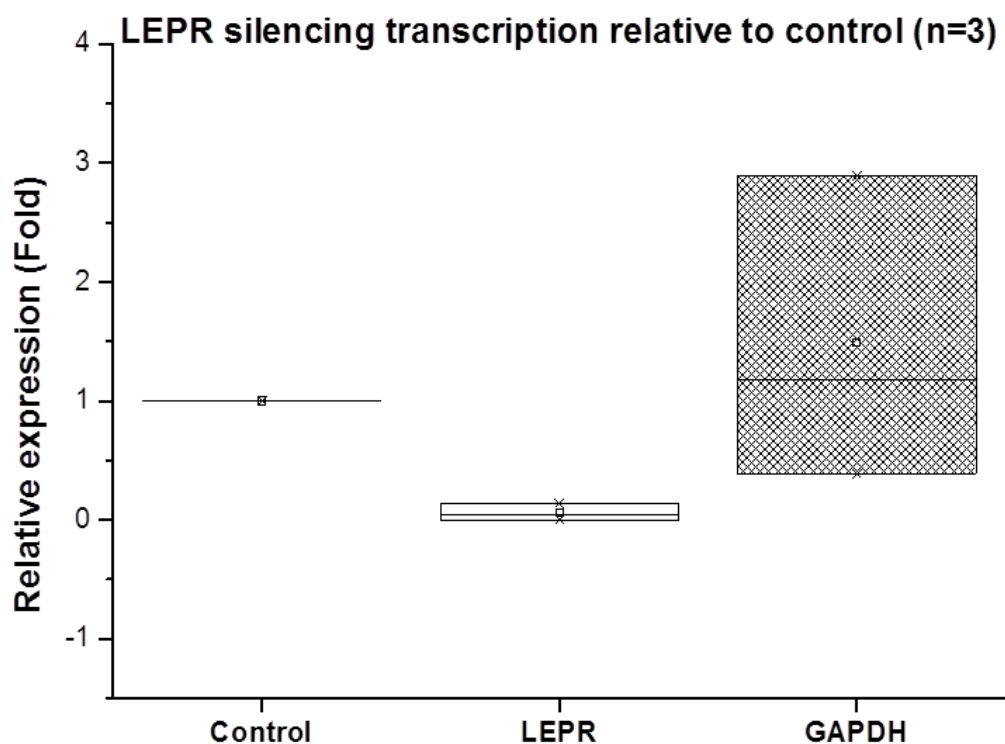


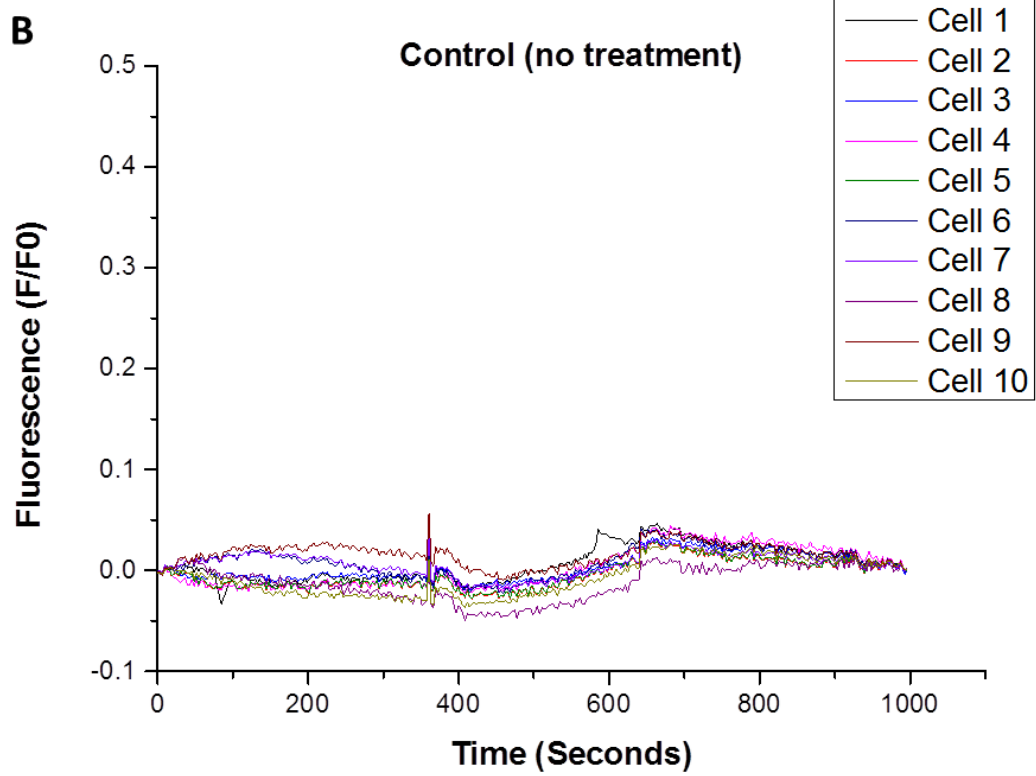
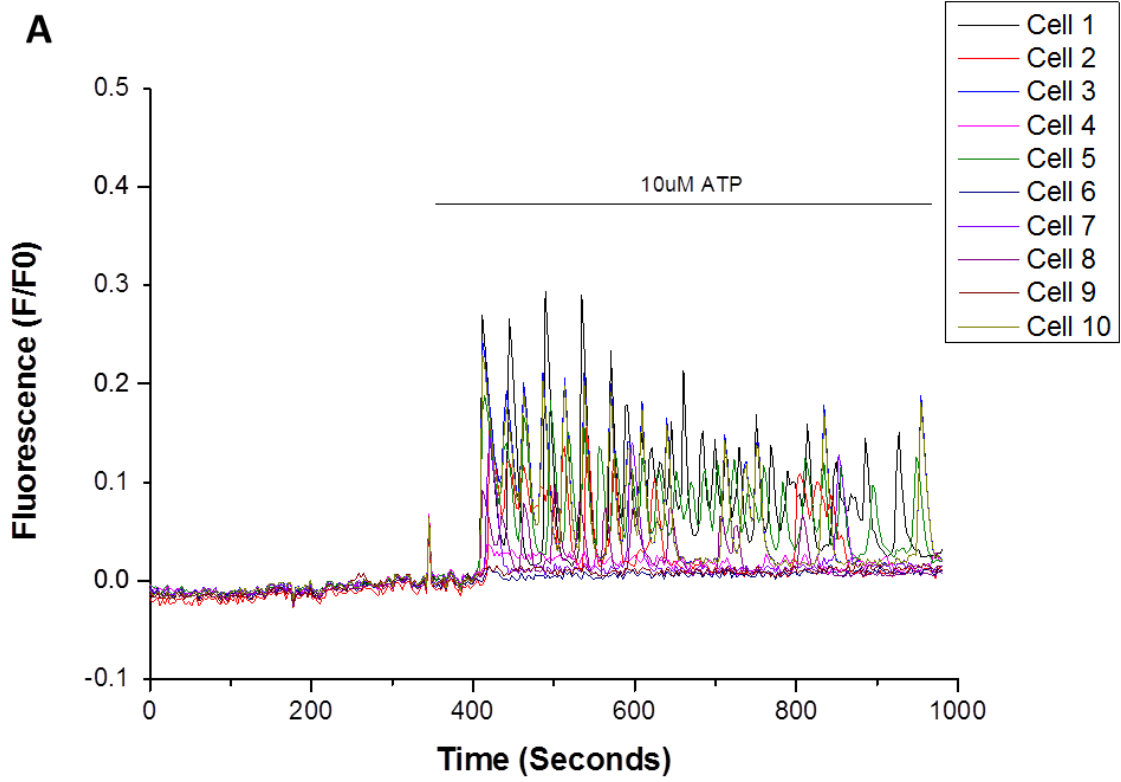
Figure 39: LEPR gene silencing in cultured human brain stem astrocytes

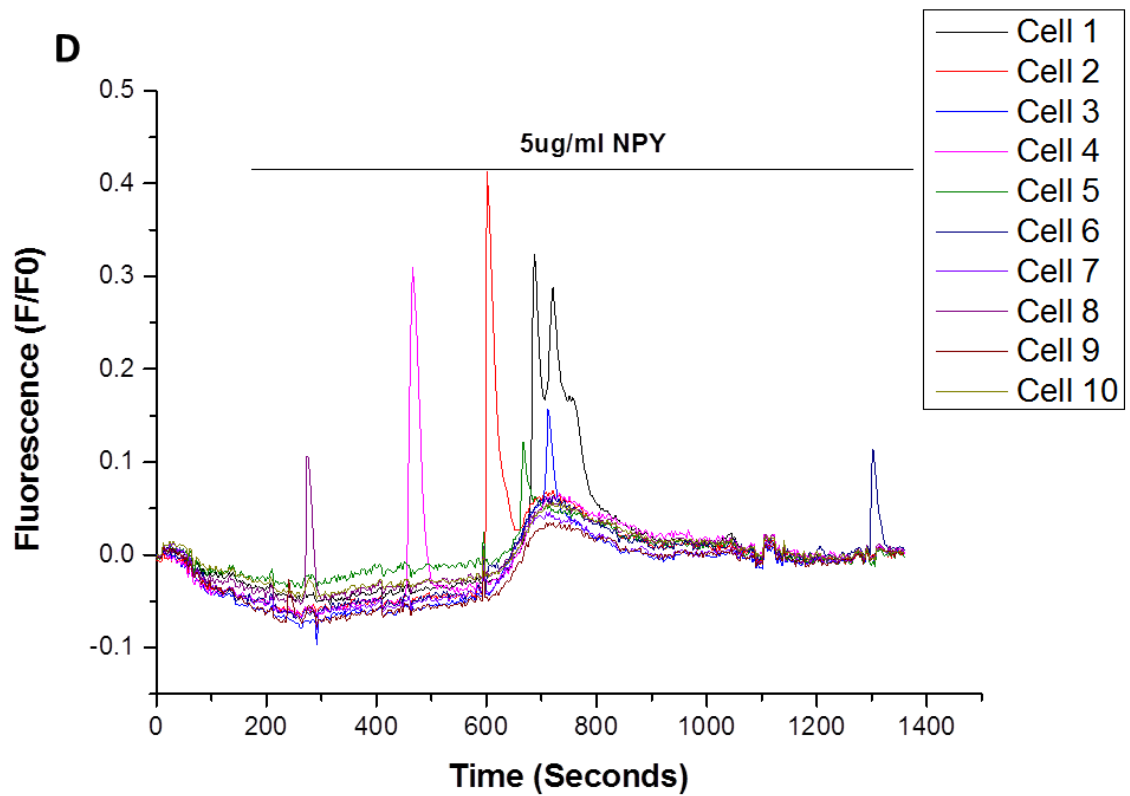
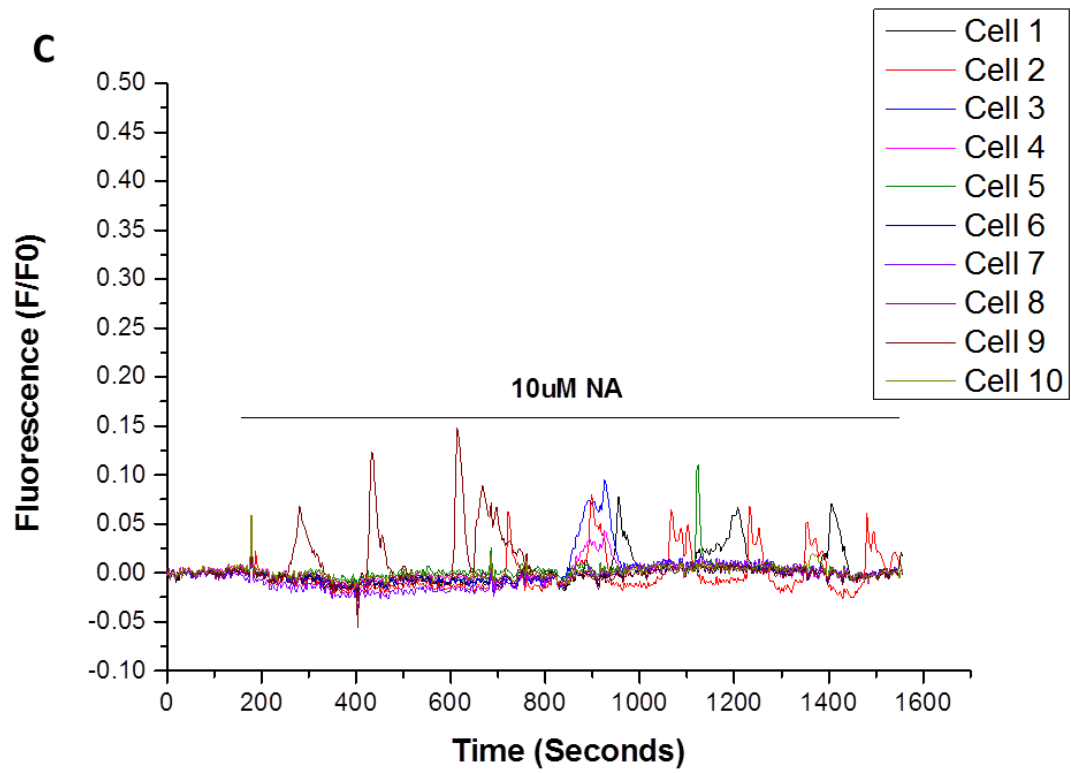
The results did not reach statistical significance, although the trend in gene expression showed that compared to the control samples (displayed as a reference value of 1) leptin receptor gene expression lowered to zero percent of control expression, while GAPDH expression varied from 50% to 300% of control expression. Unfortunately, negative control

samples could not be displayed due to the samples being compromised during reverse transcription.

3.4.10 Astrocyte intracellular calcium signalling in response to NA and NPY

The quantity of intracellular calcium via fluorescence microscopy and time-lapse digital photography was also explored due to evidence in the literature of a known ability of NPY to influence cytosolic Ca^{2+} levels (173), cultured astrocytes following NPY and/or noradrenaline exposure were recorded using Fluo-4 (a calcium-sensitive dye) to monitor cytosolic calcium. After initial testing for a general response to ATP, which is a known stimulator of fluctuation of the intracellular Ca^{2+} levels (132) and would confirm the viability of the astrocytes the results, spanning over a series of incubations showed (as illustrated in examples by Figure 40) a variety of responses, specifically of a cyclical nature compared to the regular background activity of the astrocyte (Figure 40B) which still denoted cyclical fluctuations yet of a much smaller magnitude compared to acute NPY exposure (Figure 40D) or noradrenaline (Figure 40C). The combination of the two molecules also yielded a response after an initial control period of roughly 1-2 minutes; in the case of samples that received exposure to NA, NPY, ATP or both, the frequency of the waves differed in nature and intensity as shown by the graphs in Figure 40 yet were not quantifiable precisely in amplitude.





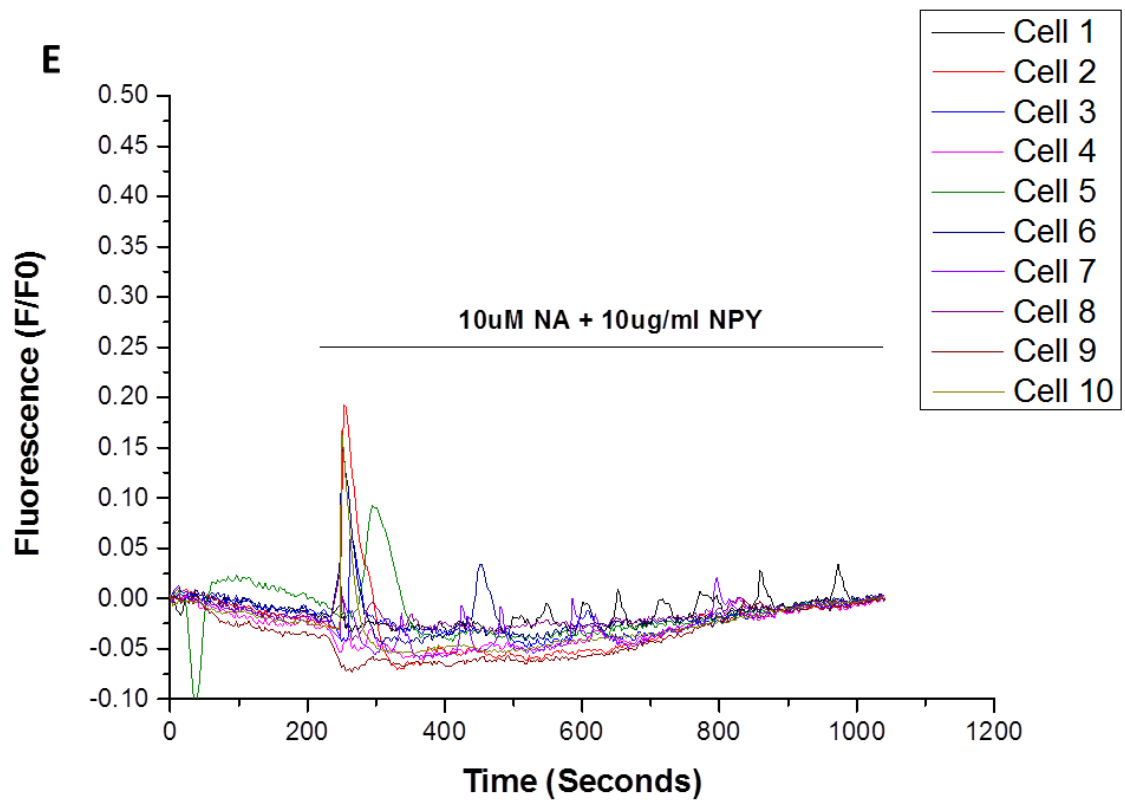


Figure 40: Intracellular Ca²⁺ oscillations in randomly selected astrocyte culture regions of interest astrocytes with addition (after a 1-2 minute resting state to observe baseline activity) of: (A) 10 uM ATP (B) No treatment (C) 10uM Noradrenaline, and (D) NPY and (E) a combination of both

Chapter 4

Discussion

4.1 Clinical data

4.1.1 Patient population results

The overall population of patients screened using the criteria described in Chapter 2 showed a sub-set of patients (21.5% of total numbers, as shown by Table 1) which fit the criteria used to isolate MHO individuals. What is very interesting about the differences between the MHO individuals and the rest of the population is that the PO/DM group does not show a difference in age and BMI, yet the quantity of circulating insulin is significantly higher and is not sufficient to maintain a level of fasting plasma glucose comparable to the MHO group. Circulating triglycerides are also higher and show an interesting and significantly higher change in the PO/DM population, going in line with the results shown in other studies which have caused serum triglycerides to be one of the possible additional biomarkers for the discrimination of patients from metabolically healthy and unhealthy (174,175). The circulating adipokine data shown in Table 2 shows a clear difference in circulating NPY (significantly higher in the PO/DM group) between the two groups, which suggests that with proper and precise detection (ideally gas chromatography and mass spectrometry) levels of NPY could be assayed as a biomarker indicative of metabolic status of a patient in a clinical setting. Other studies have also looked at NPY as a marker of possible onset of hypertension in obesity (176) and given the relative ease of detection it could be feasible in a hospital to also detect metabolically unhealthy obesity. Higher adiponectin levels in the MHO population are in line with previous reports of higher adiponectin levels associated with “healthier” metabolic phenotypes (177,178). The post-surgical follow-up data in Table 4 appears to confirm that the levels of insulin and glucose (therefore also HOMA-IR) ameliorate only in the PO/DM category in a significant manner, despite the significant drop in BMI for both groups. NPY levels seem to drop post-surgery in both populations following surgery, although the trend does not reach significance in both groups, possibly due to low numbers which could reach significance if the population is enlarged. It is also worthy of note that blood pressure data was not gathered during the follow-up visits due to clinical time constraints, and in future studies this would be paramount to the determination

of NPY levels decreasing to be possibly correlated with the possible decrease of hypertensive symptoms in the PO patient group.

Cholesterol levels appear to change in both groups and significantly so, but this could be a result of the end of pharmacological therapy after surgery and therefore a transitory phenomenon which could stabilise in longer periods of time. Adiponectin levels increased in both groups, yet the MHO population still maintained a higher level compared to the PO and diabetics. These results appear to point towards a greater benefit gained from bariatric surgery by the PO/DM population, and that MHO patients discerned from the others by biomarkers such as circulating NPY could be given alternative means of more effective and less invasive treatment in a clinical setting.

The issue of common identification criteria for the patients still stands, and the results point to an even greater need for common definitions of MHO/PO characterisation due to our observation of such differences even in a morbidly obese population, and the variety of definitions used to characterise the newly studied MHO patient group (as discussed in Chapter 2). Indeed, the number of patients approaching 22% of total in the Caucasian population confirms and increasingly enforces the idea being put forward that would describe the mere measure of BMI as inadequate in describing the multitude of metabolic abnormalities associated with obesity (179). The prevalence of “healthy obesity”, as defined by the absence of diagnosed comorbidities in a set obese population, shows that the current BMI measure for “unhealthy” and “healthy” obesity could be too broad for the new stratified approach to modern medical care which is becoming more prevalent as a greater number of factors behind human disease are being uncovered. Some progress is being made with the emergence of studies suggesting a broader view beyond BMI (75,179), but the need for a consensus is required for a more precise approach to the problem.

4.1.2 Adipose tissue explants secretion

The adipose tissue from both patient groups (Table 3) did not show any statistically significant differences in local adipokine secretion save for subcutaneous leptin, which was

significantly higher in the PO group. This could be due to the established fact in previous studies carried out by Skurk *et al.* in 2007 that larger adipocytes are known to be able to secrete more quantities of leptin (180), and therefore could be an indication of the fact that the subcutaneous adipocytes of the PO/DM group could be larger compared to the MHO group. Since other studies show that larger adipocytes are also more insulin resistant (181) this could be an indication of localised peripheral insulin resistance in the adipose tissue. What is also worthy of note is the lack of any statistical significance in local inflammatory marker secretion among the two groups, despite a trend towards a higher MCP-1 secretion in the omental adipose tissue of the PO/DM group, possibly showing that localised inflammation could not be the initial factor in the onset of insulin resistance as previously thought. NPY levels also did not change significantly at a local level.

4.1.3 IL-6 secretion in response to IL-1 β stimulation

From the data showed in Figure 20, the subcutaneous adipose tissue explanted from the subset of patients used in the study appeared to be responsive to the well-known effects of IL-1 β on IL-6 gene activation and secretion (182), even after 65 hours post-sample collection. This allowed for the use of the tissue in transcriptional regulation studies regarding inflammatory micro-RNAs responsible for that were carried out subsequently.

4.1.4 Summary of clinical data

Despite not having differences in age and BMI, 21.5% of patients observed and isolated under MHO criteria had significantly lower fasting plasma glucose, insulin, HOMA-IR levels as well as triglycerides. Circulating NPY was significantly higher in the groups observed and anti-inflammatory adipokines such as adiponectin were higher in the MHO group, and showed lesser amelioration in insulin levels compared to the PO group when undergoing bariatric surgery. There were no differences in locally secreted inflammatory adipokines between the groups in both adipose tissue depots, and leptin was significantly higher in the subcutaneous depot, suggesting larger adipocytes in the subcutaneous depots of the adipose tissue, which could also

mean worsened insulin sensitivity of the tissue itself. NPY was significantly higher in the PO/DM group, and could also suggest a higher level of SNS activity in these patients.

4.2 Histology

4.2.1 Adipocyte area

Looking at the adipocyte areas (Table 6) in the subcutaneous, and omental depot of the adipose tissue belonging to the metabolically healthy obese group, a statistically significant difference towards smaller adipocytes among MHO patients is evident in both depots, with the median area of the adipocytes being considerably larger in the PO. The adipocyte population graphed in Figure 21 appears to shift towards greater frequencies of larger adipocytes in the PO patient group, and is made very clear by the population graphs of the PO adipocytes (Figure 21, shown in green) displaying a more prominent shape in the greater area adipocytes of the higher portion of the Y axis. This results indicates in a statistically significant manner that both OM and SC depots of the PO population have larger (and therefore more insulin resistant) adipocytes, and could explain the greater secreted quantity of leptin by the subcutaneous adipocyte explants described in the previous section. This discrepancy in adipocyte size could point towards an effective dysfunction of the adipose tissue due to the theory of impaired tissue expansion, and could also indicate the presence of a slowed adipocyte turnover rate as described by previous studies (48).

4.2.2 CD68+ cell infiltration in adipose tissue

The results displayed in Table 7 and Figure 22 show no real statistical difference in the quantity of CD68+ stain cells in the adipose tissue of the patients, and despite the presence of these cells the quantity of the apparent stain was neither different not only SC and OM depots, nor between MHO and PO individuals. Previously characterised foci of CD68+ cell aggregation, referred to as “crown-like structures” (48) have been observed (Figure 22) in the tissue in line with animal studies, yet they did not seem to appear frequently or to be discriminatory towards

a single patient population. Statistical significance possibly could be lacking due to numbers of samples not being high enough, but from personal observation of the tissue the cell aggregation areas seemed rare and not really indicative of possible patient phenotype. These results, along with the lack of significant difference in locally secreted inflammatory adipokines do not seem to point to inflammation being the primary insult to the adipose tissue at a local level as argued by other groups (41). This does not exclude the idea that inflammation could be present as an accessory mechanism to the onset of insulin resistance once the primary factors such as impaired adipocyte turnover and adipocyte hypertrophy have come into play, but from the data it does not appear to be the primary cause of dysfunction in Caucasian morbidly obese patients.

4.2.3 Overall NPY receptor staining in adipose tissue

The staining present in the adipose tissue did not show any statistically significant differences in NPY staining (Table 8), therefore not indicating any overall striking differences in staining, yet the receptor staining was detectable visually (Figure 23) and appeared to be abundantly expressed throughout the tissue, suggesting a susceptibility of the adipose tissue to the effects of NPY secretion in possibly an autocrine as well as paracrine and endocrine manner. The evidence showing that adipocytes are susceptible to NPY signalling in a way that affects the functioning of glucose transporters (160) in an insulin-independent manner suggests that peripherally secreted NPY could be an accessory cause to adipose tissue dysfunction in patients that have a higher secretion level of the peptide. What also appeared interesting from the images analysed was that NPY receptor staining was concentrated around vessels especially, which led to a more precise investigation of the staining around the microvessels of the tissue depots which will be described in the next section.

4.2.4 NPY receptor staining in adipose tissue vessels

What became apparent after a closer and more sectorial observation of the staining (Table 9) was that the levels of NPY receptor associated with any vessels present in the adipose tissue in both groups had a greater intensity in the PO group in both depots for Y5 receptor and in only the subcutaneous for Y1 (Figure 24A and Figure 24B). This could point to a role of NPY receptors

Y1 and Y5 in the adipose tissue which is more confined to vascular reactivity and vascular responses to sympathetic nervous system stimulation.

The idea that NPY-potentiated vasoconstriction could be happening is supported by animal studies carried out which show potentiation of vasoconstrictive effects of neurotransmitters such as noradrenaline happening in both arteries and veins of animal models (149,150,183) and the difference in the localised vessel staining between the two populations (with greater levels of staining in the PO subcutaneous tissue) could also point to a greater sensitivity to circulating NPY levels, greater vasoconstriction in the tissue at a local level and the possibility of the tissue also being more prone to hypoxic conditions, which are known to cause insulin resistance in adipocytes (184).

Overall this human data also points to an important aspect of adipose tissue biology, which is the important role that is played by perivascular fat and its signalling in influencing vascular and microvascular reactivity. The role of perivascular fat not only in major blood vessel function (185) but also in local adipose tissue vascular function has been extensively discussed in recent years (186). It is a known fact that lack of vascular reactivity deriving from the presence of heightened local inflammation of the adipose tissue microvessels not only leads to lack of vasodilation and hypoxic conditions as previously discussed, and increased NPY signalling in PO individuals exacerbate NA-mediated vasoconstriction as shown in previous research could be a part of the alterations that lead to the problems leading to insulin resistance in humans.

4.2.5 Summary of histological investigation data

Histology investigation following the preliminary clinical data showed that not only did the tissue show differences in adipocyte size but that it also showed no statistically significant difference in the presence of CD68+ positive cells, which were present although not markedly more in the tissue of the PO group. The staining for NPY showed that receptors Y1 and Y5 were expressed and therefore showing a level of sensitivity in both depots, yet after an initial screen showing no difference in overall expression, the levels of staining associated with the

microvessels of the adipose tissue showed a significantly higher level of staining in Y5 for both depot and in the subcutaneous for Y1 in PO patients compared to the MHO group.

This would suggest a higher susceptibility at the vascular level to the effects of NPY signalling, that could also suggest additional hypoxic conditions caused by decreased blood flow at the local level that could increase insulin resistance in the adipose tissue of the PO patients in response to SNS activity. This type of hypothesis could also be confirmed by looking at the co-localisation of sympathetic nerve fibres with the NPY receptor staining, to also confirm differences in sympathetic innervation at the adipose tissue level.

An aspect that could also be interesting to explore in future studies is the presence of differences in UCP1 expression between depots and patient groups, in order to assess whether NPY signalling is having a “browning effect” on the tissue at the local level, or on the contrary is inhibiting the regular development and function of brown adipose tissue in humans, since this effect has been explored systemically in animal models with studies such as Chao *et al.* (187) showing that RNAi-mediated NPY expression knockdown in the dorsomedial hypothalamus led to an increase in brown adipose tissue depots, decreased white adipose tissue depots. Observing the presence and difference in prevalence of UCP1 expression in human adipose tissue between the two patient groups could be an interesting facet to the expression of NPY receptors in the adipose tissue, and could possibly point to more intricate differences not visible merely by npy receptor differences alone.

4.3 Tissue RNA transcriptional studies

4.3.1 PPAR γ expression in adipose tissue

The initial analysis of the morphological characteristics of MHO and PO adipose tissue allowed the hypothesis that the presence of enlarged adipocytes in the PO group could be due to the difference in the quantity of adipogenic signals the tissue is subjected to, and therefore a difference from the smaller, more numerous adipocytes that could be populating the MHO tissue to the fewer, larger and more insulin resistant adipocytes that could be present in the PO tissue. By looking at the transcription level of a master adipogenic switch like PPAR γ (Figure 25) the results showed a trend towards more adipogenic “signal” in the PO adipose tissue by about 50% of MHO expression levels, and about the same with the diabetics in the subcutaneous depot. The trend appeared to be different in the omental tissue, with lesser PPAR γ expressed in the PO group and the DM group, almost to show less adipogenesis occurring with worsening metabolic status as to show impaired remodelling of the tissue. The limitations to these results on the other hand are that statistical significance was not reached in the differences in gene expression, and that a higher transcription level and more active adipogenic signalling at the RNA level could not exactly translate to the effect being seen at the cellular level, with many other regulators of signalling coming into play in the differentiation of pre-adipocytes into adipocytes.

The level of PPAR γ transcription effectively does seem to reach a higher level in obese individuals in both subcutaneous and omental adipose tissue, compared to lean ones as shown by other studies (188,189), although the difference in expression appears to be minimal as well. Increasing numbers of the screened patients for all populations would probably show a significant trend in the total data, and investigations at the protein level for downstream-activated or upstream signalling proteins of PPAR γ could give a clearer picture of what is happening in the tissue of the PO and DM groups with respect to adipogenesis.

Also, medication taken by the DM group might tamper with PPAR γ signalling, given the direct effect of medication such as the thiazolidinedione group of drugs which act directly on PPAR γ levels.

4.3.2 SCD1 expression

The idea of observing expression levels of the enzyme Stearoyl-CoA-desaturase 1 was devised due to its importance in converting various saturated fatty acids in mono-unsaturated fatty acids (MUFA) and for the link between local MUFA levels and inflammation of the adipose tissue, since they are hypothesized to be inflammatory activators of Toll-like receptor 4 (59,66), and could play an important part in the different lipid homeostasis and lipotoxicity that could arise from its activity raising inflammation levels locally and exacerbating insulin resistance. The results in Figure 26 show that despite there being a lack of statistical significance between the groups (possibly due to low numbers), the expression of SCD1 mRNA showed a trend towards being considerably higher in the PO adipose tissue compared to the MHO. The diabetic group appeared to show lower SCD1 expression in subcutaneous adipose tissue. However, despite the higher level of expression in the PO individuals, various studies have shown that a discrepancy between SCD1 expression levels and SCD1 protein levels in the adipose tissue exist (170) when observed in the morbidly obese, and therefore that looking at mRNA levels in the tissue might not be the most precise way to determine SCD1 activity. Ideally, further studies in this type of enzyme should be carried out with precise quantification of protein levels via western blotting, or by direct quantification of secreted PUFA levels by the adipose tissue itself using techniques like gas chromatography lined with mass spectrometry or a specific colorimetric assay. The results from the DM group may also be influenced by the medication some of the patients in the group might be taking as well, which could tamper with results at the local level.

4.3.3 NPY receptor expression

The presence of NPY receptors in adipose tissue has been established in various studies (155), as well as the fact that they are direct promoters of adipogenesis and pre-adipocyte differentiation *in vitro* (157), and also inhibitors of adipose tissue lipolysis (159). Figure 27

summarised the experiments designed to detect the presence of NPY receptors 1 and 5, which were found to be the most abundantly expressed receptors in the adipose tissue in previous real-time PCR experiments and studies by Lafontan *et al.* (158), with the results not reaching statistical significance in their changes yet showing an interesting trend towards lesser quantities of receptors expressed with worsening of metabolic status, and increased Y5 expression with the worsening of metabolic status. Y1 receptor expression is known to be lower in lean individuals compared to obese individuals (190), yet the differences in expression between metabolic profile of morbidly obese individuals has never been explored, and our results despite a lack of statistical significance would show a trend towards lower expression of the receptor in the adipose tissue with a worsened metabolic phenotype. This could be due to the down-regulation of the receptor at the gene level after its stimulation in a negative-feedback loop caused by higher circulating levels stimulating the receptor more frequently than in MHO individuals. The stimulation of Y1 receptor could be causing a decrease in insulin sensitivity by the blocking of translocation of GLUT transporters reported in studies such as Gericke *et al.* 2012 (160), as well as levels of basal lipolytic potential of the adipocytes being affected, causing them to retain lipids and remain larger than other adipocytes less subject to NPY signalling.

Y5 expression on the other hand appeared to increase in the adipose tissue of the PO and DM individuals in both depots, which is also interesting due to the recent hypotheses of Y5 receptors being involved in the remodelling and angiogenic processes of the tissue (155,156,191). The increased transcription of the receptor could point to a vascular response of the tissue towards angiogenesis, which could support the impaired remodelling hypothesis behind adipose tissue dysfunction. Since the histology results showed a level of expression on the surface of the adipocytes as well as the vessels in the adipose tissue, the confirmation of the presence of NPY receptors 1 and 5 in the adipose tissue points to an interesting role for NPY and SNS activity on the regular functioning of the adipose tissue and the onset of its degeneration in PO and DM individuals.

4.3.4 Adipose tissue siRNA electroporation and knockdown of miR-146b

The data displayed by Figure 28 clearly shows an increase of miR-146b expression in the mimic siRNA electroporated in the subcutaneous adipose tissue compared to the levels of miR-146b expressed in the negative controls. The inhibitor siRNAs electroporated, as expected, appear to have decreased the level of expression also compared to the negative controls, demonstrating that the electroporation experiment has worked as expected. On the other hand, the decreased intracellular levels of miR-146b did not appear to influence the inflammatory response that IL-1 β elicited by causing increased secretion of IL-6.

This could possibly indicate that the microRNA does not appear to have a direct role in IL-6 secretion regulation in adipose tissue. The limitations to this experiment were that it was carried out on a limited number of samples, and that the levels of IL-1 β used to elicit an inflammatory response were relatively high. Nevertheless, it demonstrated that microRNA regulation in human subcutaneous adipose tissue using adipose tissue in a method similar to the one carried out by Puri *et al.* (168) was possible.

4.3.5 Summary of transcription data

Adipose tissue, while being susceptible to the modulation of gene expression in tissue as shown by the electroporation experiment, shows lack of any statistically significant changes in gene expression between the depots of the adipose tissue in all three groups. The trends presented by the transcription data showed PPAR γ transcription appearing to be higher in the PO group for subcutaneous adipose tissue and equal to MHO patients for the DM group, while the relative expression appeared to decrease with worsening metabolic status in the omental. The expression of SCD1 appeared higher in the PO group but lower in the diabetics for subcutaneous tissue and higher in PO and DM groups for omental tissue. With respect to NPY receptors, the most abundantly expressed receptors (Y1 and Y5) in the adipocytes showed a trend in lower expression in PO and DM groups for both depots, yet a higher expression in PO and DM groups and in both depots with Y5 receptor. While PPAR γ and SCD1 expression levels could not reflect protein levels and therefore not be entirely indicative of functionality

differences, the presence of NPY receptors Y1 and Y5 as confirmed by the histology data suggest that the adipocytes are susceptible to their activation, and could have effects on angiogenesis and tissue remodelling via Y5 receptor and glucose homeostasis and lipolysis control via Y1 receptor function.

4.4 Astrocyte data

4.4.1 NPY receptor immunohistochemistry data

Figure 30A clearly shows a very strong expression of NPY receptor Y1 and a lesser quantity of Y5 receptor (Figure 30B), given that the digital acquisition gain has to be adjusted much more strongly in order to visualise the Y5 antibody staining. What was interesting about this difference in the quantity of receptors present was that this also reflected the RNA expression of Y1 and Y5 in the astrocytes which will be discussed in the next section. There was no non-specific binding by the secondary and primary antibodies since the negative controls used were completely dark and showed no staining. Given the presence of the receptors in the immunohistochemistry imaging and previous studies demonstrating the responsiveness of astrocytes to NPY (192) as well as proof of expression, these results also show their presence in this primary cell line, allowing further experiments regarding the effect of the peptide.

4.4.2 Responsiveness of the receptors to NPY at the mRNA level

Since the quality of the primary cells as a working model for NPY responsiveness was assessed after the receptors were found on the cell surface, the results of real-time PCR analysis of NPY receptor transcription that was subsequently carried out are shown in Figure 31. The receptors interestingly mimicked the results of the immunohistochemistry data, with Y1 receptor being the most abundantly expressed and Y5 being present at a lower level and being harder to detect even in its transcription. Leptin receptor mRNA expression, which was known to be expressed in rat astrocytes in other studies (193), was also observed in order to ascertain that the astrocytes were sensitive to the effects of other hormones and were as close as possible to their chemoreceptor role in the human brain stem that they would normally present, and the expression of adrenergic receptor β_2 was investigated due to its sensitivity to catecholamines modelling SNS activity. The results for Y1 and Y5 receptor did not reach statistical significance in the changes exerted by the presence of NPY, yet the trend showed a slight increase in expression for both Y1 and Y5 receptors (Figure 31 A and B) after exposure to NPY in an overnight incubation, and could be attributed to the cell responding to the presence of NPY signalling by

slightly up-regulating its receptors. β_2 receptor did not seem to change expression level significantly, although after NPY exposure expression appeared to decrease slightly. The decrease in expression is an interesting effect, and was decided to be explored later in further incubations. Exposure of the astrocytes to Leptin decreased expression of its own receptor significantly, possibly suggesting responsiveness and down-regulation of the receptor in behaviour different to that of an NPY signalling response. This desensitization effect has already been observed in hypothalamic astrocytes (194) following prolonged leptin exposure with the different length of the time that the peptides are present in the medium, since leptin could have a longer half-life ensuring that signalling continues for a longer response which could regulate a negative feedback loop and desensitising the astrocytes at the mRNA level as well as with intracellular signalling. These results show that NPY receptor can be readily detected at the mRNA level in the astrocytes, and that sensitivity and ligand response at the transcription level could be different due to different signalling pathways involved in the response, and with the presence of leptin mRNA transcription as well as adrenergic receptor transcription the primary cells show to be an interesting model for brain stem function in relation to SNS activity.

4.4.3 Astrocyte receptor mRNA in response to SNS activity (Noradrenaline/NPY) data

The next step in the determination of receptor transcription in the astrocytes was to mimic the characteristics of chronic level of SNS activity on the cell population and to see how receptor transcription was affected. Figure 32 shows the various incubations with NPY and/or noradrenaline, and the effects on adrenergic receptors α_2 (later found to also be expressed in the astrocytes) and β_2 , as well as NPY receptor Y1, the most abundantly expressed receptor in the astrocyte according to the mRNA expression data. Figure 32A shows the differences in gene expression resulting from incubation with noradrenaline (at 0.01 μ M), with the only significant difference being a decrease in α_2 expression in line with other animal studies in cardiac tissue showing a decrease in receptor expression following stimulation with noradrenaline (195). β_2 levels did not seem to change significantly, possibly suggesting that the astrocytes might be more sensitive to α_2 stimulation rather than β_2 . The same decrease in α_2 expression can be

observed at a higher concentration of noradrenaline (0.1 μ M, Figure 32B), yet there is also a significant decrease in Y1 receptor expression. The reason for the decrease of Y1 expression may be due to the signalling pathway could be due to the role of NPY as a co-transmitter of noradrenaline (155), where maybe an excessive stimulation of noradrenaline as mimicked by a higher concentration could mean a negative feedback in its co-transmitter receptors as well, in a concerted manner of self-regulation from excessive stimulation. Figure 32C shows mRNA transcription changes from a dose of NPY (2.3nM or 10ng/ml), showing no significant differences between the groups. The fact that NPY alone does not affect receptor transcription at all could mean that its effects are solely in concert with noradrenaline signalling. Interesting effects were seen in the combinations of noradrenaline with NPY (Figures 32D and E), where the lower concentration of noradrenaline (Figure 32D) caused the expected decrease in α_2 expression, yet the decrease occurred also with β_2 receptors as well. The fact that β_2 receptors were also down-regulated in a significant manner could mean that NPY is also causing an increased stimulation of the intracellular signalling of noradrenaline as described by previous studies in other tissues such as in rabbit smooth muscle cells (149), and therefore causing down regulation of the β_2 receptors as well. Raising the concentration of noradrenaline though did not seem to elicit any significant changes in receptor expression, although Y1 expression significantly increased in an opposite manner to that of noradrenaline alone. A possible explanation to this opposite effect could be due to differences in secondary messengers inside the cell that the combined presence of noradrenaline and NPY causes, namely via alpha-adrenoceptors and calcium levels (196) observed in rat brain, with this potentiation causing possibly different gene expression profiles. What is clear from this RNA expression data is that despite a lack of consistently statistically significant changes for the combinatorial treatment of noradrenaline and NPY, the results and reaction to co-stimulation is very different from treatment with single molecules at the mRNA transcription level in this cell line, which could underlie changes in intracellular secondary messengers and overall cellular responses.

4.4.4 Astrocyte inflammatory cytokine secretion data

The data summarised in Figure 33, depicting the secretion of MCP-1 (B) and IL-6 (A), showed a very interesting difference between the secretions of the two inflammatory cytokines in response to noradrenaline and NPY. MCP-1 (Figure 33B) showed significant differences from the control population only in the IL-1 β positive control and when incubated solely with NPY. Since the existing evidence linking NPY signalling and MCP-1 secretion is scarce, the fact that a significant difference in MCP-1 secretion and NPY exposure is an interesting fact by itself.

Astrocytes are known to secrete MCP-1 as a neuroprotective response to viral infections and inflammation in general (197), and there is also evidence of increased MCP-1 production by astrocytes with stimulation of adrenergic β_1 and β_2 receptors in human astrocytes and the activation of intracellular protein kinase A activity (198), yet the results in these experiments show a trend towards increased MCP-1 secretion but no statistical significance possibly due to low numbers or simply due to the inhibitory effects of α -adrenoceptors being stimulated simultaneously by noradrenaline. Nevertheless, MCP-1 secretion appears to be increased by NPY alone.

IL-6 secretion (Figure 33A) on the other hand was very interesting to observe since statistically significant differences were observed in all incubations except for the lower dose of NA. IL-6 levels increased not only by treating the cells with every treatment done with the use of noradrenaline or npy, but a statistically higher difference was also observed between the higher dose of noradrenaline and the same dose with the addition of NPY, almost to denote a synergistically higher secretory response in tandem with NPY. There is evidence proving that IL-6 secretion is increased by NA stimulation in animal models (199), and that synergistic release of IL-6 with other peptides such as vasoactive intestinal peptide (VIP) is possible (200), yet NPY as a co-stimulator of IL-6 release has not yet been ascertained and could be mediating the mechanism in a similar way to previous studies demonstrating the increase of intracellular secondary messengers such as cyclic AMP which are very important in eliciting a local inflammatory response .

4.4.5 Intracellular secondary messengers and IL-6

Figure 34 and Figure 35 show the changes in intracellular messengers of two separate intracellular signalling pathways that were in the experiments following IL-6 release assays with noradrenaline and NPY, cAMP and pSTAT3 (JAK-STAT pathway), respectively. In Figure 34, the response elicited by NPY and noradrenaline is very clear, with 30 minutes (A), showing the most prominent response with significant increases from the untreated levels of cAMP for noradrenaline, combination of NPY and NA and the positive control, yet not for NPY on its own.

At other time points, namely 1 hour (Figure 34B) and 3 hours (Figure 34C) this significant difference disappears and is no longer visible, suggesting a rapid and quickly disappearing cAMP wave after stimulation. The 30 minute increase in cytosolic cAMP levels proves the responsiveness of the adrenoceptors to NA stimulation as expected as well as the increase in the positive IL-1 β control within a short timeframe, yet still showing the synergistic effect of the presence of NPY at the cAMP level with the NPY/NA combination incubation raising the intracellular cAMP levels the highest. This appears to be very interesting given studies pointing towards NPY having an inhibitory effect on adenylyl cyclase (201,202), yet there is also evidence of a synergistic effect of NPY on adrenoceptor-mediated pathways (203), which could suggest an interaction in a common secondary messenger between adrenoceptor and NPY receptor secondary messengers. The increase in intracellular cAMP after stimulation with the various molecules would also explain the increase in IL-6 secretion, given that in other cell types IL-6 release is mediated by the same secondary messenger (204).

Figure 35 shows the response to NA and NPY via the phosphorylation of the JAK/STAT signalling pathway, with significant differences in signalling shown with NPY and NA as soon as 30 minutes after the start of the incubation (Figure 35A), although the greatest significant differences were seen at one hour after start (Figure 35B), albeit the positive control lacked a statistically significant increase and only showed a trend. What is also interesting in these results though is that pSTAT3 levels still appear to be the highest in the combination of NA with NPY. At three hours, there is a decrease in the amount of phosphorylated STAT3 levels, with the highest significant being the positive control and NPY incubations. The reason for the levels of

pSTAT3 decreasing below control could be due to a compensatory inhibitory effect in the cell after stimulation of the signalling pathway. What could be a limitation to the investigation of this specific secondary messenger in this cell type is that STAT3 is phosphorylated also as a response to IL-6 binding to its receptor (205), and therefore the secreted IL-6 in response to the increased intracellular cAMP levels in the cell could bind to the cell in an autocrine manner and elicit a JAK/STAT response by itself. Nevertheless, the quantity of cAMP found to be increased by NA and NPY synergistically these series of experiments give an interesting basis on which to show the increased effect of peripheral NPY signalling and chronic SNS activity on the regular function of brain stem astrocytes.

4.4.6 cAMP levels and IL-6 release in brain stem astrocytes

To confirm the fact that IL-6 secretion was mediated by the presence of heightened levels of cAMP in the astrocytes, cAMP levels were heightened artificially in the cells overnight via the use of phosphodiesterase inhibitors (dbcAMP and IBMX) and adenylyl cyclase activators (Forskolin). Figure 36 shows that after an overnight incubation with the drugs, acting in two separate ways to heighten the levels of cAMP in the cytosol, IL-6 release from the astrocytes received a dramatic and statistically significant increase compared to the control population. These results clearly show the type of effect seen in other studies regarding the release of IL-6 mediated by cAMP, and clearly show the effect of the adrenoceptor pathway being involved in the heightened inflammation level, yet still do not explain the synergistic effect that these cells show when treated in combination with NPY.

4.4.7 IL-6 and lactate release data

Since a greater quantity of paracrine and autocrine signalling by secreted IL-6 was explored in the previous experiments, the next step in the determination of an abnormal function of the astrocytes was to examine whether the cells changed behaviour in any of their regular functions in the presence of heightened inflammation levels and whether this could cause a long-term dysfunction in their role of metabolic support for the neuronal circuits they surround. Figure 37 shows a very marked increase in the release of lactate, which is significantly higher from the first

time point of 1 hour up to 24 hours after the start of the incubation. This difference in lactate secretion from cells that have a metabolism apt to providing lactate to surrounding cells as proved by previous research showing a much more marked tendency to produce and secrete lactate more than needed by the cell in various energetic states (206,207). This increased lactate production compared to basal levels could be due to an immune response, of which astrocytes are known to be players in the brain and CNS (208), yet the increased levels of the molecule beyond normal ranges could be detrimental to the astrocytes themselves by causing acidosis for which there is evidence *in vitro* from previous studies (209), but what could be more interesting is the effect of this excessive lactate secretion on the function of neuronal circuits, since recent evidence generated from *in vivo* studies points to lactate secreted from astrocytic origins as a direct player in the functioning of neuronal circuits such as in the locus ceruleus (210). There is also evidence pointing towards an increased toxicity of lactate in aged neurons, which could also mean a greater vulnerability of neural networks in the CNS and brain to overall heightened levels of lactate for a prolonged period of time such as during chronically high levels of stress with concerted signalling of NPY and NA in the brain stem. This type of excess imbalance is not directly proven to be problematic to the functioning of neural circuitry such as the chemo sensitive astrocytes in the brain stem, but *in vivo* studies pointing towards a chronic exposure of NPY as problematic for baroreflex control (166), and other diseases like OSA and hypertension in human obese patients being linked with circulating NPY levels (164) show that more investigation in this dysfunction of astrocyte is absolutely needed, given increased localized inflammation and abnormal control of lactate secretion as an inflammatory response to NA and NPY stimulation.

4.4.8 Astrocyte cytokine array

The heightening of inflammation levels caused by noradrenaline and NPY stimulation of astrocytes was postulated to not be confined to IL-6 secretion, as there could be many other cytokines up-regulated by synergistic effects of the NA and NPY. In order to test this, a cytokine

panel array was carried out on astrocyte cell populations to possibly point to different cytokines which could also be secreted.

The results of this experiment in Figure 38 show 4 cytokines that we found to change from the control array to the exposed arrays, namely IL-8, IL-1ra, CXCL1, and Interferon- γ . IL-8 secretion in astrocytes is known to be mediated by the JAK-STAT pathway (211), therefore an increase in IL-6 and an autocrine response to the molecule could also cause an up-regulation of other inflammatory cytokines such as IL-8 like the one observed in the array. IL-1ra up regulation as seen in the NA+NPY population also is indicative of an IL-6 response since it is known to be secreted as an anti-inflammatory cytokine in response to IL-6 stimulation (212). CXCL1, an inflammatory chemokine, is also known to be secreted as a result of IL-6 stimulation in other cell types (213) and its increase in the array can also be linked to autocrine IL-6 exposure in the medium. Interferon gamma, a cytokine implicated in neuronal degeneration *in vitro* (214) and up regulated in our array, is known to have converging intracellular signals with IL-6 (215), therefore could be secreted also as a response to IL-6 receptor autocrine activation.

The results shown by this array show that many other cytokines are up-regulated in response to local IL-6 and increased inflammation levels, which could set the stage for a possible degeneration of function of the astrocytes themselves, and therefore their adjacent neuronal networks and is further proof of the theory that localized inflammation levels caused by excessive adrenergic receptor signaling boosted by raised NPY levels could be leading to excessive dysfunction in the brain stem.

4.4.9 Astrocyte leptin receptor gene silencing

The concept of using the cell line as a possible model for indicating the damage caused by chronically elevated SNS activity in the brain stem also meant that the *in vitro* model could be used to simulate the conditions of chronic elevation of other hormones. This could be done by down regulating their receptors as well as being used to isolate the receptors responsible for the increased inflammatory response.

This would mean setting up a gene silencing experiment in order to develop a way to eliminate the expression of specific receptors: in the experiments (Figure 39) that we started to test whether it was possible to silence genes in these astrocytes via the use of short interfering (siRNA), used to silence the leptin receptor which had its expression become virtually undetectable compared to the control sample, as opposed to the varying amount of transcription of another control gene, GAPDH which had not been affected experimentally. It is needed to be said that the negative control in this experiment did not show any expression due to the samples not being viable for real-time PCR, yet the leptin samples do show a variation in relative expression which is quite striking, and show a promising idea that gene silencing could be possible when confirmed with further experimentation. Evidence of gene silencing being effective with *in vitro* cultured astrocytes has been shown in previous studies (216), and this type of technique could prove very valid in determining the receptors precisely responsible for the synergistic inflammatory response in the astrocytes.

4.4.10 Intracellular Ca²⁺ levels in astrocytes

Cytosolic Ca²⁺ levels, heightened in waves by the release and replenishment of intracellular calcium stores are very important players in the responses to many external stimuli in astrocytes such as with leptin signalling (194,217), intracellular communication (140), and was one of the main initial findings which led to the consolidation of the astrocyte being much more involved in synaptic and neuronal activity as merely that of a scaffolding for neurons as previously thought (132). In the series of incubations carried out with a calcium-specific dye monitoring responses to noradrenaline and NPY in Ca²⁺-free medium, with examples of the incubations

shown by Figure 40. Initial testing with ATP, a known elicitor of intracellular Ca^{2+} levels (Figure 40A) showed that the cells were responsive to the molecule with easily detectable oscillatory waves seen by selecting 10 cells at random and recording the resulting oscillations. The control activity of the cell (Figure 40B) was monitored by, along with incubations with noradrenaline (Figure 40C), NPY (Figure 40D) and the combination of the molecules (Figure 40E). The results for the control incubation were as expected, with spontaneous oscillations occurring during the incubation as would occur with normal signalling (Figure 40B). Incubations with the addition of $10\mu\text{M}$ NA caused a wave-like intracellular calcium response (Figure 40C) when the molecule was introduced in the medium, which persisted for minutes after the initial dose was given. Since noradrenaline is not specific to α or β adrenoceptors, yet the only documented adrenoceptors in astrocytes which appear to have calcium as a secondary messenger system are the α_1 group, which are thought to be implicated in the function of long-term synaptic remodelling after prolonged stimulation (218,219), it appears as though these adrenoceptors are being stimulated by noradrenaline and are eliciting a response via intracellular Ca^{2+} levels, and this could be evidence pointing to the fact that despite their being expressed at a very low and almost undetectable way at the RNA level, α_1 receptors are present on the membrane and eliciting a response in these cells. Oscillations occurred when the cells were exposed to $10\mu\text{g/ml}$ of neuropeptide Y (Figure 40D), with the difference that the oscillations appeared to have a higher intensity compared to the ones elicited by NA. This shows that the evidence previously gathered in other studies in the literature showing the ability of NPY receptors to open intracellular calcium stores (173,203,220) is valid in the case of these cells as well, and could be contributing to the activation of protein kinases like protein kinase C (221) as well as the traditional protein kinase A pathway activated by β -adrenoceptors. The combination of the molecules also showed a prolonged oscillatory response as well, yet the activation of both secondary messengers (cAMP, Ca^{2+}) could be simultaneously activated in a synergistic way like described in other cell types. This system of activation, of which previous studies in other cell types (222) have shown to be cross-talking between cAMP and Ca^{2+} stores in the cell could be a possible explanation for

this increased combinatory effect of NA + NPY, and therefore could be important in explaining the increased inflammatory response elicited by the two molecules.

Future work with respect to these experiments would be geared not only towards the selective inhibition via pharmacological means of the NPY and/or adrenergic receptors that could be responsible for the cytoplasmic Ca^{2+} fluctuations in the cell line, but would also involve the concomitant use of mitochondrial calcium dyes such as Rhod-2 in order to see which Ca^{2+} stores are also involved in the responses.

4.4.11 Summary of astrocyte data

Using a brain stem astrocyte primary cell line to simulate the effect prolonged heightened levels of NPY and noradrenaline could have on the functioning of specific areas of the CNS, such as the RVLN and other centres of breathing control, it was found that α and β adrenergic receptors and NPY receptors were expressed on the astrocytes, that they changed expression levels when exposed to their ligands and that the exposure of the astrocytes to noradrenaline and NPY caused a higher secretion of interleukin-6, yet the two molecules simultaneously caused a synergistic effect which was reflected in the cytoplasmic levels of secondary messengers like cAMP. The levels of IL-6 that were found to be increased were also indicative of metabolic dysfunction in the astrocyte by showing an increased secretion of lactate by the astrocytes, and the secreted IL-6 was shown to cause the secretion of other inflammatory mediators as an autocrine response by the cells. The cells also showed oscillatory calcium waves when exposed to NA and NPY, implying the presence activation of α_1 -adrenoceptors on the astrocytes as well, which could underlie the synergistic effect in inflammation of NA and NPY by further increasing levels of intracellular calcium in a concerted action of NPY and adrenoceptors as well as traditional cAMP mediated responses of β -adrenoceptors.

The detection of increased lactate levels following inflammatory IL-6 stimulation in the astrocytes shows that an important aspect of neuronal regulation is modified by the increased inflammation levels. Lactate, as also discussed in the introduction, is an important molecule responsible for not only along with glutamate in the consolidation of long-term synaptic

potentiation associated with memory development as shown in animal models (223,224), but also in the regular activation of neighbouring neurons (210).

This data then could point to the increased level of lactate secretion due to a heightened level of local inflammation, which could lead to more to a more impaired function of the astrocyte itself (as also observed in other astrocyte types in animal models) and referred to as “reactive astrocyte” phenotype, or “astrogliosis” (225). Initially observed in neural tissue scarring and characterised by the impaired function and morphological characteristics of the astrocyte itself, there are a great number of molecular markers determining a reactive astrocyte phenotype (226), yet differences in the markers that the phenotype shows can be observed according to how the inflammation was elicited (225).

This astrocyte data suggests a heightened local inflammation state, and therefore more research should be carried out in the functional characterisation of this heightened inflammation level by exploring common astrogliosis markers in the cell line at the RNA and protein level and could give promising results in the determination of proper function of the astrocytes in this inflamed state and elucidation of the function of peripheral NPY signalling on the central nervous system in obesity in a human primary cell line.

4.5 Conclusions, limitations and future work

4.5.1 Intracellular boost of noradrenergic signalling by NPY via Ca^{2+} levels

The data shown by the astrocytes which describes this increase in inflammatory signalling is with respect to previous knowledge of astrocytic function and of regulation of neural circuits of the brain stem interesting since it brings a good amount of novel insight to the possible mechanisms underlying the onset of comorbidities such as OSA, hypertension and metabolic dysfunctions of the adipose tissue caused by the presence of increased NPY levels boosting the quantity of inflammatory signalling mediated by catecholamines, at both the CNS level with brain stem astrocytes being the main players and in adipose tissue as well.

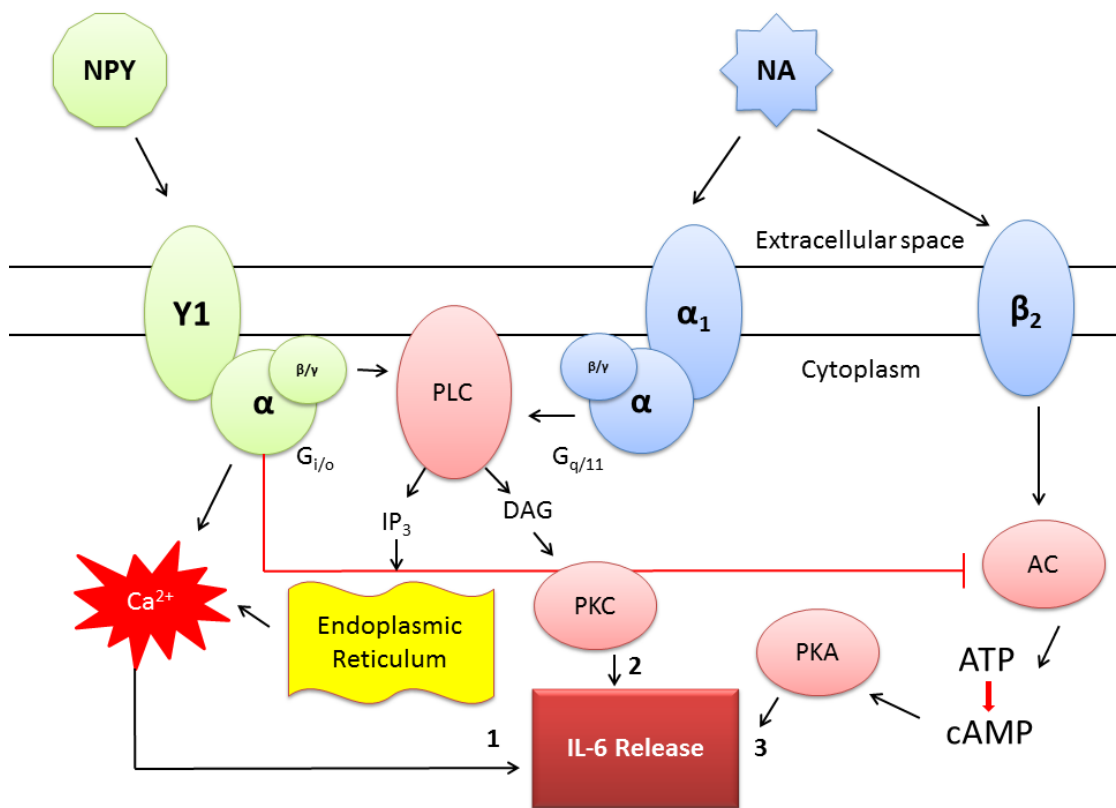


Figure 41: possible mechanisms for potentiation of IL-6 release from astrocytes caused by noradrenaline and NPY in unison

(PLC = Phospholipase C, PKC = Protein Kinase C, PKA = Protein Kinase A, AC = Adenyl Cyclase, DAG = Diacylglycerol, IP_3 = inositol trisphosphate, black arrow = activation, red line = inhibition)

From the data gathered in the astrocyte experiments and what is known in the literature the mechanism for this synergy, the picture that emerges is that of increased and exacerbated calcium responses and cAMP responses that are being elicited by both NPY and noradrenaline,

meaning that as shown by Figure 41, the actual presence of NA and NPY in combination stimulates both α and β adrenoceptors, with α_1 adrenoceptor appearing to be responsible for the calcium increase given the fluorescence data and the known literature (218), as well as the direct stimulation of calcium by NPY receptor Y1 as demonstrated by the fluorescence data and previous studies (203). What is interesting to observe though is that despite the levels of Ca^{2+} increasing, the action of Y1 receptor is known to be inhibitory of adenylyl cyclase and intracellular cAMP levels in other cell types such as vascular smooth muscle cells or in interaction with other cAMP-mediated hormone responses (173,227), yet the data from the astrocytes appears to show that cAMP levels are still higher than those of the cells exposed to NA alone, suggesting that the pathway is not as inhibited as in other cell types, or that the sheer amount of noradrenaline could be activating the pathway regardless of the actual levels of both neurotransmitters. Another possibility that could explain the occurrence of the activation of both neurotransmitters is the evidence of cross-talk between the two secondary messenger signalling pathways (222,228–230), which could show specific interaction in this cell type as well. This raised level of both secondary messengers, which in the case of phospholipase C activation as done by Y1 receptor and α_1 -adrenoceptor activate isoforms of protein kinase C via phospholipase activation (203,231) , and in the case of cAMP levels activate protein kinase A both converge on the same result of signalling the secretion of interleukin-6 (232), and causing the downstream increase in signalling in a synergistic manner (pathways 1, 2 and 3 in figure 38). With this synergistic action observed in other cell types and with other hormones along with neuropeptide Y, and the results from the astrocyte data and the heightened presence of the molecule in the circulation of morbidly obese patients with states of heightened SNS activity shows that it is very important to study the process in detail and to elucidate whether this type of concomitant signalling is behind the onset of a worsening metabolic phenotype in the human metabolism, and the effects of neuropeptide Y's concerted action with SNS activity on overall inflammation levels in other parts of the CNS.

Recent studies for example, Park *et al.* (233), showing that the elimination of NPY signalling via knockout of the NPY gene in rats reduces adiposity despite no change in food intake could lead an interesting type of further hypothesis to this study: that the targeting of NPY signalling from the periphery to the CNS in an inhibitory manner via receptor antagonists or monoclonal antibodies could mean that the paracrine and endocrine effects of the signalling could be eliminated, with the comorbidities arising from functional impairment of the astrocytes due to heightened inflammation in the brain stem possibly partially reversed in humans as well. More work is to be done to confirm this type of hypothesis in the ways described previously in this section.

4.5.2 Limitations of the astrocyte model and future work

The limitations of this model is that the *in vitro* signaling experiments in the cell line could not be ideal in reproducing the quantities of circulating neuropeptide Y in physiological conditions, yet these experiments represent a starting point for more elaborate research, with specific agonists and antagonists of α and β adrenoceptors which could be used to nullify or single out the effects of specific types of adrenoceptors, as well as the use of specific agonists of various NPY receptors in order to ascertain which receptors are responsible for the observed effects. Also, another experiment which could be developed is the use of phorbol esters to activate protein kinase C and to see whether the additive effect is observed as well. Another limitation to this study is the lack of western blotting experiments to the adrenergic and the neuropeptide Y receptors themselves, which could be done to determine the changes of the receptors expressed at the protein level given the lack of significant differences in the experiments exploring mRNA levels, which could also be due to small numbers of the samples examined. What could also be investigated is the effect of these chronically heightened inflammation levels on the quantity of receptors for other hormones such as leptin, which is very well known to be expressed by these astrocytes (147), and the effects it could have on their ability to sense the hormone from the bloodstream in the RVLM. The gene silencing experiments could also prove interesting in isolating the receptors responsible for this synergy as well, and would also be definitely considered for future work in the field.

As previously also mentioned in the relevant data summary sections, the future work with respect to astrocytes could also be to explore the inflammation markers that are associated with the reactive astrocyte state observed in other models of disease and whether they could be found in the case of chronic NPY + NA stimulation in order to describe whether this state could also occur at the level of the brain stem and after NPY-potentiated NA signaling.

4.5.3 Development of an animal model

Given the results of the *in vitro* model, the next logical step in the development of an even more accurate model for long term stress and SNS activity on the brain stem would be the development of an animal model, either mouse or rat, that could be used for long-term exposure to catecholamines and NPY levels, so the effects of this type of synergistic signaling could be observed in brain stem tissue slices isolated from the animals or even looking at the way the control of breathing and blood pressure is affected. Similar studies such as Xie *et al.* 2012 have been carried out with rats and long-term exposure to NPY (166), and were an inspiration in the development of these experiments to begin with.

Long-term stress has been observed by other studies like Abe *et al.* 2010 also point to NPY as having a pivotal role in the degeneration of metabolic function in the periphery, but brain stem astrocyte activity and its direct link to the synchronization and control of neural networks like the types seen in other circuits and described in the introduction of this thesis have not yet been linked, and the *in vitro* data generated by this study shows that there is room for further investigation in the matter in an animal model.

An animal model could also allow for the design of an experiment involving knockout mutants for NPY receptor genes like the ones used in studies of Park *et al.* 2014 (233), and this the effects of nullifying the role of NPY receptors via knockdown/knockout or pharmacological means could prove useful in the understanding of their role in the interplay between central nervous system and peripheral signaling.

Immunohistochemistry for local IL-6 levels in the brain stem after long-term circulating NPY exposure on brain stem tissue slices could prove further the hypothesis that local inflammation could be driving the dysfunction observed in other animal models such as Xie *et al.*, and further reinforce the evidence gathered by the *in vitro* experiments. An animal model could also provide indication as to the functionality of the astrocytes (and neural circuits of the RVLN) with respect to other hormones important for metabolic control of the adipose tissue and blood pressure, such as Angiotensin II and Leptin, as well as giving the opportunity to look at the functionality

(such as the presence of insulin resistance as a result of heightened circulating NPY and catecholamine levels) of the peripheral tissues of the animal at the same time in order to observe NPY secretion rate.

What could be a limitation between the use of human-derived astrocyte cell lines and a rat model on the other hand is that given evidence that there are differences in cell functionality in the regulation of inflammation between human and rat astrocytes as shown by evidence in the literature (234), the applicability of results could be different compared to a human *in vitro* model. Nevertheless, the overall view of NPY's peripheral and central effects that an animal model could offer would give extremely important results in the elucidation of the link between stress, peripheral tissue function and its effects on the central nervous system.

A possible way this study could be prolonged in the use of an animal model would be to combine the methodology of Xie *et al.* (166), with the long-term administration of NPY from the periphery, seeing the central effects this could have on brain stem astrocyte function either *in vivo* directly from brain stem slices or from isolated astrocytes of the rat brain stem cultured *in vitro*. Also, the study of NPY knockout mice such as the study by Park *et al.* (233) and their reactivity according to Y1, Y5 receptor specificity, in order to isolate the receptor which is being targeted at the central nervous system level and its inflammatory action on the astrocytes therein could be studied.

4.5.4 DPP-IV and its effects on NPY signalling

One of the aspects that were not fully investigated in this study was the effect of Dipeptidyl Peptidase-IV (or DPP-IV) on NPY's ability to target specific NPY receptors compared to others on the cell surface. Since receptor specificity could change the effects of NPY's ability to affect intracellular signalling, as seen with adipocytes and is an important step in NPY processing with other cells as well (159,235,236), the inhibition of DPP-IV by using specific drugs such as one belonging to the gliptin class of DPP-IV inhibitors could give insight into which NPY receptors are mediating the synergistic effect on the astrocyte cell line. DPP-IV expression levels and protein levels investigated in the adipose tissue of the patients directly via real-time PCR or western

blotting could prove very useful in the determination of a preferential receptor being activated *in vivo* in the adipose tissue and causing a difference in lipolytic potential of the adipocytes at the local level, which could also explain the hypertrophy results shown by the histology investigation. The results shown in this thesis, despite DPP-IV inhibition on the other hand are still valid since they demonstrate physiological conditions as much as possible, and therefore are reflecting the physiological amount of DPP-IV activity in the cells as much as possible.

4.5.5 Precise NPY detection

What has also emerged during the work on NPY levels in this thesis is the difference in detectable levels of circulating NPY between the various studies in the literature and the results gathered by the means of this study. Various studies show varying overall levels of circulating NPY (153,164,176,237) compared to the results shown by our investigation, although serum NPY was relatively different and therefore indicative of overall circulating levels regardless of quantity. What should be ameliorated in the future of studying the peptide is the detection method, possibly changing from a sandwich ELISA used in this thesis to more elaborate methods such as gas chromatography and mass spectrometry, two methods that are more precise in their detection of NPY levels and becoming viable in a clinical setting as well as much more popular in the scientific community. Undoubtedly they are more expensive than ELISA detection, yet the development of more economical and cheaper means of clinical analysis with the continuous refinement of the technologies cited could prove more advantageous in the future.

4.5.6 The need for a common MHO definition

What is shown from the results shown in this thesis, which range from the population study at the clinical level to tissue studies at the organ level and *in vitro* studies at the cellular level is that the molecular mechanisms underlying the regulation of SNS activity, metabolic function and overall reaction of the human body to excessive energy intake can vary dramatically according to the factors at play, and this happening in a population which was kept at the same age, BMI and ethnic group, so already in a condition of being a subset singled out from the

population of a developed country. This type of diversity that this group of patients and other groups has observed could have a variety of effects and is a very important source of information for more detailed studies like this one, yet the difference in the discrimination of patients between studies, and the lack of central approval from a global organization like the World Health Organisation of a common MHO definition makes the accurate study of the phenomenon and the search for hypothetic biomarkers (such as the proposed Neuropeptide Y in this thesis) difficult.

Studies into the incidence of MHO characteristics among obese populations are going in the right direction by starting to adopt unifying criteria (179) and also to take more complex variables than the mere measurement of body mass index into account to classify patients in separate metabolic groups. But a coordinated effort is needed for a more stratified and precise approach to the emerging problem of obesity in the developed world, which as research progresses and refines its techniques to solve the problems and burdens that obesity entails, is also revealing a much more complex and diverse multi-variant phenomenon involving not only the adipose tissue and its energetics, but also the regulatory mechanisms which change according to patient type.

Bibliography

Bibliography

1. WHO. Obesity: preventing and managing the global epidemic. World Health Organ Tech Rep Ser. 2000;
2. Sims EA, Danforth E. Expenditure and Storage of Energy in Man. *J Clin Invest.* 1987;79:1019–25.
3. Morgan, E Dent M. The economic burden of obesity. 2010;(October).
4. Dent, M Chrisopoulos S, Mulhall C RC. Bariatric surgery for obesity. *Natl Obes Obs.* 2010;(August).
5. Hilton S, Patterson C, Teyhan A. Escalating coverage of obesity in UK newspapers: the evolution and framing of the “obesity epidemic” from 1996 to 2010. *Obesity (Silver Spring).* 2012 Aug;20(8):1688–95.
6. Allender S, Rayner M. The burden of overweight and obesity-related ill health in the UK. *Obes Rev.* 2007 Sep;8(5):467–73.
7. Lau DCW, Douketis JD, Morrison KM, Hramiak IM, Sharma AM, Ur E. 2006 Canadian clinical practice guidelines on the management and prevention of obesity in adults and children [summary]. *CMAJ.* 2007 Apr 10;176(8):S1–13.
8. Kahn SE, Hull RL, Utzschneider KM. Mechanisms linking obesity to insulin resistance and type 2 diabetes. *Nature.* 2006 Dec 14;444(7121):840–6.
9. Hofbauer KG, Nicholson JR. Pharmacotherapy of obesity. *Exp Clin Endocrinol Diabetes.* 2006 Oct;114(9):475–84.
10. Van Gaal LF, Mertens IL, De Block CE. Mechanisms linking obesity with cardiovascular disease. *Nature.* 2006 Dec 14;444(7121):875–80.
11. Muniyappa R, Sowers JR. Role of insulin resistance in endothelial dysfunction. *Rev Endocr Metab Disord.* 2013 Mar;14(1):5–12.
12. Kerr SMP, Livingstone MBE, McCrorie T a, Wallace JMW. Endothelial dysfunction associated with obesity and the effect of weight loss interventions. *Proc Nutr Soc.* 2011 Nov;70(4):418–25.
13. Hall JE, Brands MW, Henegar JR. Mechanisms of hypertension and kidney disease in obesity. *Ann N Y Acad Sci.* 1999 Nov 18;892(601):91–107.
14. Lobato NS, Filgueira FP, Akamine EH, Tostes RC, Carvalho MHC, Fortes ZB. Mechanisms of endothelial dysfunction in obesity-associated hypertension. *Brazilian J Med Biol Res.* 2012 May;45(5):392–400.
15. Toda N, Okamura T. Obesity impairs vasodilatation and blood flow increase mediated by endothelial nitric oxide: An overview. *J Clin Pharmacol.* 2013 Sep 9;(September).

16. Hall JE. The kidney, hypertension, and obesity. *Hypertension*. 2003 Mar;41(3 Pt 2):625–33.
17. Dorresteijn J a N, Visseren FLJ, Spiering W. Mechanisms linking obesity to hypertension. *Obes Rev*. 2012 Jan;13(1):17–26.
18. Usmani ZA, Chai-Coetzer CL, Antic N a, McEvoy RD. Obstructive sleep apnoea in adults. *Postgrad Med J*. 2013 Mar;89(1049):148–56.
19. Drager LF, Togeiro SM, Polotsky VY, Lorenzi-Filho G. Obstructive Sleep Apnea: A CardioMetabolic Risk in Obesity and Metabolic Syndrome. *J Am Coll Cardiol*. 2013 Jun 12;62(7).
20. Lam JCM, Mak JCW, Ip MSM. Obesity, obstructive sleep apnoea and metabolic syndrome. *Respirology*. 2012 Feb;17(2):223–36.
21. Toschi-Dias E, Trombetta IC, Dias da Silva VJ, Maki-Nunes C, Cepeda FX, Alves M-JNN, et al. Time delay of baroreflex control and oscillatory pattern of sympathetic activity in patients with metabolic syndrome and obstructive sleep apnea. *AJP Hear Circ Physiol*. 2013 Jan 25;304(7):H1038–44.
22. Zámbo V, Simon-Szabó L, Szelényi P, Kereszturi E, Bánhegyi G, Csala M. Lipotoxicity in the liver. *World J Hepatol*. 2013 Oct 27;5(10):550–7.
23. Koo S-H. Nonalcoholic fatty liver disease: molecular mechanisms for the hepatic steatosis. *Clin Mol Hepatol*. 2013 Sep;19(3):210–5.
24. Asrih M, Jornayvaz FR. Inflammation as a potential link between nonalcoholic fatty liver disease and insulin resistance. *J Endocrinol*. 2013 Sep;218(3):R25–36.
25. Kanuri G, Bergheim I. In Vitro and in Vivo Models of Non-Alcoholic Fatty Liver Disease (NAFLD). *Int J Mol Sci*. 2013 Jan;14(6):11963–80.
26. Krahmer N, Farese R V, Walther TC. Balancing the fat: lipid droplets and human disease. *EMBO Mol Med*. 2013 Jul;5(7):905–15.
27. Ye J. Mechanisms of insulin resistance in obesity. *Front Med*. 2013 Mar;7(1):14–24.
28. DeFronzo R. Insulin resistance. A multifaceted syndrome responsible for NIDDM, obesity, hypertension, dyslipidemia, and atherosclerotic cardiovascular disease. *Diabetes Care*. 1991;14(3):173–94.
29. Grundy SM, Brewer HB, Cleeman JI, Smith SC, Lenfant C. Definition of metabolic syndrome: Report of the National Heart, Lung, and Blood Institute/American Heart Association conference on scientific issues related to definition. *Circulation*. 2004 Jan 27;109(3):433–8.
30. Hardy OT, Czech MP, Corvera S. What causes the insulin resistance underlying obesity? *Curr Opin Endocrinol Diabetes Obes*. 2012 Apr;19(2):81–7.
31. Saltiel A. Insulin signalling and the regulation of glucose and lipid metabolism. *Nature*. 2001;414(December):799–806.

32. Abdul-Ghani M a, DeFronzo R a. Pathogenesis of insulin resistance in skeletal muscle. *J Biomed Biotechnol.* 2010 Jan;2010:476279.
33. DeFronzo R a, Tripathy D. Skeletal muscle insulin resistance is the primary defect in type 2 diabetes. *Diabetes Care.* 2009 Nov;32 Suppl 2:S157–63.
34. Heptulla R, Smitten a, Teague B, Tamborlane W V, Ma YZ, Caprio S. Temporal patterns of circulating leptin levels in lean and obese adolescents: relationships to insulin, growth hormone, and free fatty acids rhythmicity. *J Clin Endocrinol Metab.* 2001 Jan;86(1):90–6.
35. Randle, PJ, Garland PB, Hales CN, Newsholme EA. The glucose fatty-acid cycle. Its role in insulin sensitivity and the metabolic disturbances of diabetes mellitus. *Lancet.* 1963 Apr 13;1(7285):785–9.
36. Elks M. Fat oxidation and diabetes of obesity: the Randle hypothesis revisited. *Med Hypotheses.* 1990;(9):257–60.
37. Samuel VT, Petersen KF, Shulman GI. Lipid-induced insulin resistance: unravelling the mechanism. *Lancet. Elsevier Ltd;* 2010 Jun 26;375(9733):2267–77.
38. Bremer A a, Mietus-Snyder M, Lustig RH. Toward a unifying hypothesis of metabolic syndrome. *Pediatrics.* 2012 Mar;129(3):557–70.
39. Kawano Y, Cohen DE. Mechanisms of hepatic triglyceride accumulation in non-alcoholic fatty liver disease. *J Gastroenterol.* 2013 Apr;48(4):434–41.
40. Wiernsperger N. Hepatic function and the cardiometabolic syndrome. *Diabetes Metab Syndr Obes.* 2013 Jan;6:379–88.
41. Greenberg AS, Obin MS. Obesity and the role of adipose tissue in inflammation and metabolism. *Am J Clin Nutr.* 2006 Feb;83(2):461S – 465S.
42. Rosen ED, Spiegelman BM. Adipocytes as regulators of energy balance and glucose homeostasis. *Nature.* 2006 Dec 14;444(7121):847–53.
43. Karastergiou K, Mohamed-Ali V. The autocrine and paracrine roles of adipokines. *Mol Cell Endocrinol.* 2010 Apr;318(1-2):69–78.
44. Trayhurn P, Bing C, Wood IS. Adipose tissue and adipokines--energy regulation from the human perspective. *J Nutr.* 2006 Jul;136(7 Suppl):1935S – 1939S.
45. Adamczak M, Wiecek A. The adipose tissue as an endocrine organ. *Semin Nephrol. Elsevier Inc.;* 2013 Jan;33(1):2–13.
46. Procaccini C, De Rosa V, Galgani M, Carbone F, La Rocca C, Formisano L, et al. Role of Adipokines Signaling in the Modulation of T Cells Function. *Front Immunol.* 2013 Jan;4(October):332.
47. Strissel KJ, Stancheva Z, Miyoshi H, Perfield JW, Defuria J, Jick Z, et al. Adipocyte Death, Adipose Tissue Remodeling, and Obesity Complications. *Time.* 2007;56(December).

48. Cinti S, Mitchell G, Barbatelli G, Murano I, Ceresi E, Faloia E, et al. Adipocyte death defines macrophage localization and function in adipose tissue of obese mice and humans. *J Lipid Res.* 2005 Nov;46(11):2347–55.
49. Olefsky JM, Glass CK. Macrophages, inflammation, and insulin resistance. *Annu Rev Physiol.* 2010 Mar;72:219–46.
50. Sun K, Kusminski C. Adipose tissue remodeling and obesity. *J Clin Invest.* 2011;121(6).
51. Gregor MF, Hotamisligil GS. Inflammatory Mechanisms in Obesity. *Annu Rev Immunol.* 2010 Apr 5;
52. Hotamisligil GS. Inflammation and metabolic disorders. *Nature.* 2006 Dec 14;444(7121):860–7.
53. Yoshizaki T, Kusunoki C, Kondo M, Yasuda M, Kume S, Morino K, et al. Autophagy regulates inflammation in adipocytes. *Biochem Biophys Res Commun.* Elsevier Inc.; 2011 Dec 1;417(1):352–7.
54. Lee A-H, Heidtman K, Hotamisligil GS, Glimcher LH. Dual and opposing roles of the unfolded protein response regulated by IRE1{alpha} and XBP1 in proinsulin processing and insulin secretion. *Proc Natl Acad Sci U S A.* 2011 May 9;108(21):8885–90.
55. Kovsan J, Blüher M, Tarnovscki T, Klötting N, Kirshtein B, Madar L, et al. Altered autophagy in human adipose tissues in obesity. *J Clin Endocrinol Metab.* 2011 Feb;96(2):E268–77.
56. Hummasti S, Hotamisligil GS. Endoplasmic reticulum stress and inflammation in obesity and diabetes. *Circ Res.* 2010 Sep 3;107(5):579–91.
57. Arner E, Westermark PO, Spalding KL, Britton T, Rydén M, Frisén J, et al. Adipocyte turnover: relevance to human adipose tissue morphology. *Diabetes. Am Diabetes Assoc;* 2010;59(1):105.
58. Smith J, Al-Amri M, Dorairaj P, Sniderman A. The adipocyte life cycle hypothesis. *Clin Sci (Lond).* 2006 Jan;110(1):1–9.
59. Cusi K. The role of adipose tissue and lipotoxicity in the pathogenesis of type 2 diabetes. *Curr Diab Rep.* 2010 Aug;10(4):306–15.
60. Oh DY, Morinaga H, Talukdar S, Bae EJ, Olefsky JM. Increased macrophage migration into adipose tissue in obese mice. *Diabetes.* 2012 Feb;61(2):346–54.
61. Brown BN, Sicari BM, Badylak SF. Rethinking regenerative medicine: a macrophage-centered approach. *Front Immunol.* 2014 Jan;5(November):510.
62. Fujisaka S, Usui I, Iikutani M, Aminuddin a, Takikawa a, Tsuneyama K, et al. Adipose tissue hypoxia induces inflammatory M1 polarity of macrophages in an HIF-1 α -dependent and HIF-1 α -independent manner in obese mice. *Diabetologia.* 2013 Jun;56(6):1403–12.
63. Fischer-Posovszky P, Wang Q a, Asterholm IW, Rutkowski JM, Scherer PE. Targeted deletion of adipocytes by apoptosis leads to adipose tissue recruitment of alternatively activated M2 macrophages. *Endocrinology.* 2011 Aug;152(8):3074–81.

64. Prieur X, Mok CYL, Velagapudi VR, Núñez V, Fuentes L, Montaner D, et al. Differential Lipid Partitioning Between Adipocytes and Tissue Macrophages Modulates Macrophage Lipotoxicity and M2/M1 Polarization in Obese Mice. *Diabetes*. 2011 Jan 24;60(March):797–809.
65. Wood IS, Stezhka T, Trayhurn P. Modulation of adipokine production, glucose uptake and lactate release in human adipocytes by small changes in oxygen tension. *Pflugers Arch*. 2011 Sep;462(3):469–77.
66. Fessler MB, Rudel LL, Brown JM. Toll-like receptor signaling links dietary fatty acids to the metabolic syndrome. *Curr Opin Lipidol*. 2009 Oct;20(5):379–85.
67. Mauvoisin D, Mounier C. Hormonal and nutritional regulation of SCD1 gene expression. *Biochimie*. Elsevier Masson SAS; 2011 Jan;93(1):78–86.
68. Ferrannini E, Natali a, Bell P, Cavallo-Perin P, Lalic N, Mingrone G. Insulin resistance and hypersecretion in obesity. European Group for the Study of Insulin Resistance (EGIR). *J Clin Invest*. 1997 Sep 1;100(5):1166–73.
69. Stefan N, Kantartzis K, Machann J, Schick F, Thamer C, Rittig K, et al. Identification and characterization of metabolically benign obesity in humans. *Arch Intern Med*. 2008 Aug 11;168(15):1609–16.
70. Blüher M. The distinction of metabolically “healthy” from “unhealthy” obese individuals. *Curr Opin Lipidol*. 2010 Feb;21(1):38–43.
71. Brochu M. What Are the Physical Characteristics Associated with a Normal Metabolic Profile Despite a High Level of Obesity in Postmenopausal Women? *J Clin Endocrinol Metab*. 2001 Mar 1;86(3):1020–5.
72. Karelis AD. Metabolically healthy but obese individuals. *Lancet*. 2008 Oct;372(9646):1281–3.
73. Primeau V, Coderre L, Karelis a D, Brochu M, Lavoie M-E, Messier V, et al. Characterizing the profile of obese patients who are metabolically healthy. *Int J Obes*. Nature Publishing Group; 2011 Jul;35(7):971–81.
74. Wildman RP, Muntner P, Reynolds K, McGinn AP, Rajpathak S, Wylie-Rosett J, et al. The obese without cardiometabolic risk factor clustering and the normal weight with cardiometabolic risk factor clustering: prevalence and correlates of 2 phenotypes among the US population (NHANES 1999-2004). *Arch Intern Med*. 2008 Aug 11;168(15):1617–24.
75. Velho S, Paccaud F, Waeber G, Vollenweider P, Marques-Vidal P. Metabolically healthy obesity: different prevalences using different criteria. *Eur J Clin Nutr*. Nature Publishing Group; 2010 Oct;64(10):1043–51.
76. Cameron a J. Metabolically normal obesity: a misnomer? *Int J Obes (Lond)*. 2011 Mar 15;2716–2716.
77. Franz MJ, VanWormer JJ, Crain a L, Boucher JL, Histon T, Caplan W, et al. Weight-loss outcomes: a systematic review and meta-analysis of weight-loss clinical trials with a minimum 1-year follow-up. *J Am Diet Assoc*. 2007 Oct;107(10):1755–67.

78. King DS, Dalsky GP, Clutter WE, Young D a, Staten M a, Cryer PE, et al. Effects of exercise and lack of exercise on insulin sensitivity and responsiveness. *J Appl Physiol*. 1988 May;64(5):1942–6.
79. Kantartzis K, Machann J, Schick F, Rittig K, Machicao F, Fritsche a, et al. Effects of a lifestyle intervention in metabolically benign and malign obesity. *Diabetologia*. 2011 Apr;54(4):864–8.
80. Shin M-J, Hyun YJ, Kim OY, Kim JY, Jang Y, Lee JH. Weight loss effect on inflammation and LDL oxidation in metabolically healthy but obese (MHO) individuals: low inflammation and LDL oxidation in MHO women. *Int J Obes (Lond)*. 2006 Oct;30(10):1529–34.
81. Karelis a D, Messier V, Brochu M, Rabasa-Lhoret R. Metabolically healthy but obese women: effect of an energy-restricted diet. *Diabetologia*. 2008 Sep;51(9):1752–4.
82. Janiszewski PM, Ross R. Effects of weight loss among metabolically healthy obese men and women. *Diabetes Care*. 2010 Sep;33(9):1957–9.
83. Pataky Z, Bobbioni-Harsch E, Golay a. Open questions about metabolically normal obesity. *Int J Obes (Lond)*. Nature Publishing Group; 2010 Dec;34 Suppl 2(S2):S18–23.
84. Buchwald H, Estok R, Fahrbach K, Banel D, Jensen MD, Pories WJ, et al. Weight and type 2 diabetes after bariatric surgery: systematic review and meta-analysis. *Am J Med*. Elsevier Inc.; 2009 Mar;122(3):248–56.e5.
85. Sjöström L, Narbro K, Sjöström C. Effects of bariatric surgery on mortality in Swedish obese subjects. *New Engl J*. 2007;
86. Adams TD, Gress RE, Smith SC, Halverson RC, Simper SC, Rosamond WD, et al. Long-term mortality after gastric bypass surgery. *N Engl J Med*. 2007 Aug 23;357(8):753–61.
87. Sesti G, Folli F, Perego L, Hribal ML, Pontiroli AE. Effects of weight loss in metabolically healthy obese subjects after laparoscopic adjustable gastric banding and hypocaloric diet. *PLoS One*. 2011 Jan;6(3):e17737.
88. Cummings DE, Bloom SR. At the heart of the benefits of bariatric surgery. *Nat Med*. 2012 Jan;18(3):358–9.
89. Durward CM, Hartman TJ, Nickols-Richardson SM. All-cause mortality risk of metabolically healthy obese individuals in NHANES III. *J Obes*. 2012 Jan;2012(Cvd):460321.
90. Hivert M-F, Sullivan LM, Fox CS, Nathan DM, D'Agostino RB, Wilson PWF, et al. Associations of adiponectin, resistin, and tumor necrosis factor-alpha with insulin resistance. *J Clin Endocrinol Metab*. 2008 Aug;93(8):3165–72.
91. De Luis DA, Aller R, Izaola O, Conde R, Gonzalez Sagrado M. The ratio of adiponectin to HOMA as an index of metabolic syndrome in obese women. *Ann Nutr Metab*. 2011 Oct;58(4):301–6.
92. Blüher M, Rudich A, Klötting N, Golan R, Henkin Y, Rubin E, et al. Two patterns of adipokine and other biomarker dynamics in a long-term weight loss intervention. *Diabetes Care*. 2012 Feb;35(2):342–9.

93. Weyer C, Foley JE, Bogardus C, Tataranni P a, Pratley RE. Enlarged subcutaneous abdominal adipocyte size, but not obesity itself, predicts type II diabetes independent of insulin resistance. *Diabetologia*. 2000 Dec;43(12):1498–506.
94. Chandalia M, Lin P, Seenivasan T, Livingston EH, Snell PG, Grundy SM, et al. Insulin resistance and body fat distribution in South Asian men compared to Caucasian men. *PLoS One*. 2007 Jan;2(8):e812.
95. Danforth E. Failure of adipocyte differentiation causes type II diabetes mellitus? *Nat Genet*. 2000 Sep;26(1):13.
96. Dubois SG, Heilbronn LK, Smith SR, Albu JB, Kelley DE, Ravussin E. Decreased expression of adipogenic genes in obese subjects with type 2 diabetes. *Obesity (Silver Spring)*. 2006 Sep;14(9):1543–52.
97. O'Connell J, Lynch L, Cawood TJ, Kwasnik A, Nolan N, Geoghegan J, et al. The relationship of omental and subcutaneous adipocyte size to metabolic disease in severe obesity. *PLoS One*. 2010 Jan;5(4):e9997.
98. O'Connell J, Lynch L, Hogan a, Cawood TJ, O'Shea D. Preadipocyte factor-1 is associated with metabolic profile in severe obesity. *J Clin Endocrinol Metab*. 2011 Apr;96(4):E680–4.
99. Nagy ZS, Czimmerer Z, Szanto A, Nagy L. Pro-inflammatory cytokines negatively regulate PPAR γ mediated gene expression in both human and murine macrophages via multiple mechanisms. *Immunobiology*. Elsevier GmbH.; 2013 Nov;218(11):1336–44.
100. Richard AJ, Amini-Vaughan Z, Ribnicky DM, Stephens JM. Naringenin inhibits adipogenesis and reduces insulin sensitivity and adiponectin expression in adipocytes. *Evid Based Complement Alternat Med*. 2013 Jan;2013:549750.
101. McLaughlin T, Deng a, Yee G, Lamendola C, Reaven G, Tsao PS, et al. Inflammation in subcutaneous adipose tissue: relationship to adipose cell size. *Diabetologia*. 2010 Feb;53(2):369–77.
102. McLaughlin T, Sherman a, Tsao P, Gonzalez O, Yee G, Lamendola C, et al. Enhanced proportion of small adipose cells in insulin-resistant vs insulin-sensitive obese individuals implicates impaired adipogenesis. *Diabetologia*. 2007 Aug;50(8):1707–15.
103. Biddinger SB, Kahn CR. From mice to men: insights into the insulin resistance syndromes. *Annu Rev Physiol*. 2006 Jan;68:123–58.
104. Tontonoz P, Kim JB, Graves R a, Spiegelman BM. ADD1: a novel helix-loop-helix transcription factor associated with adipocyte determination and differentiation. *Mol Cell Biol*. 1993 Aug;13(8):4753–9.
105. Horton JD, Goldstein JL, Brown MS. SREBPs: activators of the complete program of cholesterol and fatty acid synthesis in the liver. *J Clin Invest*. 2002 May;109(9):1125–31.
106. Shimomura I, Bashmakov Y, Ikemoto S, Horton JD, Brown MS, Goldstein JL. Insulin selectively increases SREBP-1c mRNA in the livers of rats with streptozotocin-induced diabetes. *Proc Natl Acad Sci U S A*. 1999 Nov 23;96(24):13656–61.

107. Chen G, Liang G, Ou J, Goldstein JL, Brown MS. Central role for liver X receptor in insulin-mediated activation of Srebp-1c transcription and stimulation of fatty acid synthesis in liver. *Proc Natl Acad Sci U S A*. 2004 Aug 3;101(31):11245–50.
108. De Ferranti S, Mozaffarian D. The perfect storm: obesity, adipocyte dysfunction, and metabolic consequences. *Clin Chem*. 2008 Jun;54(6):945–55.
109. Al-Hasani H, Joost H-G. Nutrition-/diet-induced changes in gene expression in white adipose tissue. *Best Pract Res Clin Endocrinol Metab*. 2005 Dec;19(4):589–603.
110. Shimomura I, Hammer RE, Richardson J a., Ikemoto S, Bashmakov Y, Goldstein JL, et al. Insulin resistance and diabetes mellitus in transgenic mice expressing nuclear SREBP-1c in adipose tissue: model for congenital generalized lipodystrophy. *Genes Dev*. 1998 Oct 15;12(20):3182–94.
111. Saisho Y, Hirose H, Roberts R, Abe T, Kawabe H, Itoh H. C-reactive protein, high-molecular-weight adiponectin and development of metabolic syndrome in the Japanese general population: a longitudinal cohort study. *PLoS One*. 2013 Jan;8(9):e73430.
112. Dai X-P, Liu Z-Q, Xu L-Y, Gong Z-C, Huang Q, Dong M, et al. Association of plasma epinephrine level with insulin sensitivity in metabolically healthy but obese individuals. *Auton Neurosci*. Elsevier B.V.; 2012 Apr 3;167(1-2):66–9.
113. Kong L, Zhu J, Han W, Jiang X, Xu M, Zhao Y, et al. Significance of serum microRNAs in pre-diabetes and newly diagnosed type 2 diabetes: a clinical study. *Acta Diabetol*. 2010 Sep;
114. Ferland-McCollough D, Ozanne SE, Siddle K, Willis AE, Bushell M. The involvement of microRNAs in Type 2 diabetes. *Biochem Soc Trans*. 2010 Dec;38(6):1565–70.
115. Saper CB. The central autonomic nervous system: conscious visceral perception and autonomic pattern generation. *Annu Rev Neurosci*. 2002 Jan;25:433–69.
116. Guyenet PG. The sympathetic control of blood pressure. *Nat Rev Neurosci*. 2006 May;7(5):335–46.
117. Troisi RJ, Weiss ST, Parker DR, Sparrow D, Young JB, Landsberg L. Relation of obesity and diet to sympathetic nervous system activity. *Hypertension*. 1991 May 1;17(5):669–77.
118. Bartness T, Shrestha Y. Sensory and sympathetic nervous system control of white adipose tissue lipolysis. *Mol Cell* 2010;318:34–43.
119. Migliorini RH, Garofalo M a, Kettelhut IC. Increased sympathetic activity in rat white adipose tissue during prolonged fasting. *Am J Physiol*. 1997 Feb;272(2 Pt 2):R656–61.
120. Bartness TJ, Song CK, Shi H, Bowers RR, Foster MT. Brain–adipose tissue cross talk. *Proc Nutr Soc*. 2007 Mar 7;64(01):53–64.
121. Mohamed-Ali V, Flower L, Sethi J, Hotamisligil G, Gray R, Humphries SE, et al. beta-Adrenergic regulation of IL-6 release from adipose tissue: in vivo and in vitro studies. *J Clin Endocrinol Metab*. 2001 Dec;86(12):5864–9.

122. Sandi C. Stress, cognitive impairment and cell adhesion molecules. *Nat Rev Neurosci*. 2004 Dec;5(12):917–30.
123. Rutters F, Fleur S, Lemmens S, Born J, Martens M, Adam T. The Hypothalamic-Pituitary-Adrenal Axis, Obesity, and Chronic Stress Exposure: Foods and HPA Axis. *Curr Obes Rep*. 2012 Aug 16;1(4):199–207.
124. Pasquali R, Vicennati V. Activity of the hypothalamic-pituitary-adrenal axis in different obesity phenotypes. *Int J Obes Relat Metab Disord*. 2000 Jun;24 Suppl 2:S47–9.
125. Björntorp P, Rosmond R. Neuroendocrine abnormalities in visceral obesity. *Int J Obes Relat Metab Disord*. 2000 Jun;24 Suppl 2:S80–5.
126. Wiedmer P, Chaudhary N, Rath M, Yi C-X, Ananthakrishnan G, Nogueiras R, et al. The HPA axis modulates the CNS melanocortin control of liver triacylglyceride metabolism. *Physiol Behav*. Elsevier Inc.; 2012 Feb 1;105(3):791–9.
127. Peckett AJ, Wright DC, Riddell MC. The effects of glucocorticoids on adipose tissue lipid metabolism. *Metabolism*. Elsevier Inc.; 2011 Nov;60(11):1500–10.
128. Bartness TJ, Song CK. Thematic review series: adipocyte biology. Sympathetic and sensory innervation of white adipose tissue. *J Lipid Res*. 2007 Aug;48(8):1655–72.
129. Giordano A, Frontini A, Murano I, Tonello C, Marino MA, Carruba MO, et al. Regional-dependent increase of sympathetic innervation in rat white adipose tissue during prolonged fasting. *J Histochem Cytochem*. 2005 Jun;53(6):679–87.
130. Boyda HN, Procyshyn RM, Pang CCY, Barr a M. Peripheral adrenoceptors: the impetus behind glucose dysregulation and insulin resistance. *J Neuroendocrinol*. 2013 Mar;25(3):217–28.
131. Lafontan M, Moro C, Berlan M, Crampes F, Sengenès C, Galitzky J. Control of lipolysis by natriuretic peptides and cyclic GMP. *Trends Endocrinol Metab*. 2008;19(4):130–7.
132. Halassa MM, Fellin T, Haydon PG. The tripartite synapse: roles for gliotransmission in health and disease. *Trends Mol Med*. 2007 Feb;13(2):54–63.
133. Perea G, Navarrete M, Araque A. Tripartite synapses: astrocytes process and control synaptic information. *Trends Neurosci*. 2009 Aug;32(8):421–31.
134. Gourine A V, Kasparov S. Astrocytes as brain interoceptors. *Exp Physiol*. 2011 Apr;96(4):411–6.
135. Bouzier-Sore A-K, Pellerin L. Unraveling the complex metabolic nature of astrocytes. *Front Cell Neurosci*. 2013 Jan;7(October):179.
136. Barros LF, Deitmer JW. Glucose and lactate supply to the synapse. *Brain Res Rev*. Elsevier B.V.; 2010 May;63(1-2):149–59.
137. Fillenz M, Lowry JP, Boutelle MG, Fray a E. The role of astrocytes and noradrenaline in neuronal glucose metabolism. *Acta Physiol Scand*. 1999 Dec;167(4):275–84.

138. Walls a B, Heimbürger CM, Bouman SD, Schousboe a, Waagepetersen HS. Robust glycogen shunt activity in astrocytes: Effects of glutamatergic and adrenergic agents. *Neuroscience*. IBRO; 2009 Jan 12;158(1):284–92.
139. Cornell-Bell a H, Finkbeiner SM, Cooper MS, Smith SJ. Glutamate induces calcium waves in cultured astrocytes: long-range glial signaling. *Science*. 1990 Jan 26;247(4941):470–3.
140. Zonta M, Carmignoto G. Calcium oscillations encoding neuron-to-astrocyte communication. *J Physiol Paris*. 2002;96(3-4):193–8.
141. Haydon P, Carmignoto G. Astrocyte control of synaptic transmission and neurovascular coupling. *Physiol Rev*. 2006;1009–31.
142. Deschepper CF. Peptide receptors on astrocytes. *Front Neuroendocrinol*. 1998 Jan;19(1):20–46.
143. Gourine A V, Kasymov V, Marina N, Tang F, Figueiredo MF, Lane S, et al. Astrocytes control breathing through pH-dependent release of ATP. *Science*. 2010 Jul 30;329(5991):571–5.
144. Parys B, Côté a, Gallo V, De Koninck P, Sík a. Intercellular calcium signaling between astrocytes and oligodendrocytes via gap junctions in culture. *Neuroscience*. Elsevier Inc.; 2010 Jun 2;167(4):1032–43.
145. Allard C, Carneiro L, Grall S, Cline BH, Fioramonti X, Chrétien C, et al. Hypothalamic astroglial connexins are required for brain glucose sensing-induced insulin secretion. *J Cereb Blood Flow Metab*. 2013 Dec 4;(October):1–8.
146. Okada Y, Sasaki T, Oku Y, Takahashi N, Seki M, Ujita S, et al. Preinspiratory calcium rise in putative pre-Botzinger complex astrocytes. *J Physiol*. 2012 Oct 1;590(Pt 19):4933–44.
147. Pan W, Hsuchou H, Jayaram B, Khan RS, Huang EY-K, Wu X, et al. Leptin action on nonneuronal cells in the CNS: potential clinical applications. *Ann N Y Acad Sci*. 2012 Aug;1264(1):64–71.
148. Fuente-Martín E. Leptin regulates glutamate and glucose transporters in hypothalamic astrocytes. *J* 2012;122(11).
149. Edvinsson L, Ekblad E, Håkanson R, Wahlestedt C. Neuropeptide Y potentiates the effect of various vasoconstrictor agents on rabbit blood vessels. *Br J Pharmacol*. 1984 Oct;83(2):519–25.
150. Ekblad E, Edvinsson L, Wahlestedt C, Uddman R, Håkanson R, Sundler F. Neuropeptide Y co-exists and co-operates with noradrenaline in perivascular nerve fibers. *Regul Pept*. 1984 Apr;8(3):225–35.
151. Tatemoto K. Neuropeptide Y: complete amino acid sequence of the brain peptide. *Proc Natl Acad* 1982;79(September):5485–9.
152. Rasmusson AM, Schnurr PP, Zukowska Z, Scioli E, Forman DE. Adaptation to extreme stress: post-traumatic stress disorder, neuropeptide Y and metabolic syndrome. *Exp Biol Med (Maywood)*. 2010 Oct;235(10):1150–62.

153. Barceló A, Barbé F, Llompart E, de la Peña M, Durán-Cantolla J, Ladaría A, et al. Neuropeptide Y and leptin in patients with obstructive sleep apnea syndrome: role of obesity. *Am J Respir Crit Care Med*. 2005 Jan 15;171(2):183–7.
154. Shi Y-C, Baldock P a. Central and peripheral mechanisms of the NPY system in the regulation of bone and adipose tissue. *Bone*. Elsevier Inc.; 2012 Feb;50(2):430–6.
155. Hirsch D, Zukowska Z. NPY and Stress 30 Years Later: The Peripheral View. *Cell Mol Neurobiol*. 2012 Jan 24;
156. Kuo LE, Kitlinska JB, Tilan JU, Li L, Baker SB, Johnson MD, et al. Neuropeptide Y acts directly in the periphery on fat tissue and mediates stress-induced obesity and metabolic syndrome. *Nat Med*. 2007 Jul;13(7):803–11.
157. Yang K, Guan H, Arany E, Hill DJ, Cao X. Neuropeptide Y is produced in visceral adipose tissue and promotes proliferation of adipocyte precursor cells via the Y1 receptor. *FASEB J*. 2008 Jul;22(7):2452–64.
158. Serradeil-Le Gal C, Lafontan M, Raufaste D, Marchand J, Pouzet B, Casellas P, et al. Characterization of NPY receptors controlling lipolysis and leptin secretion in human adipocytes. *FEBS Lett*. 2000 Jun 16;475(2):150–6.
159. Kos K, Baker a R, Jernas M, Harte a L, Clapham JC, O’Hare JP, et al. DPP-IV inhibition enhances the antilipolytic action of NPY in human adipose tissue. *Diabetes Obes Metab*. 2009 Apr;11(4):285–92.
160. Gericke MT, Schröder T, Kosacka J, Nowicki M, Klötting N, Spanel-Borowski K. Neuropeptide Y impairs insulin-stimulated translocation of glucose transporter 4 in 3T3-L1 adipocytes through the Y1 receptor. *Mol Cell Endocrinol*. Elsevier Ireland Ltd; 2012 Jan 2;348(1):27–32.
161. Peirce V, Carobbio S, Vidal-Puig A. The different shades of fat. *Nature*. 2014 Jun 5;510(7503):76–83.
162. Plum L, Rother E, Münzberg H, Wunderlich FT, Morgan D a, Hampel B, et al. Enhanced leptin-stimulated Pi3k activation in the CNS promotes white adipose tissue transdifferentiation. *Cell Metab*. 2007 Dec;6(6):431–45.
163. Bi S, Li L. Browning of white adipose tissue: role of hypothalamic signaling. *Ann N Y Acad Sci*. 2013 Oct;1302:30–4.
164. Li N-F, Yao X-G, Zhu J, Yang J, Liu K-J, Wang Y-C, et al. Higher levels of plasma TNF-alpha and neuropeptide Y in hypertensive patients with obstructive sleep apnea syndrome. *Clin Exp Hypertens*. 2010 Jan;32(1):54–60.
165. Abe K, Kuo L, Zukowska Z. Neuropeptide Y is a mediator of chronic vascular and metabolic maladaptations to stress and hypernutrition. *Exp Biol Med (Maywood)*. 2010 Oct;235(10):1179–84.
166. Xie F, Zhang R, Yang C, Xu Y, Wang N, Sun L, et al. Long-term Neuropeptide Y Administration in the Periphery Induces Abnormal Baroreflex Sensitivity and Obesity in Rats. *Cell Physiol Biochem*. 2012 Jan;29(1-2):111–20.

167. Livak KJ, Schmittgen TD. Analysis of relative gene expression data using real-time quantitative PCR and the $2^{-\Delta\Delta C(T)}$ Method. *Methods*. 2001 Dec;25(4):402–8.
168. Puri V, Chakladar A, Virbasius J V, Konda S, Powelka AM, Chouinard M, et al. RNAi-based gene silencing in primary mouse and human adipose tissues. *J Lipid Res*. 2007 Feb;48(2):465–71.
169. Lehrke M, Lazar M a. The many faces of PPARgamma. *Cell*. 2005 Dec 16;123(6):993–9.
170. García-Serrano S, Moreno-Santos I, Garrido-Sánchez L, Gutierrez-Repiso C, García-Almeida JM, García-Arnés J, et al. Stearoyl-CoA desaturase-1 is associated with insulin resistance in morbidly obese subjects. *Mol Med*. 2011;17(3-4):273–80.
171. Taganov KD, Boldin MP, Chang K-J, Baltimore D. NF-kappaB-dependent induction of microRNA miR-146, an inhibitor targeted to signaling proteins of innate immune responses. *Proc Natl Acad Sci U S A*. 2006 Aug 15;103(33):12481–6.
172. Sheedy FJ, O’Neill L a J. Adding fuel to fire: microRNAs as a new class of mediators of inflammation. *Ann Rheum Dis*. 2008 Dec;67 Suppl 3:iii50–5.
173. Pons J, Kitlinska J, Jacques D, Perreault C, Nader M, Everhart L, et al. Interactions of multiple signaling pathways in neuropeptide Y-mediated bimodal vascular smooth muscle cell growth. *Can J Physiol Pharmacol*. 2008 Jul;86(7):438–48.
174. Labruna G, Pasanisi F, Nardelli C, Caso R, Vitale DF, Contaldo F, et al. High leptin/adiponectin ratio and serum triglycerides are associated with an “at-risk” phenotype in young severely obese patients. *Obesity (Silver Spring)*. Nature Publishing Group; 2011 Jul;19(7):1492–6.
175. Van Vliet-Ostaptchouk J V, Nuotio M-L, Slagter SN, Doiron D, Fischer K, Foco L, et al. The prevalence of metabolic syndrome and metabolically healthy obesity in Europe: a collaborative analysis of ten large cohort studies. *BMC Endocr Disord*. 2014 Feb 1;14(1):9.
176. Baltazi M, Katsiki N, Savopoulos C, Iliadis F, Koliakos G, Hatzitolios AI. Plasma neuropeptide Y (NPY) and alpha-melanocyte stimulating hormone (a-MSH) levels in patients with or without hypertension and/or obesity: a pilot study. *Am J Cardiovasc Dis*. 2011 Jan;1(1):48–59.
177. Gustafsson S, Lind L, Söderberg S, Ingelsson E. Associations of circulating adiponectin with measures of vascular function and morphology. *J Clin Endocrinol Metab*. 2010 Jun;95(6):2927–34.
178. Aguilar-Salinas C a, García EG, Robles L, Riaño D, Ruiz-Gomez DG, García-Ulloa AC, et al. High adiponectin concentrations are associated with the metabolically healthy obese phenotype. *J Clin Endocrinol Metab*. 2008 Oct;93(10):4075–9.
179. Roberson LL, Aneni EC, Maziak W, Agatston A, Feldman T, Rouseff M, et al. Beyond BMI: The “Metabolically healthy obese” phenotype & its association with clinical/subclinical cardiovascular disease and all-cause mortality -- a systematic review. *BMC Public Health*. 2014 Jan;14(1):14.
180. Skurk T, Alberti-Huber C, Herder C, Hauner H. Relationship between adipocyte size and adipokine expression and secretion. *J Clin Endocrinol Metab*. 2007 Mar;92(3):1023–33.

181. Roberts R, Hodson L, Dennis a L, Neville MJ, Humphreys SM, Harnden KE, et al. Markers of de novo lipogenesis in adipose tissue: associations with small adipocytes and insulin sensitivity in humans. *Diabetologia*. 2009 May;52(5):882–90.
182. Akira S, Isshiki H, Nakajima T, Kinoshita S, Nishio Y, Natsuka S, et al. Regulation of expression of the interleukin 6 gene: structure and function of the transcription factor NF-IL6. *Ciba Found Symp*. 1992 Jan;167:47–62; discussion 62–7.
183. Wiest R, Jurzik L, Moleda L, Froh M, Schnabl B, von Hörsten S, et al. Enhanced Y1-receptor-mediated vasoconstrictive action of neuropeptide Y (NPY) in superior mesenteric arteries in portal hypertension. *J Hepatol*. 2006 Mar;44(3):512–9.
184. Hosogai N, Fukuhara A, Oshima K, Miyata Y, Tanaka S, Segawa K, et al. Adipose tissue hypoxia in obesity and its impact on adipocytokine dysregulation. *Diabetes*. 2007 Apr;56(4):901–11.
185. Yudkin JS, Eringa E, Stehouwer CD a. “Vasocrine” signalling from perivascular fat: a mechanism linking insulin resistance to vascular disease. *Lancet*. 2005;365(9473):1817–20.
186. Houben a J, Eringa EC, Jonk a M, Serne EH, Smulders YM, Stehouwer CD. Perivascular Fat and the Microcirculation: Relevance to Insulin Resistance, Diabetes, and Cardiovascular Disease. *Curr Cardiovasc Risk Rep*. 2012 Feb;6(1):80–90.
187. Chao P-T, Yang L, Aja S, Moran TH, Bi S. Knockdown of NPY expression in the dorsomedial hypothalamus promotes development of brown adipocytes and prevents diet-induced obesity. *Cell Metab*. Elsevier Inc.; 2011 May 4;13(5):573–83.
188. Ruschke K, Fishbein L, Dietrich A. Gene expression of PPAR γ and PGC-1 α in human omental and subcutaneous adipose tissues is related to insulin resistance markers and mediates beneficial effects. *Eur J* 2010;162(3):515–23.
189. Tinahones FJ, Garrido-Sanchez L, Miranda M, García-Almeida JM, Macias-Gonzalez M, Ceperuelo V, et al. Obesity and insulin resistance-related changes in the expression of lipogenic and lipolytic genes in morbidly obese subjects. *Obes Surg*. 2010 Nov;20(11):1559–67.
190. Sitticharoon C, Chatree S, Churintaraphan M. Expressions of neuropeptide Y and Y1 receptor in subcutaneous and visceral fat tissues in normal weight and obese humans and their correlations with clinical parameters and peripheral metabolic factors. *Regul Pept*. Elsevier B.V.; 2013 Jul 6;185C:65–72.
191. Lee EW, Michalkiewicz M, Kitlinska J, Kalezic I, Switalska H, Yoo P, et al. Neuropeptide Y induces ischemic angiogenesis and restores function of ischemic skeletal muscles. *J Clin Invest*. 2003 Jun;111(12):1853–62.
192. St-Pierre J a, Nouel D, Dumont Y, Beaudet a, Quirion R. Sub-population of cultured hippocampal astrocytes expresses neuropeptide Y Y(1) receptors. *Glia*. 2000 Mar;30(1):82–91.
193. Hsueh H, Pan W, Barnes M, Kastin A. Leptin receptor mRNA in rat brain astrocytes. *Peptides*. 2009;30(12):2275–80.

194. Hsuchou H, He Y, Kastin AJ, Tu H, Markadakis EN, Rogers RC, et al. Obesity induces functional astrocytic leptin receptors in hypothalamus. *Brain*. 2009 Apr;132(Pt 4):889–902.
195. Zhao M, Hagler HK, Muntz KH. Regulation of alpha 1-, beta 1-, and beta 2-adrenergic receptors in rat heart by norepinephrine. *Am J Physiol*. 1996 Nov;271(5 Pt 2):H1762–8.
196. Clark JT, Gist RS, Kalra SP, Kalra PS. Alpha 2-adrenoceptor blockade attenuates feeding behavior induced by neuropeptide Y and epinephrine. *Physiol Behav*. 1988 Jan;43(4):417–22.
197. Eugenin E a., D’Aversa TG, Lopez L, Calderon TM, Berman JW. MCP-1 (CCL2) protects human neurons and astrocytes from NMDA or HIV-tat-induced apoptosis. *J Neurochem*. 2003 May 6;85(5):1299–311.
198. Morioka N, Abe H, Araki R, Matsumoto N, Zhang FF, Nakamura Y, et al. A β 1/2 adrenergic receptor-sensitive intracellular signaling pathway modulates CCL2 production in cultured spinal astrocytes. *J Cell Physiol*. 2014 Mar;229(3):323–32.
199. Norris JG, Benveniste EN. Interleukin-6 production by astrocytes: induction by the neurotransmitter norepinephrine. *J Neuroimmunol*. 1993 Jun;45(1-2):137–45.
200. Maimone D, Cioni C, Rosa S, Macchia G, Aloisi F, Annunziata P. Norepinephrine and vasoactive intestinal peptide induce IL-6 secretion by astrocytes: synergism with IL-1 beta and TNF alpha. *J Neuroimmunol*. 1993 Aug;47(1):73–81.
201. Kassis S, Olasmaa M, Terenius L, Fishman PH. Neuropeptide Y inhibits cardiac adenylate cyclase through a pertussis toxin-sensitive G protein. *J Biol Chem*. 1987 Mar 15;262(8):3429–31.
202. Pedrazzini T, Pralong F, Grouzmann E. Neuropeptide Y: the universal soldier. *Cell Mol Life ...*. 2003;60:350–77.
203. Selbie LA, Darby K, Schmitz-Peiffer C, Browne CL, Herzog H, Shine J, et al. Synergistic interaction of Y1-neuropeptide Y and alpha 1b-adrenergic receptors in the regulation of phospholipase C, protein kinase C, and arachidonic acid production. *J Biol Chem*. 1995 May 19;270(20):11789–96.
204. Fiebich BL, Schleicher S, Spleiss O, Czygan M, Hüll M. Mechanisms of prostaglandin E2-induced interleukin-6 release in astrocytes: possible involvement of EP4-like receptors, p38 mitogen-activated protein kinase and protein kinase C. *J Neurochem*. 2001 Dec;79(5):950–8.
205. Kojima H, Inoue T, Kunimoto H, Nakajima K. IL-6-STAT3 signaling and premature senescence. *Jak-Stat*. 2013 Oct 1;2(4):e25763.
206. Shulman R, Hyder F, Rothman D. Lactate efflux and the neuroenergetic basis of brain function. *NMR Biomed*. 2001;389–96.
207. Swanson RA, Benington JH. Astrocyte glucose metabolism under normal and pathological conditions in vitro. *Dev Neurosci*. 1996 Jan;18(5-6):515–21.

208. Farina C, Aloisi F, Meinl E. Astrocytes are active players in cerebral innate immunity. *Trends Immunol.* 2007 Mar;28(3):138–45.
209. Norenberg MD, Mozes LW, Gregorios JB, Norenberg LO. Effects of lactic acid on astrocytes in primary culture. *J Neuropathol Exp Neurol.* 1987 Mar;46(2):154–66.
210. Tang F, Lane S, Korsak a., Paton JFR, Gourine a. V., Kasparov S, et al. Lactate-mediated glia-neuronal signalling in the mammalian brain. *Nat Commun. Nature Publishing Group;* 2014 Feb 11;5:1–13.
211. De la Iglesia N, Konopka G, Lim K-L, Nutt CL, Bromberg JF, Frank D a, et al. Deregulation of a STAT3-interleukin 8 signaling pathway promotes human glioblastoma cell proliferation and invasiveness. *J Neurosci.* 2008 Jun 4;28(23):5870–8.
212. Steensberg A, Fischer CP, Keller C, Møller K, Pedersen BK. IL-6 enhances plasma IL-1ra, IL-10, and cortisol in humans. *Am J Physiol Endocrinol Metab.* 2003 Aug;285(2):E433–7.
213. Roy M, Richard J-F, Dumas A, Vallières L. CXCL1 can be regulated by IL-6 and promotes granulocyte adhesion to brain capillaries during bacterial toxin exposure and encephalomyelitis. *J Neuroinflammation.* 2012 Jan;9:18.
214. Suzumura A, Takeuchi H, Zhang G, Kuno R, Mizuno T. Roles of glia-derived cytokines on neuronal degeneration and regeneration. *Ann N Y Acad Sci.* 2006 Nov;1088:219–29.
215. Yuan J, Wegenka U. The Signalling Pathways of Interleukin-6 and Gamma Interferon Converge by the Activation of Different Transcription Factors Which Bind to Common Responsive DNA Elements. ... *Cell Biol.* 1994;
216. Nicchia GP, Frigeri A, Liuzzi GM, Svelto M. Inhibition of aquaporin-4 expression in astrocytes by RNAi determines alteration in cell morphology, growth, and water transport and induces changes in ischemia-related genes. *FASEB J.* 2003 Aug;17(11):1508–10.
217. Pasti L, Volterra A. Intracellular calcium oscillations in astrocytes: a highly plastic, bidirectional form of communication between neurons and astrocytes in situ. *J* 1997;17(20):7817–30.
218. Gibbs ME, Bowser DN. Astrocytic adrenoceptors and learning: alpha1-adrenoceptors. *Neurochem Int. Elsevier Ltd;* 2010 Nov;57(4):404–10.
219. Duffy S, MacVicar B. Adrenergic calcium signaling in astrocyte networks within the hippocampal slice. *J Neurosci.* 1995;15(August).
220. Endoh T, Nobushima H, Tazaki M. Neuropeptide Y modulates calcium channels in hamster submandibular ganglion neurons. *Neurosci Res. Elsevier Ireland Ltd and Japan Neuroscience Society;* 2012 Aug;73(4):275–81.
221. Neary JT, Norenberg LO, Norenberg MD. Calcium-activated, phospholipid-dependent protein kinase and protein substrates in primary cultures of astrocytes. *Brain Res.* 1986 Oct 22;385(2):420–4.
222. Vajanaphanich M, Schultz C, Tsien RY, Traynor-Kaplan AE, Pandol SJ, Barrett KE. Cross-talk between calcium and cAMP-dependent intracellular signaling pathways.

- Implications for synergistic secretion in T84 colonic epithelial cells and rat pancreatic acinar cells. *J Clin Invest.* 1995 Jul;96(1):386–93.
223. Stehberg J, Moraga-Amaro R, Salazar C, Becerra A, Echeverría C, Orellana J a, et al. Release of gliotransmitters through astroglial connexin 43 hemichannels is necessary for fear memory consolidation in the basolateral amygdala. *FASEB J.* 2012 Sep;26(9):3649–57.
 224. Nedergaard M, Verkhratsky A. Artifact versus reality--how astrocytes contribute to synaptic events. *Glia.* 2012 Jul;60(7):1013–23.
 225. Pekny M, Nilsson M. Astrocyte activation and reactive gliosis. *Glia.* 2005 Jun;50(4):427–34.
 226. Ridet JL, Privat A, Malhotra SK, Gage FH. Reactive astrocytes: cellular and molecular cues to biological function. *Trends Neurosci.* 1997 Dec;20(12):570–7.
 227. Kapoor JR, Sladek CD. Substance P and NPY differentially potentiate ATP and adrenergic stimulated vasopressin and oxytocin release. *Am J Physiol Regul Integr Comp Physiol.* 2001 Jan;280(1):R69–78.
 228. Zaccolo M, Pozzan T. cAMP and Ca²⁺ interplay: a matter of oscillation patterns. *Trends Neurosci.* 2003 Feb;26(2):53–5.
 229. Bruce JL, Straub S V, Yule DI. Crosstalk between cAMP and Ca²⁺ signaling in non-excitable cells. *Cell Calcium.* 2003 Dec;34(6):431–44.
 230. Cooper DM, Mons N, Karpen JW. Adenylyl cyclases and the interaction between calcium and cAMP signalling. *Nature.* 1995 Mar 30;374(6521):421–4.
 231. Chen CC, Wang JK, Chen WC, Lin SB. Protein kinase C eta mediates lipopolysaccharide-induced nitric-oxide synthase expression in primary astrocytes. *J Biol Chem.* 1998 Jul 31;273(31):19424–30.
 232. Erta M, Quintana A, Hidalgo J. Interleukin-6, a major cytokine in the central nervous system. *Int J Biol Sci.* 2012 Jan;8(9):1254–66.
 233. Park S, Fujishita C, Komatsu T, Kim SE, Chiba T, Mori R, et al. NPY antagonism reduces adiposity and attenuates age-related imbalance of adipose tissue metabolism. *FASEB J.* 2014 Dec;28(12):5337–48.
 234. Satoh J, Lee YB, Kim SU. T-cell costimulatory molecules B7-1 (CD80) and B7-2 (CD86) are expressed in human microglia but not in astrocytes in culture. *Brain Res.* 1995 Dec 15;704(1):92–6.
 235. Rosmaninho-Salgado J, Marques AP, Estrada M, Santana M, Cortez V, Grouzmann E, et al. Dipeptidyl-peptidase-IV by cleaving neuropeptide Y induces lipid accumulation and PPAR- γ expression. *Peptides.* Elsevier Inc.; 2012 Sep;37(1):49–54.
 236. Mentlein R, Dahms P, Grandt D, Krüger R. Proteolytic processing of neuropeptide Y and peptide YY by dipeptidyl peptidase IV. *Regul Pept.* 1993 Dec 10;49(2):133–44.

237. Bernet F, Dedieu JF, Laborie C, Montel V, Dupouy JP. Circulating neuropeptide Y (NPY) and catecholamines in rat under resting and stress conditions. Arguments for extra-adrenal origin of NPY, adrenal and extra-adrenal sources of catecholamines. *Neurosci Lett.* 1998 Jun 26;250(1):45–8.